Molecular Meccano. 4. The Self-Assembly of [2]Catenanes Incorporating Photoactive and Electroactive π-Extended Systems[1]

Peter R. Ashton,[†] Roberto Ballardini,*[,⊥] Vincenzo Balzani,*[,‡] Alberto Credi,[‡] Maria Teresa Gandolfi,[‡] Stephan Menzer,[§] Lluïsa Pérez-García,[†] Luca Prodi,[‡] J. Fraser Stoddart,*[,†] Margherita Venturi,[‡] Andrew J. P. White,[§] and David J. Williams*[,§]

Contribution from the School of Chemistry, University of Birmingham, Edgbaston, Birmingham B15 2TT, U.K., Istituto FRAE-CNR, Via Gobetti 101, I-40129 Bologna, Italy, Dipartimento di Chimica "G. Ciamician" dell' Università, Via Selmi 2, I-40126 Bologna, Italy, and the Chemical Crystallography Laboratory, Department of Chemistry, Imperial College, South Kensington, London SW7 2AY, U.K.

Received December 2, 1994. Revised Manuscript Received August 17, 1995[⊗]

Abstract: Six new [2]catenanes, which have been constructed by efficient (38−64%) template-directed methods incorporate (a) within their crown-10 components hydroquinone and/or 1,5-dioxynaphthalene residues as π-donors and (b) within their tetracationic cyclophane components, bipyridinium and/or *trans*-bis(pyridinium)ethylene units as π-acceptors, the latter as potential photochemically-addressable functions. Four of the [2]catenanes exhibit translational isomerism in solution, as evidenced by dynamic ^{1}H NMR spectroscopic studies. The preferred isomers have a 1,5-dioxynaphthalene residue inside the tetracationic cyclophane components and a bipyridinium unit inside the crown-10 components. Where the [2]catenanes have crystallized, X-ray crystallography has revealed that the predominant isomer in solution is the one that exists in the crystal—for example, only *one* amongst *four* possible translational isomers is detected in solution at low temperatures as well as in the solid state, in the case of the [2]catenane containing two different π-donors [hydroquinone and 1,5-dioxynaphthalene rings] and two different π-acceptors [bipyridinium and *trans*-bis(pyridinium)ethylene units]. The isomer populations in solution are also indicated by electrochemical experiments. There is evidence in the case of the [2]catenane composed of bisparaphenylene-34-crown-10 and a tetracationic cyclophane incorporating a bipyridinium unit as well as a *trans*-bis(pyridinium)ethylene unit of being able to switch the translational isomer preference by reducing and oxidizing sequentially the bipyridinium unit electrochemically. These results illustrate the progress that is being made toward the construction of controllable [2]catenanes. A detailed photochemical and photophysical investigation has shown that, although the *trans*-bis(pyridinium)ethylene units undergo efficient *trans* → *cis* photochemical process even when incorporated in a cyclophane structure, the corresponding [2]catenanes cannot be photoaddressed because of the presence of low energy charge-transfer levels.

In part 1 of this series of papers, we reported[2] a highly efficient (70%) template-directed synthesis[3] of a [2]catenane (Figure 1), incorporating two viologen units in its tetracationic cyclophane component and two hydroquinone rings in its macrocyclic polyether component. The search for more selective recognition processes between the components of [2]catenanes of this kind requires the identification of modified π-accepting and π-donating building blocks for incorporation into the tetracationic cyclophane and macrocyclic polyether components, respectively. These considerations led us to self-assemble the series of [2]catenanes (Figure 2) incorporating (1) π-extended tetracationic cyclophanes, wherein the bipyridinium units have inserted centrally within them any functional group which maintains the coplanarity as well as the conjugation of the system and (2) π-extended macrocyclic polyethers where benzene and naphthalene rings are the aromatic building blocks. Since some vinylogous viologens, such as $[BMBIPYE]^{2+}$, have

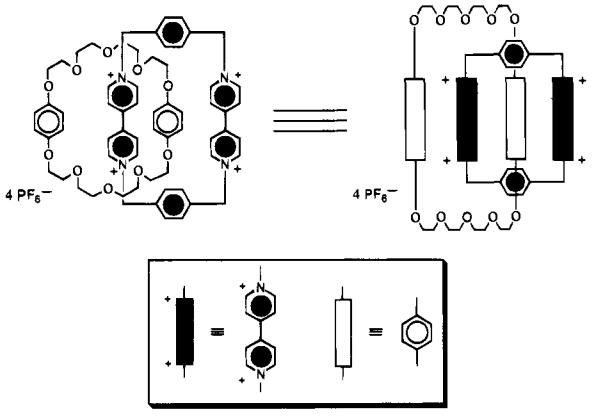

Figure 1. The structural formula and cartoon version of the {[2]-[BPP34C10]-[BBIPYBIXYCY]catenane}$[PF_6]_4$ formed between bis-*p*-phenylene-34-crown-10 and bis(paraquat-*p*-phenylene).

[†] University of Birmingham.
[⊥] Istituto FRAE-CNR, Bologna.
[‡] Università di Bologna.
[§] Imperial College.
[⊗] Abstract published in *Advance ACS Abstracts*, October 1, 1995.

(1) Molecular Meccano 3. Amabilino, D. B.; Anelli, P. L.; Ashton, P. R.; Brown, G. R.; Córdova, E.; Godinez, L. A.; Hayes, W.; Kaifer, A. E.; Philp, D.; Slawin, A. M. Z.; Spencer, N.; Stoddart, J. F.; Tolley, M. S.; Williams, D. J. *J. Am. Chem. Soc.* **1995**, *117*, 11142−11170.

(2) Anelli, P. L.; Ashton, P. R.; Ballardini, R.; Balzani, V.; Delgado, M.; Gandolfi, M. T.; Goodnow, T. T.; Kaifer, A. E.; Philp, D.; Pietraszkiewicz, M.; Prodi, L.; Reddington, M. V.; Slawin, A. M. Z.; Spencer, N.; Stoddart, J. F.; Vicent, C.; Williams, D. J. *J. Am. Chem. Soc.* **1992**, *114*, 193−218.

(3) For reviews on template-directed synthesis, see: (a) Chambron, J.-C.; Dietrich-Buchecker, C. O.; Sauvage, J.-P. *Top. Curr. Chem.* **1993**, *165*, 131−162. (b) Anderson, S.; Anderson, H. L.; Sanders, J. K. M. *Acc. Chem. Res.* **1993**, *26*, 469−475. (c) Hoss, R.; Vögtle, F. *Angew. Chem., Int. Ed. Engl.* **1994**, *33*, 375−384.

0002-7863/95/1517-11171$09.00/0

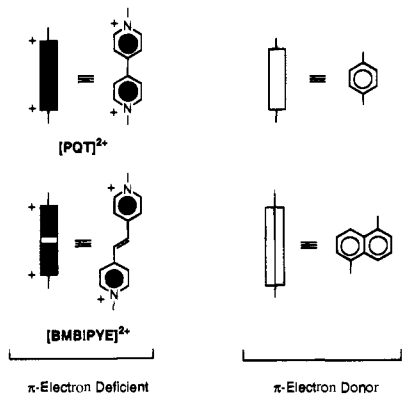

Figure 2. The building blocks, as both cartoons and formulas, employed in the construction of the new [2]catenanes.

already been synthesized[4] in order to modify the properties and functions of $[PQT]^{2+}$, we were attracted by the idea of incorporating them into a set of new self-assembled [2]-catenanes. Several reasons led us to choose the vinylogous derivative $[BMBIPYE]^{2+}$ of $[PQT]^{2+}$ as a π-extended viologen. These reasons included (1) its weaker affinity for binding π-electron donors and (2) its higher reduction potential,[5] which makes the unit suitable for the construction of potentially controllable [2]catenanes.[6,7] On the other hand, its incorporation into the tetracationic cyclophane component increases the size of its cavity, meaning that it could be used in combination with larger aromatic units present in the macrocyclic polyether component. It was anticipated that new structural and dynamic properties would emerge as a result of the "looser" structures associated with the new [2]catenanes as well as the translational isomerism[8] that occurs in these desymmetrized [2]catenanes.[6,9] Furthermore, they are electrochemically and photochemically active and, as such, could be attractive building blocks for the construction of switchable molecules. These were our expectations. Now, we report a full range[7] of experiments and discuss the results obtained from them.

Results and Discussion

Names and Cartoons. It will be convenient to employ acronyms composed of letters and numbers to identify the compounds displayed in the schemes and figures. Thus, 1,4-bis(bromomethyl)benzene is abbreviated to BBB, 1,4-dihydroxybenzene to 1/4DHB, 1,5-dihydroxynaphthalene to 1/5DHN, bis-*p*-phenylene-34-crown-10 to BPP34C10, 1,5-naphtho-*p*-phenylene-36-crown-10 to 1/5NPP36C10, and 1,5-dinaphtho-38-crown-10 to 1/5DN38C10. The other acronyms can be deduced on the basis of the following defintions: B stands for bis when at the beginning, for bromo when in the middle, and benzene when at the end of the name. Bn, E, H, M, N, and T stand for benzyl, ethoxy, hydroxy, methyl, naphthalene, and tosyloxy, respectively. CY, XY, and BIXY represent cyclophane, xylyl, and bisxylyl units, respectively. BP and BPE stand for the neutral 4,4′-bipyridine and (*E*)-1,2-bis(4,4′-pyridyl)-ethylene systems, and BIPY and BIPYE represent the bipyridinium and bis(pyridinium)ethylene ring systems, with the formal charges indicated in the usual manner. Paraquat is represented by $[PQT]^{2+}$. In the cartoon versions of the structural formulas, the smaller rectangles represent *para*-disubstituted benzene rings and the larger ones, bipyridinium ring systems, if shaded, and bispyridinium ethylene ring systems, if shaded with a light area in the middle of the rectangle. In both cases, the formal charges are positioned appropriately beside the cartoon. In the case of the neutral components, the rectangles are unshaded, and aromatic ring systems such as benzene and naphthalene are represented as having one and two compartments, respectively. In the Electrochemistry and Photochemistry sections, the acronyms employed (Figure 3) are different. BPP34C10 is abbreviated to BB, 1/5DN38C10 to NN, and 1/5NPP36C10 to BN. The three tetracationic cyclophanes are abbreviated by consecutive numbers with the tetracationic nature indicated by a superscript—thus, $[BBIPYBIXYCY][PF_6]_4$ is abbreviated to $\mathbf{1}^{4+}$ and so on. The [2]catenanes have been named by a combination of the acronyms for their two components—thus, $\{[2]\text{-}[BPP34C10]\text{-}[BBIPYEBIXYCY]catenane\}[PF_6]_4$ is abbreviated $\mathbf{3BB}^{4+}$.

Synthesis. The crown ether 1/5NPP36C10 can be prepared following a previously reported procedure[9a] and a new one (Scheme 1). In method A, reaction (THF/NaH) of BHEEB[2] with 1/5BTEEN[9a] gave (14%) 1/5NPP36C10. In method B, cyclization ($MeCN/Cs_2CO_3$) of 1/5BTEEEEN[10] with 1/4DHB afforded (32%) 1/5NPP36C10. The macrocyclic polyethers BPP34C10 and 1/5DN38C10 were synthesized according to literature procedures.[2,10-12]

(4) (a) Rembaum, A.; Hermann, A. M.; Stewart, F. E.; Gutmann, F. *J. Phys. Chem.* **1969**, *73*, 513–520. (b) Ashwell, G. J. *Phys. Sat. Sol.* **1978**, *86*, 705–715. (c) Bühner, M.; Geuder, W.; Hünig, S.; Koch, M.; Poll, T. *Angew. Chem., Int. Ed. Engl.* **1988**, *27*, 1553–1556. (d) Kamogawa, H.; Yamada, H. *Bull. Chem. Soc. Jpn.* **1991**, *64*, 3196–3198. (e) Muramatsu, T.; Toyota, A.; Ikegami, Y. *J. Org. Chem.* **1995**, *60*, 4925–4927.

(5) Hünig, S.; Berneth, H. *Top. Curr. Chem.* **1988**, *92*, 1–44.

(6) For communications relating to some of the results, see: (a) Ashton, P. R.; Ballardini, R.; Balzani, V.; Gandolfi, M. T.; Marquis, D. J.-F.; Pérez-García, L.; Prodi, L.; Stoddart, J. F.; Venturi, M. *J. Chem. Soc., Chem. Commun.* **1994**, 177–180. (b) Ashton, P. R.; Pérez-García, L.; Stoddart, J. F.; White, A. J. P.; Williams, D. J. *Angew. Chem., Int. Ed. Engl.* **1995**, *34*, 571–574.

(7) (a) At present, one of the most fundamental challenges offered by these intriguing molecules is to learn how to effect structural changes between their component parts, induced by external stimuli that are either chemical (ref 7b–e), electrochemical (ref 7b, 7f, 7g), or photochemical (ref 7h–n). Subsequently, this control could lead to the expression of a particular property—not only at the microscopic level of a molecule but also at the macroscopic level of a material or device (ref 7o, p). (b) Beer, P. D. *Chem. Soc. Rev.* **1989**, *18*, 409–450. (c) Bissell, R. A.; Córdova, E.; Kaifer, A. E.; Stoddart, J. F. *Nature* **1994**, *369*, 133–137. (d) Gunter, M. J.; Hockless, D. C. R.; Johnston, M. R.; Skelton, B. W.; White, A. H. *J. Am. Chem. Soc.* **1994**, *116*, 4810–4823. (e) Marsella, M. J.; Carroll, P. J.; Swager, T. M. *J. Am. Chem. Soc.* **1994**, *116*, 9347–9348. (f) Newell, A. K.; Utley, J. H. P. *J. Chem. Soc., Chem. Commun.* **1992**, 800–801. (g) Livoreil, A.; Dietrich-Buchecker, C. O.; Sauvage, J.-P. *J. Am. Chem. Soc.* **1994**, *116*, 9399–9400. (h) Balzani, V.; Scandola, F. *Supramolecular Photochemistry*; Ellis Horwood Limited: Chichester, 1991; Chapter 12. (i) Balzani, V. *Tetrahedron* **1992**, *48*, 10443–10514. (j) Ballardini, R.; Balzani, V.; Gandolfi, M. T.; Prodi, L.; Venturi, M.; Philp, D.; Ricketts, H. G.; Stoddart, J. F. *Angew. Chem., Int. Ed. Engl.* **1993**, *32*, 1301–1303. (k) Benniston, A. C.; Harriman, A. *Angew. Chem., Int. Ed. Engl.* **1993**, *32*, 1459–1461. (l) Benniston, A. C.; Harriman, A.; Lynch, V. M. *Tetrahedron Lett.* **1994**, *35*, 1473–1476. (m) Seiler, M.; Dürr, H.; Willner, I.; Joselevich, E.; Doron, A.; Stoddart, J. F. *J. Am. Chem. Soc.* **1994**, *116*, 3399–3404. (n) Bauer, M.; Müller, W. M.; Müller, U.; Rissanen, K.; Vögtle, F. *Liebigs Ann.* **1995**, 649–656. (o) Drexler, K. E. *Nanosystems: Molecular Machinery, Manufacturing and Computation*; Wiley: New York, 1992. (p) Drexler, K. E. *Annu. Rev. Biophys. Biomol. Struct.* **1994**, *23*, 377–405.

(8) (a) Schill, G.; Rissler, K.; Vetter, W. *Angew. Chem., Int. Ed. Engl.* **1981**, *20*, 187–189. (b) Rissler, K.; Schill, G.; Fritz, H.; Vetter, W. *Chem. Ber.* **1986**, *119*, 1374–1399.

(9) (a) Ashton, P. R.; Blower, M.; Philp, D.; Spencer, N.; Stoddart, J. F.; Tolley, M. S.; Ballardini, R.; Ciano, M.; Balzani, V.; Gandolfi, M. T.; Prodi, L.; McLean, C. H. *New J. Chem.* **1993**, *17*, 689–695. (b) Amabilino, D. B.; Stoddart, J. F. *Recl. Trav. Chim. Pays-Bas* **1993**, *112*, 429–430. (c) Amabilino, D. B.; Ashton, P. A.; Brown, G. R.; Hayes, W.; Stoddart, J. F.; Tolley, M. S.; Williams, D. J. *J. Chem. Soc., Chem. Commun.* **1994**, 2479–2482.

(10) Amabilino, D. B.; Stoddart, J. F. Unpublished results.

(11) Helgeson, R. C.; Tarnowski, T. L.; Timko, J. M.; Cram, D. J. *J. Am. Chem. Soc.* **1977**, *99*, 6411–6418.

(12) (a) Ashton, P. R.; Chrystal, E. J. T.; Mathias, J. P.; Parry, K. P.; Slawin, A. M. Z.; Spencer, N.; Stoddart, J. F.; Williams, D. J. *Tetrahedron Lett.* **1987**, *28*, 6367–6370. (b) Ashton, P. R.; Brown, C. L.; Chrystal, E. J. T.; Goodnow, T.; Kaifer, A. E.; Parry, K. P.; Philp, D.; Slawin, A. M. Z.; Spencer, N.; Stoddart, J. F.; Williams, D. J. *J. Chem. Soc., Chem. Commun.* **1991**, 634–639.

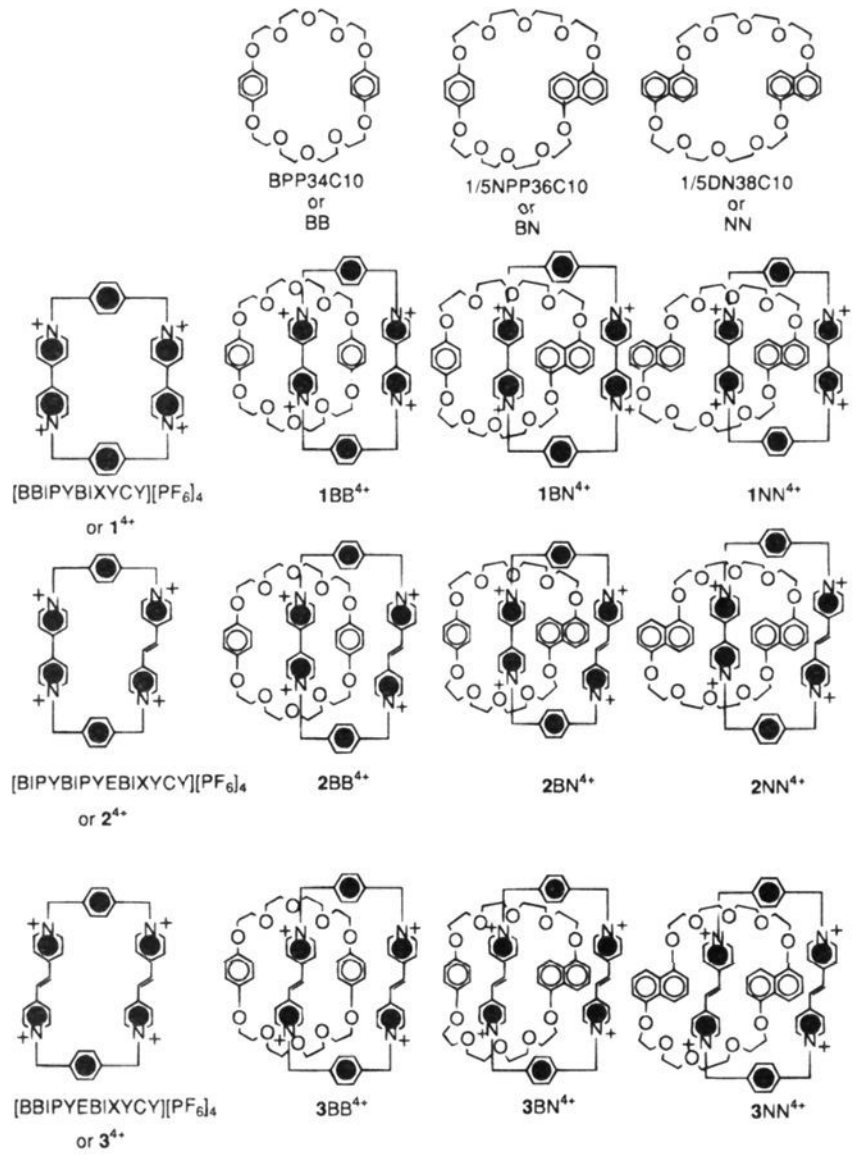

Figure 3. The acronyms for the macrocyclic polyethers, the tetracationic cyclophanes, and their corresponding [2]catenanes.

Scheme 1

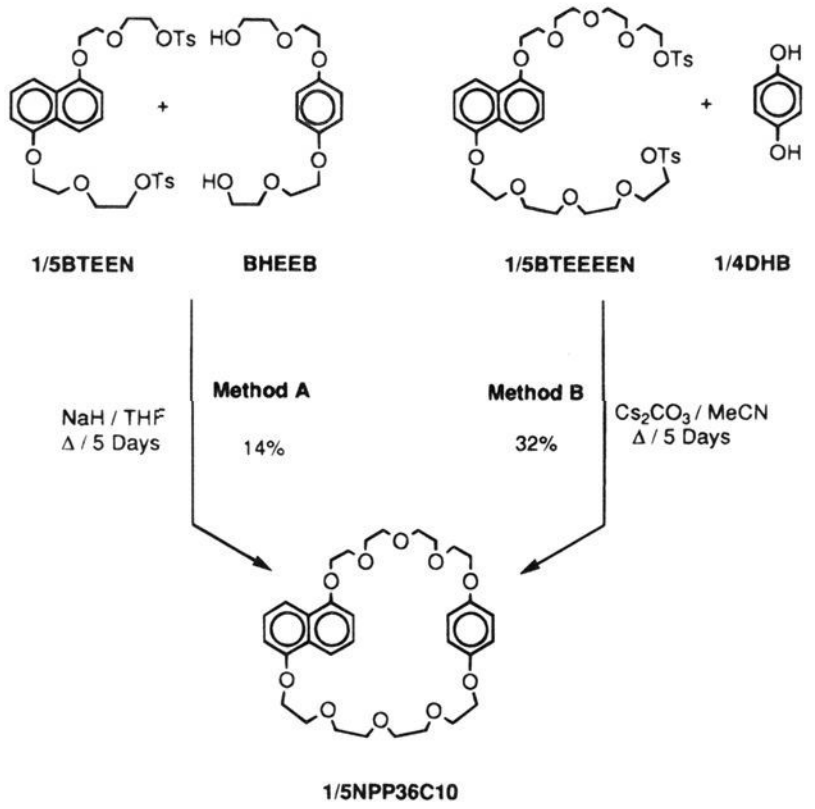

The template-directed synthesis of the cyclophane [BBIPYEBIXYCY][PF_6]$_4$ was achieved (Scheme 2) starting from [BBIPYEXY][PF_6]$_2$—obtained (84%) by reaction of (*E*)-1,2-bis(4,4′-bipyridyl)ethylene (BPE) with 1,4-bis(bromomethyl)-benzene (BBB) after counterion exchange (NH_4PF_6/H_2O)—and BBB, using 1/5BHEEN as template and DMF as the solvent. Separation of the product from the template was achieved by continuous liquid−liquid extraction of an aqueous solution of the 1:1 complex with $CHCl_3$. The template was recovered almost quantitatively (98%) from the organic phase. The aqueous phase contained the cyclophane, which, after purification and counterion exchange, afforded [BBIPYEBIXYCY]-[PF_6]$_4$. The preparation of [BBIPYEBIXYCY][PF_6]$_4$ was successful *only* in the presence of 1/5BHEEN. BHEEB exhibits *no* template effect. The larger π-surface area provided by 1/5BHEEN is presumably necessary in order to complement the extended π-system associated with the π-electron deficient bis(pyridinium)ethylene unit.

Table 1. Comparison of the Yields for the Self-Assembly of [2]Catenanes[a]

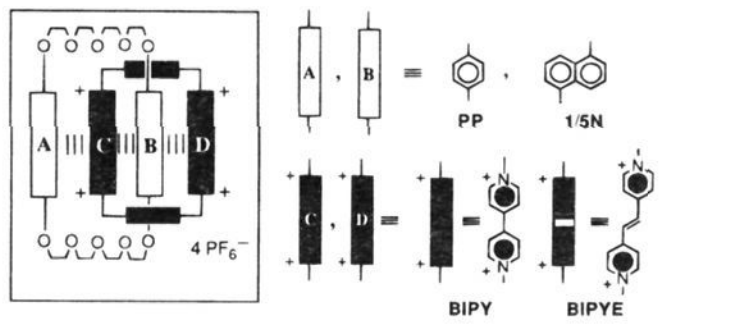

entry for the [2]catenane	crown ether A	crown ether B	cyclophane C	cyclophane D	method	solvent	yield (%)	ref
1	PP	PP	BIPY	BIPY	E	MeCN	70	2
					F	DMF	53	30
2	PP	PP	BIPY	BIPYE	F	MeCN	23	
					F	DMF	43	
					G	DMF	38	
3	PP	PP	BIPYE	BIPYE	E	MeCN	19	
					E	DMF	38	
4	PP	1/5N	BIPY	BIPY	E	MeCN	50	9a
5	PP	1/5N	BIPY	BIPYE	F	DMF	58	
6	PP	1/5N	BIPYE	BIPYE	E	DMF	49	
7	1/5N	1/5N	BIPY	BIPY	E	MeCN	51	12b
8	1/5N	1/5N	BIPY	BIPYE	F	DMF	64	
					G	DMF	59	
9	1/5N	1/5N	BIPYE	BIPYE	E	DMF	51	

[a] See Schemes 4 and 5 as well as the Experimental Section.

The cyclophane [BIPYBIPYEBIXYCY][PF_6]$_4$ was prepared (Scheme 3) by template-directed syntheses by two different routes. In method C, reaction of [BBXYBIPY][PF_6]$_2$—obtained (70%) by reaction of 4,4′-bipyridine (BP) with a large excess of 1,4-bis(bromomethyl)benzene (BBB) after counterion exchange—with (*E*)-1,2-bis(4,4′-bipyridyl)ethylene (BPE), afforded the cyclophane [BIPYBIPYEBIXYCY][PF_6]$_4$, following decomplexation of the initially formed complex by continuous liquid−liquid extraction and counterion exchange. In the second procedure (method D), [BBXYBIPYE][PF_6]$_2$—previously prepared by reaction of BPE with BBB—was reacted (DMF/NaI) with BP to give the cyclophane [BIPYBIPYEBIXYCY][PF_6]$_4$. In both cases, DMF was the solvent of choice, and 1/5BHEEN proved to be a much more efficient template than BHEEB, which gave the cyclophane in only 12% yield. The similarity (53 and 42%) of the yields, obtained when 1/5BHEEN is used as template, indicates that the structure of the tricationic intermediate, which undergoes cyclization to the tetracationic cyclophane, does not seem to govern the ring closure step.

Two different approaches were followed in self-assembling the [2]catenanes (Table 1) according to the structures of their tetracationic cyclophanes. Polar solvents (MeCN or DMF) were the ones of choice for the catenations. In general, DMF afforded higher yields of the new [2]catenanes (entries 2 and 3 in Table 1), presumably because of the increase in the solubility of the starting materials—which allows higher concentrations of reactants to be employed—and because of the fact that it facilitates the isolation of the catenated materials—"cleaner" reaction mixtures were obtained using DMF as the solvent and by taking the precaution to protect the reactions from light.

The synthesis of those [2]catenanes incorporating *two* identi-

Scheme 2

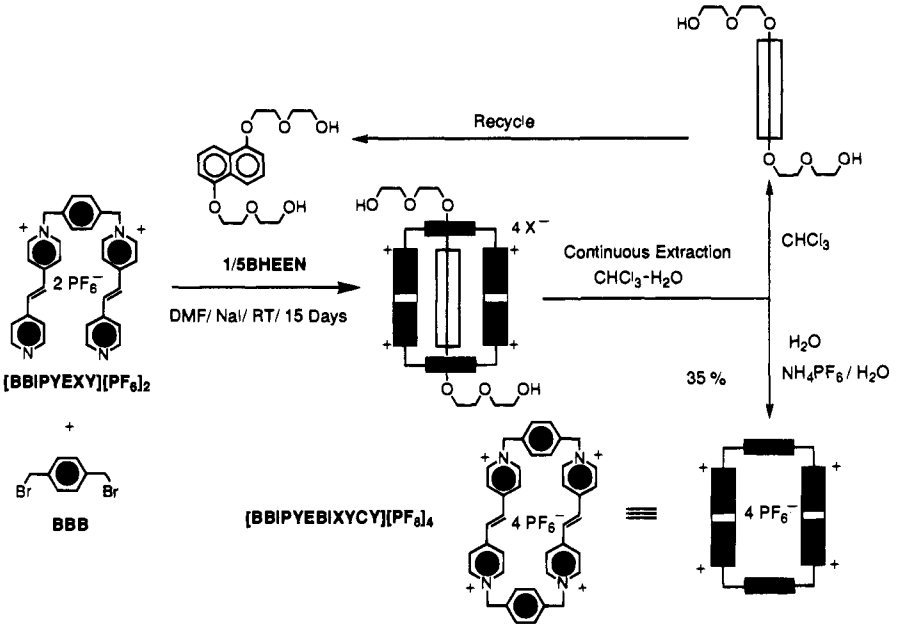

Scheme 3

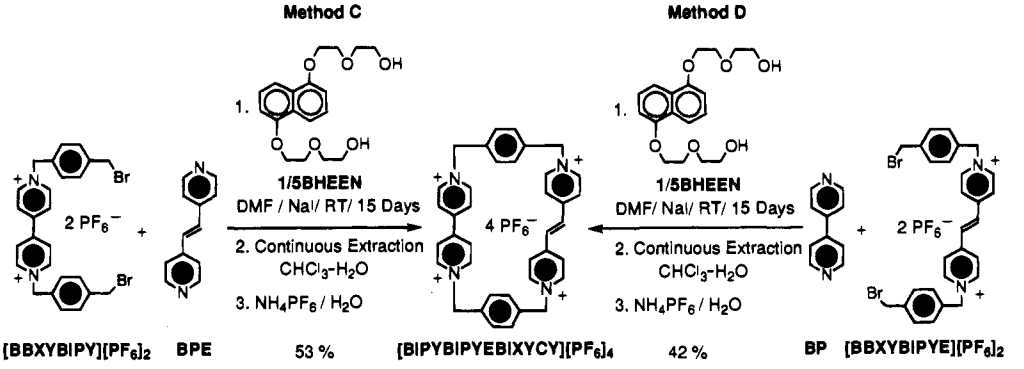

cal π-electron deficient units is described (method E) in Scheme 4. Reaction of [BBIPYEXY][PF_6]$_2$ with BBB results presumably in a tricationic intermediate which, on complexation with the appropriate macrocyclic polyether, generates the corresponding [2]catenane by undergoing template-directed cyclization. Scheme 5 illustrates the general approach used for the self-assembly of those [2]catenanes containing *one* bipyridinium unit and *one* bis(pyridinium)ethylene unit. The instantaneous formation of a complex between the macrocyclic polyether and [BBXYBIPY][PF_6]$_2$ was followed by stepwise alkylation of BPE to form (method F) the corresponding [2]catenane. In addition, two of the [2]catenanes have been synthesized by another route (method G) in order to ascertain if catenations are influenced electronically by the binding strength associated with the initially formed complex as well as by the steric requirements of the tricationic intermediate prior to the final cyclization. Thus, by reaction of [BBXYBIPYE][PF_6]$_2$ with BP in the presence of BPP34C10 or 1/5DN38C10, the corresponding [2]catenanes were isolated in yields that were only reduced by ca. 5% relative to those obtained by method F (see entries 2 and 8 in Table 1). This experimental observation suggests that neither the weaker complexes formed by the extended bipyridinium units with the aromatic crown ethers nor the geometries of the intermediates are the dominant factors for the [2]catenane formation, i.e., kinetic control appears to be the dominant feature governing the self-assembly processes.[13]

In all cases, the yields (Table 1) are influenced by the nature of both the neutral and the charged components of the [2]catenanes. Thus, in MeCN, with reference to BPP34C10 as the macrocyclic polyether component, the cyclophane incorporating two bipyridinium units affords a higher yield (70%) of the [2]catenane, than the cyclophane containing one bipyridinium and one bis(pyridinium)ethylene unit where the yield is 23%. When the [2]catenane contains a cyclophane with two extended viologen units, it is self-assembled in only 19% yield in MeCN. If we take the crown ether component as the variable one, we observe—choosing [BIPYBIPYEBIXYCY][PF_6]$_4$ as the reference cyclophane—that the self-assembly process in DMF occurs with increased efficiency (Table 1) when the hydroquinone rings are replaced progressively by 1,5-dioxynapthalene units in the crown ether component, e.g., the yield of the corresponding [2]catenanes are (i) 43% using BPP34C10, (ii) 58% using 1/5NPP36C10, and (iii) 64% using 1/5DN38C10. These observations demonstrate that the efficiencies of the catenations increase in a manner that is directly related to the number of 1,5-dioxynaphthalene units.

Two dynamic processes occur in the [2]catenanes (Scheme 6). One process (X) involves the exchange of the π-electron rich aromatic rings of the neutral macrocycle between "inside" and "alongside" environments with respect to the cyclophane. Another process (Y) involves the circumrotation of the cyclophane through the macrocyclic polyether. As a consequence of the introduction of different π-donors and π-acceptors into these systems, they undergo translational isomerism.[8] Scheme

(13) Amabilino, D. B.; Ashton, P. R.; Pérez-García, L.; Stoddart, J. F. *Angew. Chem., Int. Ed. Engl.* **1995**, in press.

Scheme 4

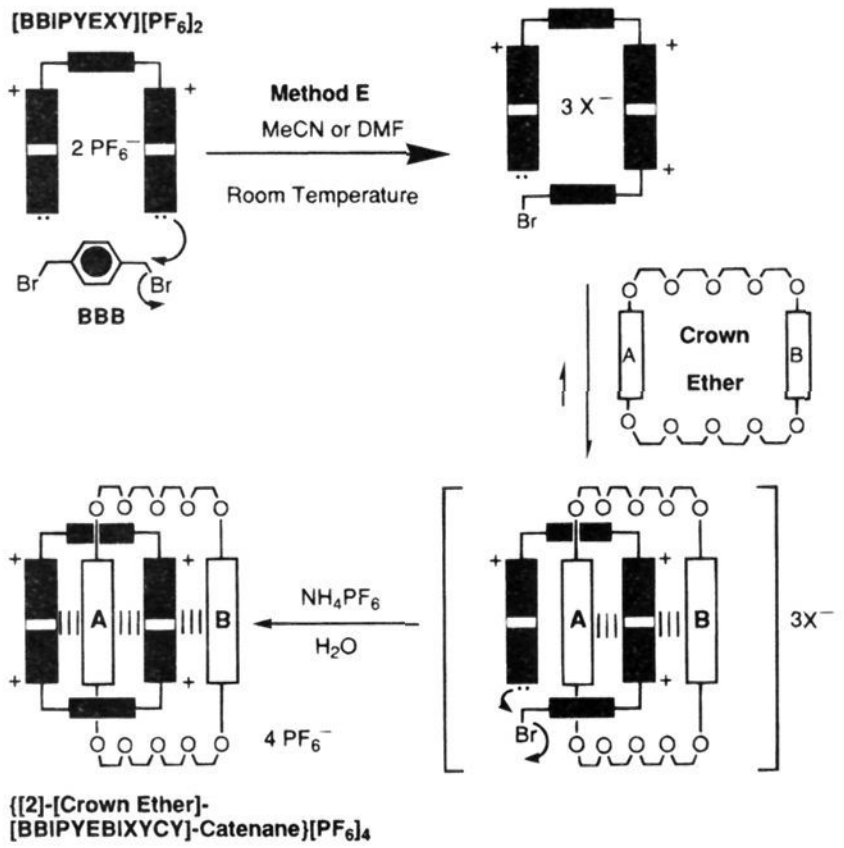

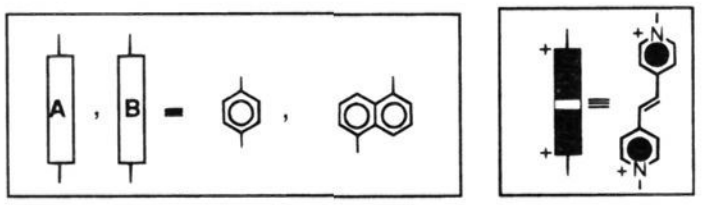

6 describes the two processes (X and Y) governing the dynamic behavior of the [2]catenanes. The situation which is described in Scheme 6 is the most complicated one, i.e., where the four recognition sites in the two interlocked rings are all different, meaning that up to four translational isomers can exist. When A = B **or** C = D, only two isomers are possible, whereas, when A = B **and** C = D, there is no possibility of the existence of translational isomerism.

X-ray Crystal Structures. The structures of some of the [2]catenanes were confirmed by obtaining single crystals of the tetrakis(hexafluorophosphate) salts which were suitable for X-ray crystallography. Some of the relevant distances and angles present in the solid-state structures of these catenanes are listed in Table 2.

In the solid state, {[2]-[1/5NPP36C10]-[BIPYBIPYEBIXY-CY]catenane][PF_6]$_4$} exists (Figure 4) as only one isomer. The macrocyclic polyether is threaded through the center of the extended cyclophane with the 1,5-dioxynaphthalene unit sandwiched between the π-electron deficient bipyridinium and bis-(pyridinium)ethylene units and with the hydroquinone ring positioned alongside its bipyridinium component. The molecule, which has crystallographic C_2 symmetry about an axis passing through the centers of the ethylenic double bond, the 1,5-dioxynaphthalene ring, the bipyridinium unit and the hydroquinone ring, is stabilized further by (i) edge-to-face interactions between the inside 1,5-dioxynaphthalene unit and the *p*-xylyl spacers of the cyclophane, and (ii) weak [C−H···O] hydrogen bonds between (a) one each of the *p*-xylyl hydrogen atoms and the central oxygen atoms of the polyether chains—the [H···O] distances are 2.49 Å and the [C−H···O] angles are 167°—and (b) one each of the α-CH pyridinium hydrogen atoms and the central oxygen atoms of the polyether chains—the [H···O] distances are 2.47 Å and the [C−H···O] angles are 169°. The incorporation of one extended viologen unit in place of the bipyridinium unit into one of the sides of the cyclophane increases significantly its overall dimensions (length from 10.3 to 11.2 Å and width from 6.8 to 7.2 Å) and alters its recognition properties. The center of the 1,5-dioxynaphthalene unit lies closer to the bipyridinium unit (3.50 Å) than to the double bond (3.72 Å) of the π-extended viologen component. In both naphthalene and hydroquinone regions in the macrocyclic polyether, the ring planes extend to include the immediately adjacent bismethyleneoxy groups, both chains adopting a

Scheme 5

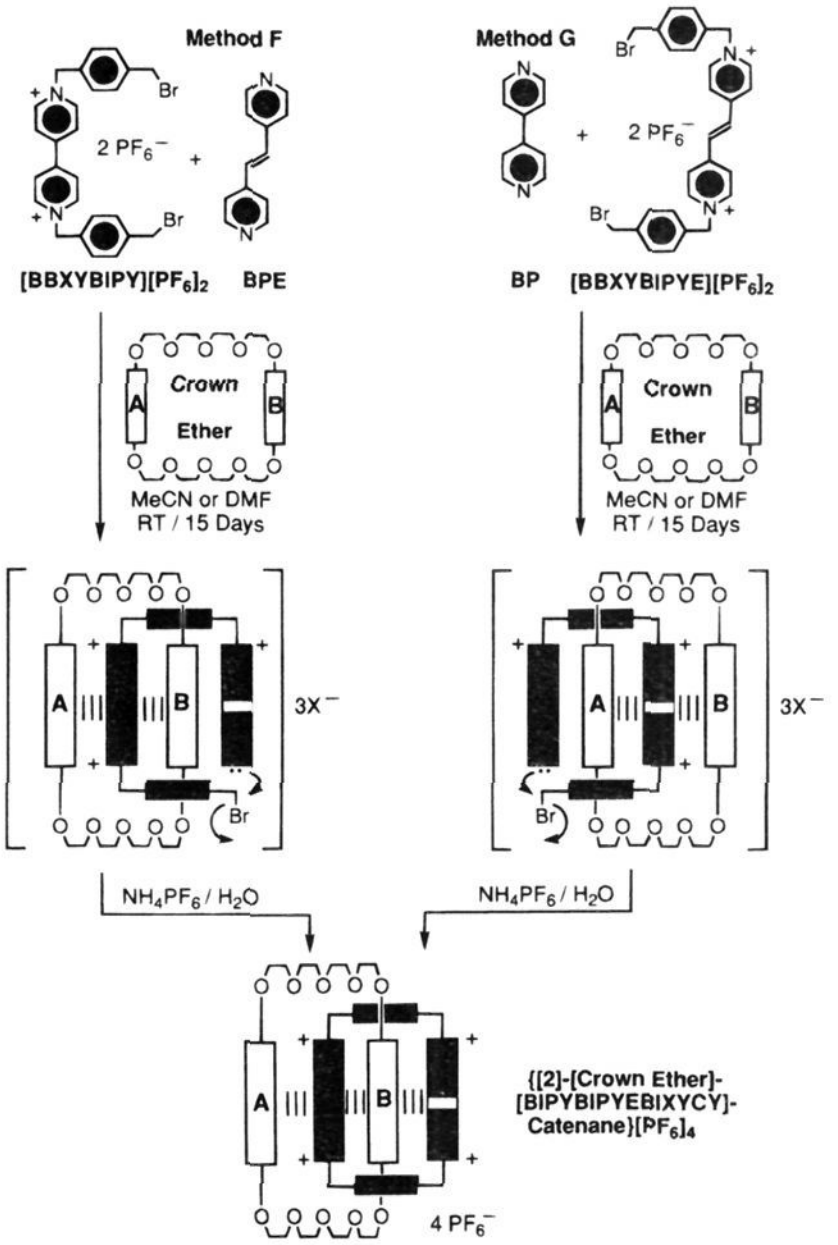

Scheme 6

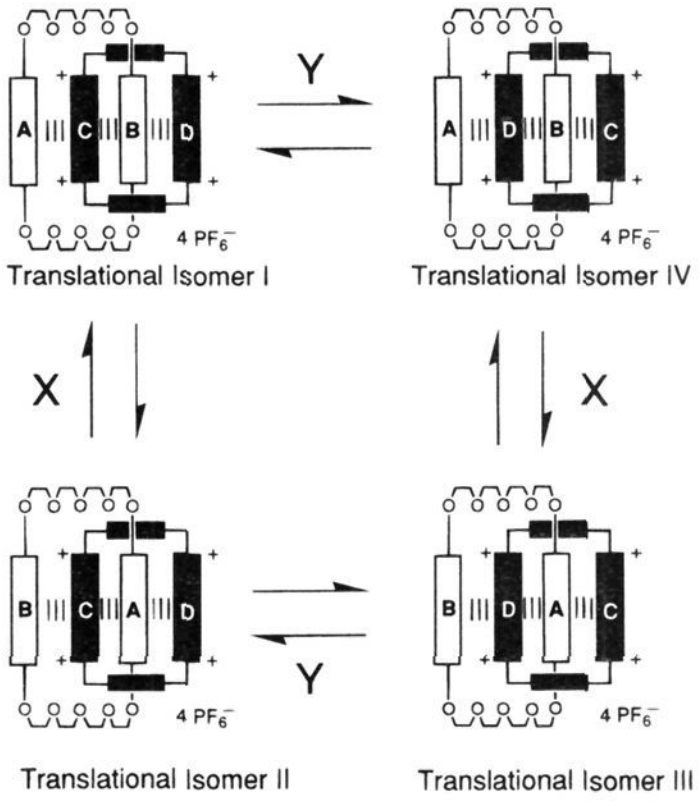

Table 2. Distances (Å) and Angles (deg) Characterizing the Molecular and Supramolecular Geometries of {[2]-[BPP34C10]-[BBIPYBIXYCY]catenane}$[PF_6]_4$,[2] {[2]-[1/5NPP36C10]-[BIPYBIPYEBIXYCY]catenane}$[PF_6]_4$, {[2]-[1/5DN38C10]-[BIPYBIPYEBIXYCY]catenane}$[PF_6]_4$, and {[2]-[1/5DN38C10]-[BBIPYEBIXYCY]catenane}$[PF_6]_4$

compound	unit[a]	θ^b	ψ^c	ϕ^d	τ^e	O(a)[f]	O(b)[f]	O(c)[f]	O(d)[f]	O(e)[f]	Z···Z[g]	Y···Y[h]	X···Y[i]	H···Y[j]	X–H···Y[k]
{[2]-[BPP34C10]-[BBIPYBIXYCY]catenane}$[PF_6]_4$	BIPY	6	24	10	47	3.98	4.42	4.16	3.34	3.88	6.8	10.3	5.1	2.8	166
	BIPY	6	26	14		4.25	4.51	4.00	4.20	4.57			5.2	2.9	157
{[2]-[1/5NPP36C10]-[BIPYBIPYEBIXYCY]catenane}$[PF_6]_4$	BIPY	10	14	10	35	4.69	4.99	4.15	3.65	4.07	7.2	11.2	5.6	2.99	143
	BIPYE	11	45	10		4.69	4.99	4.15	3.65	4.07			5.6	2.99	143
{[2]-[1/5DN38C10]-[BIPYBIPYEBIXYCY]catenane}$[PF_6]_4$	BIPY	5	14	11	49	4.12	4.36	3.82	3.26	3.92	7.1	11.3	5.5	2.8	153
	BIPYE	8	45	13		4.52	4.38	4.19	4.01	3.56			5.8	3.2	156
{[2]-[1/5DN38C10]-[BBIPYEBIXYCY]catenane}$[PF_6]_4$	BIPYE	3	27	16	49	4.66	4.21	4.19	4.50	6.19	7.0	12.6	6.0	3.4	153
	BIPYE	5	27	16		4.95	4.52	3.95	4.14	3.75			6.6	3.9	155

[a] When the indicated parameter corresponds to two different values, the value corresponding to the viologen occupying the inside cavity of the macrocyclic polyether in the [2]catenane is quoted first. [b] The twist angle θ is defined as the average of the moduli of the four C–C–C–C torsional angles about the central C–C bond within the bipyridinium residues, the anti torsional angles being reduced to 180°-α. [c] The bowing of the bipyridinium and bis(pyridinium)ethylene units is expressed by the angle ψ, subtended by the two N^+–CH_2 bonds emanating from the bipyridinium or bis(pyridinium)ethylene units. [d] The bowing of the *p*-xylene residues is expressed by the angle ϕ, subtended by the two C–CH_2 bonds emanating from the *p*-phenylene rings. [e] The twist angle τ is defined as the angle between the vector of the oxygen atoms adjacent to the aromatic residue inside the tetracationic cyclophane and the equatorial plane of the tetracation—as defined by the mean plane of the four "corner" methylene carbon atoms. [f] Distances from N^+ in the pyridinium ring encircled by the polyether chain. [g] Width of the tetracationic cyclophane defined as the distance between the centers of the bond(s) linking the pyridinium rings. [h] Length of the tetracationic cyclophane. [i] Centroid–centroid distance between the aromatic unit inside the tetracationic cyclophane and its *p*-xylyl spacer. [j] Distance between either the H-2/5 on the benzene or the H-4/8 on the naphthalene and the centers of their immediately adjacent *p*-xylyl rings. [k] Angle [C–H–centroid] at the H atom involved in the edge-to-face interaction.

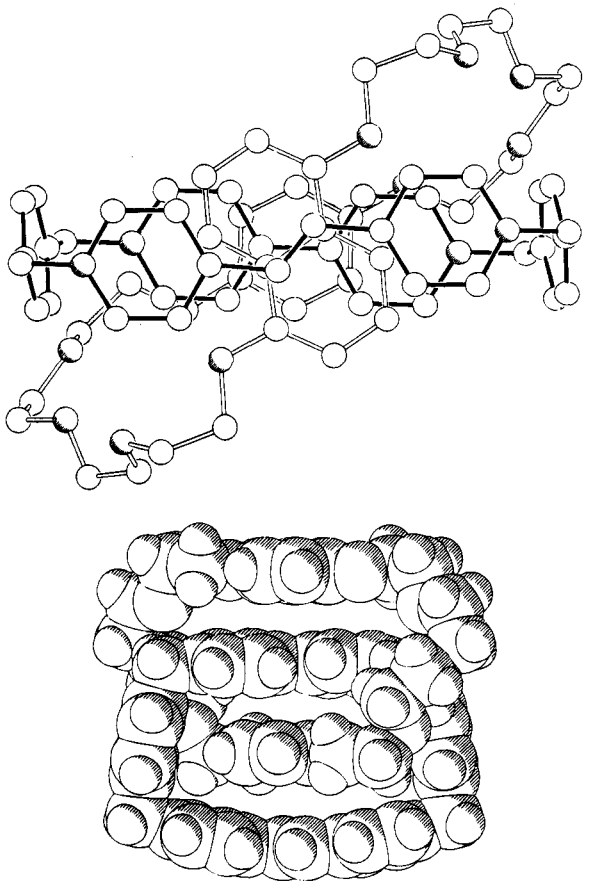

Figure 4. (a) Side-on view showing the stacking of the π-systems down the molecular C_2 axis and (b) space-filling representation in plan of {[2]-[1/5NPP36C10]-[BIPYBIPYEBIXYCY]catenane}$^{4+}$.

conformation with an anti geometry (Figure 4a). The distances of the oxygen atoms in the polyether chains to their encircled bipyridinium nitrogen atoms vary between 3.65 to 4.99 Å. The twist angles (θ) within the bipyridinium (10°) and the bis(pyridinium)ethylene (11°) units are larger than in the {[2]-[BPP34C10]-[BBIPYBIXYCY]catenane][$PF_6]_4$}. The bowing (ψ) of the viologen units (Figure 4b), with values of 14° for the bipyridinium unit and 45° for the bis(pyridinium)ethylene unit are, as expected, very different to those observed for the original [2]catenane,[2] while the bowing of the *p*-xylene residues (ϕ) remains very similar (10°). These distorsions are accompanied by changes in the angles associated with the methylene groups: they have values of 111° next to the bipyridinium unit and 108° next to the bis(pyridinium)ethylene unit. The substantial bowing (ψ = 45°) of the π-extended viologen unit is an accumulation of folds of ca. 19° for each pyridinium ring and an out-of-plane twist of 9° about the olefinic double bond. The [2]catenane forms (Figure 5) extended polar stacks in the crystals. An interesting feature of these stacks is that the double bond of the extended viologen component lies appreciably closer (3.42 Å) to the hydroquinone ring of an adjacent molecule than to the 1,5-dioxynaphthalene unit within the [2]catenane itself (3.72 Å) and indeed has a separation of less than the intramolecular distance (3.50 Å) between 1,5-dioxynaphthalene and the bipyridinium units.

The X-ray structure of {[2]-[1/5DN38C10]-[BIPYBIPYEBIXYCY]catenane]}$[PF_6]_4$ (Figure 6) shows one of the 1,5-dioxynaphthalene units to be positioned within the cyclophane sandwiched between the π-electron deficient bipyridinium and bis(pyridinium)ethylene units, with its $OC_{10}H_6O$ axis less steeply inclined to the cyclophane mean plane (τ = 49°, cf. 56° in {[2]-[1/5NPP36C10]-[BIPYBIPYEBIXYCY]catenane}$[PF_6]_4$). The

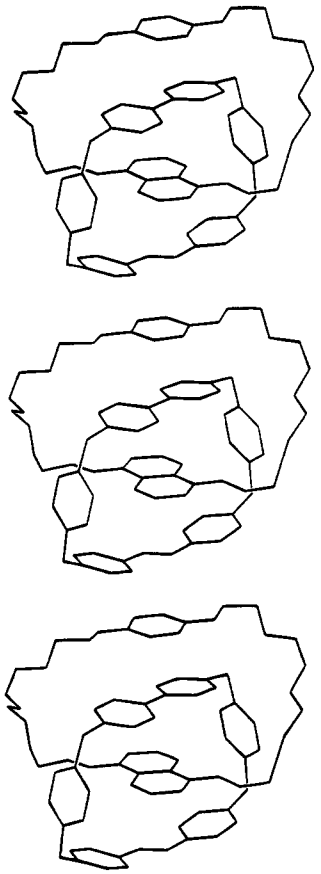

Figure 5. Part of the polar stack of π-donors and π-acceptors associated with {[2]-[1/5NPP36C10]-[BIPYBIPYEBIXYCY]catenane}$^{4+}$ in the crystal that extends along the crystallographic *b*-direction.

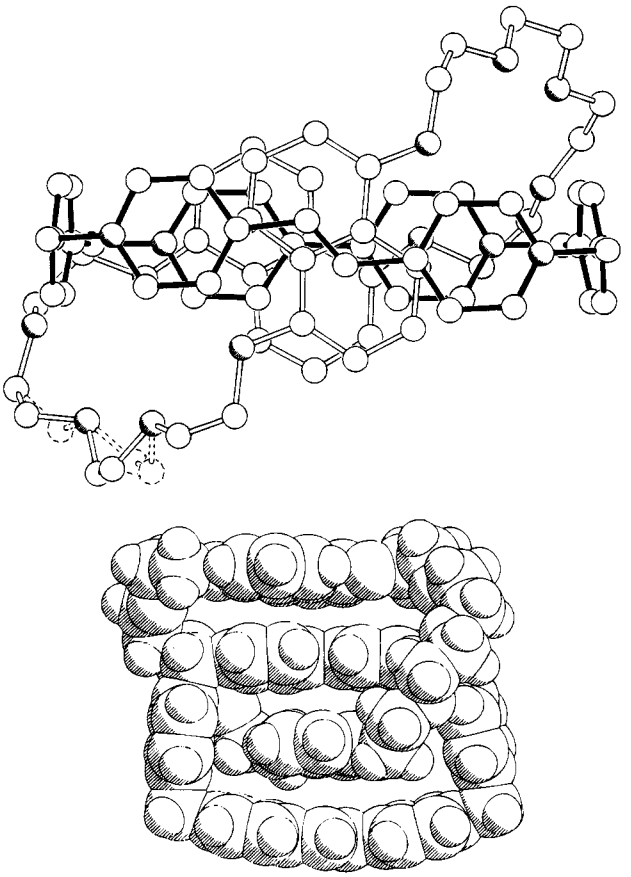

Figure 6. (a) Side-one view showing the stacking of the π-systems (the broken atoms and bonds correspond to an alternative conformation that is also present in the solid states) and (b) space-filling representation in plan of {[2]-[1/5DN38C10]-[BIPYBIPYEBIXYCY]catenane}$^{4+}$.

other 1,5-dioxyanphthalene unit lies alongside the bipyridinium unit of the cyclophane. Again, there are stabilizing (i) edge-to-face interactions between the inside 1,5-dioxynaphthalene and the *p*-xylyl spacers of the cyclophane and (ii) a series of weak [C−H···O] hydrogen bonds involving methylene, *p*-xylyl, and α-pyridinium hydrogen atoms and oxygen atoms within the polyether chains. The hydrogen bonding distances are in the range 2.29−2.52 Å. The shortest of these distances is between one of the α-CH bipyridinium hydrogen atoms and the central oxygen atom of one of the polyether chains. The other two hydrogen bonding interactions involve oxygen atoms which are diametrically opposite each other and two removed from the 1,5-dioxynaphthalene units and involve one methylene and one *p*-xylyl hydrogen atom in the cyclophane component. The [C−H···O] angles are in the range 146−155°. The dimensions of the cyclophane are essentially unchanged from those observed for the [2]catenane incorporating hydroquinone and 1,5-dioxynaphthalene units, there again being a substantial bend (ψ = 45°) in the π-extended viologen unit. The C_2 axis which characterizes the previous structure is no longer present as a result of the fact that the inside and "outside" 1,5-dioxynaphthalene residues are offset with respect to the encircled bipyridinium unit. However, they both have their $OC_{10}H_6O$ axes equally inclined to the mean plane of the cyclophane (Figure 6a). There is a retention of coplanarity between each of these residues and their associated methyleneoxy groups, both chains adopting conformations with anti geometries. There are noticeable small reductions (0.04 and 0.13 Å) in the separation between both the inside and alongside 1,5-dioxynaphthalene rings and the bipyridinium unit—3.46 and 3.41 Å, respectively—reflecting increased π-overlap between these ring systems. The [2]catenane packs (Figure 7) within the crystal to form polar stacks with a separation of 3.42 Å between the alongside 1,5-dioxynaphthalene in one molecule and the bis(pyridinium)ethylene unit of the next. This separation (3.68 Å) is once again significantly shorter than that observed between these two units within the [2]catenane molecule itself.

The solid-state structure of {[2]-[1/5DN38C10]-[BBIPYEBIXYCY]catenane}$[PF_6]_4$ reveals (Figure 8) the conventional threading of the crown ether through the center of the extended cyclophane with one of the 1,5-dioxynaphthalene units sandwiched between the pair of bis(pyridinium)ethylene units, with its $OC_{10}H_6O$ axis inclined by 49° to the mean plane of the cyclophane. The other 1,5-dioxynaphthalene unit is positioned alongside the inside bis(pyridinium)ethylene unit but is appreciably offset (Figure 8a) with respect to its inside counterpart so as to lie closer to one pyridinium ring than to the other. In addition to the normal $\pi-\pi$ stacking interactions, there are [C−H···O] hydrogen bonds involving one methylene and two α-CH pyridinium hydrogen atoms and oxygen atoms within the polyether chains. The [H···O] distance between the methylene hydrogen atom and the second oxygen atom relative to the alongside 1,5-dioxynaphthalene unit is 2.50 Å and the [C−H···O] angle is 158°. The α-CH pyridinium hydrogen atoms are involved in noticeably stronger hydrogen bonding interactions. One of these is a bifurcated hydrogen bond to the second and third oxygen atoms relative to the inside 1/5-dioxynaphthalene unit, having [H···O] distances of 2.49 and 2.35 Å, respectively, and associated [C−H···O] angles of 128 and 133°. There is a further very short [C−H···O] hydrogen bond ([H···O] = 2.29 Å; [C−H···O] angle = 158°) between the other diametrically opposite α-CH pyridinium hydrogen atom and the central oxygen atom of the polyether chain. The presence of two

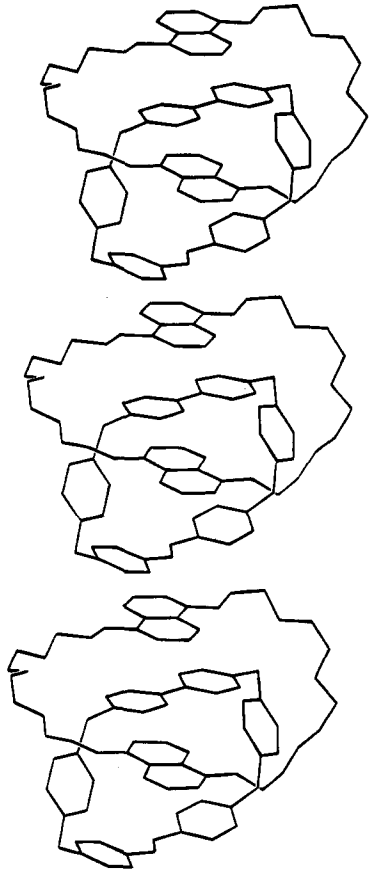

Figure 7. Part of the polar stack of π-donors and π-acceptors associated with {[2]-[1/5DN38C10]-[BIPYBIPYEBIXYCY]catenane}$^{4+}$ in the crystal that extends along the crystallographic *b*-direction.

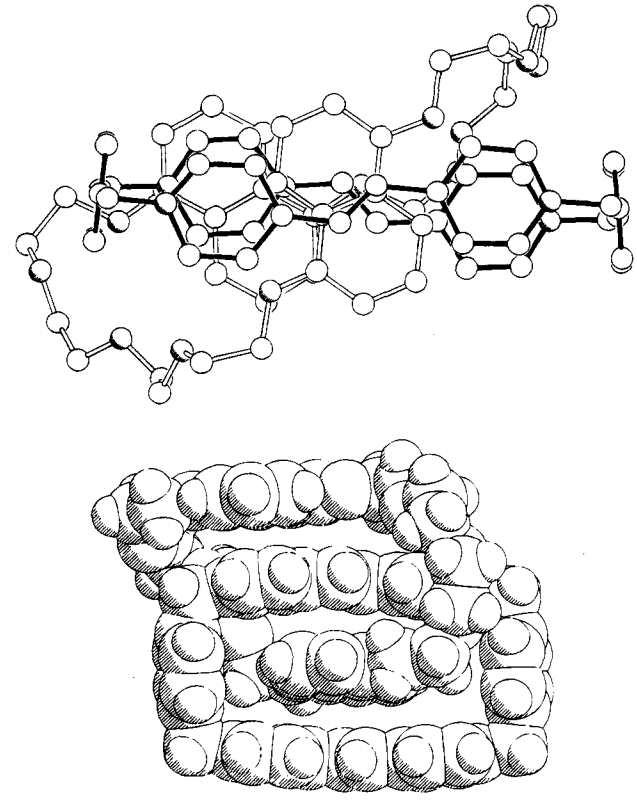

Figure 8. (a) Side-on view showing the stacking of the π systems and (b) space-filling representation in plan of {[2]-[1/5DN38C10]-[BBIPYEBIXYCY]catenane}$^{4+}$.

extended viologen units in the cyclophane produces a significant increase in its overall length (12.6 Å, cf. 11.2 Å in the previous two structures). As a consequence, the edge-to-face interactions between the inside 1,5-dioxynaphthalene unit and the two *p*-xylyl spacers of the cyclophane are reduced substantially, the [H···centroid] distances being 3.4 and 3.9 Å. The overall width of the cyclophane component remains essentially unchanged at 7.0 Å. The bending (ψ) of both bis(pyridinium)ethylene units is greatly reduced (27° for both units), whereas that for the two *p*-xylyl spacers is noticeably increased (ϕ = 16° for both spacers). The [2]catenane molecules pack, forming (Figure 9) polar stacks in the crystals. It is noticeable that there is a slight "stepping" of adjacent molecules, thus increasing the overlap between the alongside 1,5-dioxynaphthalene unit of one molecule and one of the alongside pyridinium rings of an extended viologen unit in another molecule in the stack. As observed previously with the other [2]catenanes, the $\pi-\pi$ separations between adjacent molecules (3.34 Å) are significantly shorter than those within the catenane itself, where the distances are 3.59 Å (alongside olefinic bond to inside 1,5-dioxynaphthalene), 3.45 Å (inside 1,5-dioxynaphthalene to inside olefinic bond), and 3.43 Å (inside pyridinium to alongside 1,5-dioxynaphthalene).

Mass Spectrometry. The results obtained using positive-ions FABMS are summarized in Table 3. Although some of the 1:1 complexes formed between BPP34C10, 1/5DN38C10, or 1/5NPP36C10 and substrates containing the bis(pyridinium)-ethylene unit have low K_a values (Table 4), it is usually possible to detect these complexes by FABMS, observing peaks corresponding to $[M - PF_6]^+$ and $[M - 2PF_6]^+$. Similar patterns, with losses of one and two counterions, are observed (Table 3) for the tetracationic cyclophanes. Although a 1:1 complex between [BIPYBIPYEBIXYCY][PF_6]$_4$ and 1/5BHEEN has been detected by FABMS, neither [BHEEB.BIPYBIPYEBIXYCY]-[PF_6]$_4$ nor the complexes between BHEEB or 1/5BHEEN with [BBIPYEBIXYCY][PF_6]$_4$ have been observed using this technique.

In all the cases, positive-ion FABMS of the [2]catenanes revealed (Table 3) peaks characteristic of the successive loss of one, two, and three PF_6^- counterions from the molecular ion. Peaks, corresponding to the loss of one and two PF_6^- counterions from the free cyclophane component of the [2]-catenanes, are also characteristic[14] of the fragmentations of the [2]catenane—in their cases, after loss of the neutral crown ether component.

Stability Constants. The K_a values have been evaluated[15] by titration, using a spectrophotometric method that relies on the appearance of a charge transfer band in the UV−visible spectrum of the 1:1 complex between systems containing π-electron rich and π-electron deficient aromatic units. Table 4 lists the stability constants (K_a values) and derived free energies of complexation ($-\Delta G°$ values) for the 1:1 complexes formed (Scheme 7) between BPP34C10 and [PQT][PF_6]$_2$,[2] [BMBIPYE][PF_6]$_2$, and [BBnBIPYE][PF_6]$_2$ in Me_2CO at 25 °C and for the 1:1 complexes formed (Scheme 8) between [BBI-PYBIXYCY][PF_6]$_4$,[2,16] and [BIPYBIPYEBIXYCY][PF_6]$_4$, and BHEEB and 1/5BHEEN, in MeCN at 25 °C. The data listed in Table 4 indicate that BPP34C10 binds the π-extended viologens [BMBIPYE][PF_6]$_2$ and [BBnBIPYE][PF_6]$_2$ more

(14) (a) Vetter, W.; Schill, G. *Tetrahedron* **1967**, *23*, 3079−3093. (b) Vetter, W.; Logemann, E.; Schill, G. *Org. Mass Spectrom.* **1977**, *12*, 351−369.

(15) Connors, K. A. In *Binding Constants*; Wiley Interscience: New York, 1987.

(16) A value of 5600 M^{-1} was obtained (ref 17) for the stability constant of the 1:1 complex, [1/5DN38C10·BBIPYBIXYCY][PF_6]$_4$; it corresponds to a $-\Delta G°$ value of 5.1 kcal mol^{-1}.

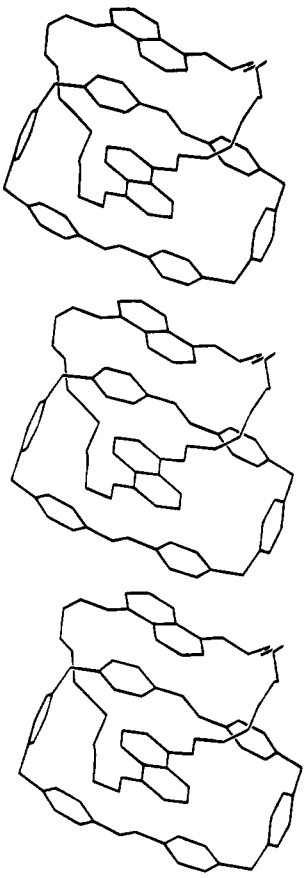

Figure 9. Part of the polar stack of π-donors and π-acceptors associated with {[2]-[1/5DN38C10]-[BBIPYEBIXYCY]catenane}$^{4+}$ in the crystal that extends along the crystallographic *b*-direction.

weakly than $[PQT][PF_6]_2$ in Me_2CO. The lower free energy of complexation for the π-extended viologen compounds is reflected in the lower chemical yields (Table 1) obtained during the self-assembly of [2]catenanes containing bis(pyridinium)-ethylene units and BPP34C10, i.e., the yields are lower than those observed during the self-assembly of the [2]catenane containing this macrocyclic polyether and bipyridinium units. However, there is not a direct correlation between the strengths of binding of compounds containing the bis(pyridinium)ethylene unit and the chemical yields of the [2]catenanes where this unit is present. This observation draws attention to the important role that other noncovalent bonding interactions play in the recognition processes that lead to the formation and stabilization of the interlocked molecules. Unfortunately, no accurate values for the binding of the π-extended viologen units with 1/5DN38C10 can be obtained on account of the relative insolubility of this macrocyclic polyether in solvents such as Me_2CO, MeCN, and DMF. The only evidence for the formation of stronger complexes with 1/5DN38C10 arises from the larger differences observed (Table 5) in the chemical shifts of the complexes with respect to their free components. However, the K_a values obtained for complex formation of [BIPYBIPYE-BIXYCY][PF_6]$_4$ with BHEEB and 1/5BHEEN indicate much stronger binding between 1,5-dioxynaphthalene rings and bis-(pyridinium)ethylene units, i.e., they are better "matching pairs" in terms of their mutual recognition. These experimental data draw attention to the relative importance of weak dispersive forces, between the π-electron rich and π-electron deficient units, and, more importantly, the need for complementarity between the π-overlapping surfaces of these units. They are reflected in the higher yields obtained for those [2]catenanes containing 1/5DN38C10 and bis(pyridinium)ethylene units and, more remarkably, by the much higher efficiency displayed by 1/5BHEEN in templating the formation of the tetracationic cyclophanes containing these π-extended viologen units.

^{1}H NMR Spectroscopy. The comparison (Table 5) between the chemical shifts of probe protons in a range of different 1:1 complexes provides a qualitative measure of the strengths of binding between the components of the complex. This information is relatively important in those situations where no additional information has been obtained from the determination of stability constants. The magnitudes of the $\Delta\delta$ values for the 1:1 complexes indicates their relatively weak nature. Although [BBnBIPYE][PF_6]$_2$ forms the strongest complexes with BPP34C10, 1/5DN38C10, and 1/5NPP36C10, in all cases they are weaker than those formed with $[PQT][PF_6]_2$ with the δ values for the olefinic protons in the π-extended viologen being the most affected. The strongest 1:1 complex is undoubtedly [BBXYBIPYE·1/5DN38C10][PF_6]$_2$, as evidenced (Table 5) by the magnitude of the shifts experienced by the protons in this complex, e.g., the olefinic protons in this complex are shielded by 1.04 ppm.

Table 6 lists the chemical shifts of [BBIPYEBIXYCY][PF_6]$_4$ and [BIPYBIPYEBIXYCY][PF_6]$_4$ and the 1:1 complexes of the latter with BHEEB and 1/5BHEEN. The low association constants (Table 4) for these complexes are a consequence of the larger dimensions of the cyclophanes. They are reflected in the relatively small changes in the chemical shifts of selected protons in the 1:1 complexes with BHEEB and 1/5BHEEN. Even in the stronger complex—namely [1/5BHEEN·BIPYBI-PYEBIXYCY][PF_6]$_4$—the $\Delta\delta$ values for both the cyclophane protons and the aromatic protons in the π-electron rich thread are deshielded only by about 0.10 ppm.

^{1}H NMR spectroscopy has been especially valuable for providing information about the nature of the translational isomerism in the [2]catenanes. Table 6 also lists ^{1}H NMR chemical shift data (δ values) as well as the chemical shift differences ($\Delta\delta$ values) for selected protons in these interlocked compounds with reference to the corresponding δ values arising from their free components. Again, the protons most affected ($\Delta\delta$ = −0.96 to −1.93 ppm) are the olefinic protons in the π-extended viologen unit. The aromatic protons in the macrocyclic polyether component experience large changes, particularly those that are oriented into the π-face of the paraphenylene spacers in the cyclophanes, as a consequence of T-type interactions—e.g., the H-4/8 protons on the naphthalene rings of 1/5DN38C10 experience a shielding of ca. 4.5 ppm.

All the new [2]catenanes exhibit temperature-dependent behavior in their ^{1}H NMR spectra. It originates from the two dynamic processes that occur in the [2]catenanes (Scheme 6). Table 7 summarizes the kinetic and thermodynamic parameters calculated[18] from the temperature-dependent ^{1}H NMR spectra recorded for the relevant [2]catenanes.

(17) Blower, M. Ph.D. Thesis, University of Birmingham, 1993.

(18) The kinetic and thermodynamic data were calculated using three procedures: (a) The *coalescence method*, where values for the rate constant k_c at the coalescence temperature (T_c) were calculated (Sutherland, I. O. *Annu. Rep. NMR Spectrosc.* **1971**, *4*, 71−235) from the approximate expression, $k_c = \pi(\Delta\nu)/(2)^{1/2}$, where $\Delta\nu$ is the chemical shift difference (in Hertz) between the coalescing signals in the absence of exchange. (b) The *exchange method*, where values of k were calculated (Sandström, J. *Dynamic NMR Spectroscopy*; Academic Press: London, 1982; Chapter 6) from the approximate expression $k = \pi(\Delta\nu)$, where $\Delta\nu$ is the difference (in Hertz) between the line width at a temperature T, where exchange of sites is taking place, and the line width in the absence of exchange. (c) In the case of a coalescing AB system, a *modified coalescence method* was used where values of k_c were calculated from the approximate expression $k_c = \pi[(\Delta\nu)^2 + J_{AB}^2]^{1/2}/(2)^{1/2}$ where $\Delta\nu$ is the difference (in Hertz) between ν_A and ν_B in the absence of exchange and J_{AB} is the coupling constant. The Eyring equation was subsequently employed to calculate $\Delta G^{\ddagger}_c$ or $\Delta G^{\ddagger}$ values at T_c or T, respectively.

Table 3. FABMS Data[a,b] for [BMBIPYEI[PF_6]$_2$, [BBnBIPYEI[PF_6]$_2$, [BBXYBIPYE][PF_6]$_2$, Their 1:1 Complexes with BPP34C10, 1/5DN38C10, and 1/5NPP36C10, the Tetracationic Cyclophanes [BBIPYEBIXYCY][PF_6]$_4$, [BIPYBIPYEBIXYCY][PF_6]$_4$, the Complex [1/5BHEEN·BIPYBIPYEBIXYCY][PF_6]$_4$, and the New [2]Catenanes

compound or complex	M[c]	M-PF_6	M-2PF_6	M-3PF_6	M-PF_6-CE[d]	M-2PF_6-CE[d]	M-3PF_6-CE[d]
[BMBIPYEI[PF_6]$_2$	(502)[e]	357	212				
[BPP34C10·BMBIPYE][PF_6]$_2$	(1038)[e]	893	748				
[1/5DN38C10·BMBIPYE][PF_6]$_2$	(1088)[e]	943	798				
[1/5NPP36C10·BMBIPYE][PF_6]$_2$	(1138)[e]	993	848				
[BBnBIPYEI[PF_6]$_2$	(654)[e]	509	364				
[BPP34C10·BBnBIPYEI[PF_6]$_2$	1190	1045	900				
[1/5DN38C10·BBnBIPYE][PF_6]$_2$	(1290)[e]	1163 (+NH_4^+)	1000 (+NH_4^+)				
[1/5NPP36C10·BBnBIPYE][PF_6]$_2$	(1476)[e]	1331	1186				
[BBXYBIPYE][PF_6]$_2$	(840)[e]	695	550				
[BPP34C10·BBXYBIPYE][PF_6]$_2$	(1376)[e]	1231 1073(-2Br)	1086				
[1/5DN38C10·BBXYBIPYEI[PF_6]$_2$	(1476)[e]	1331	1184				
[1/5NPP36C10·BBXYBIPYE][PF_6]$_2$	(1426)[e]	1281	1136				
[BBIPYEBIXYCYI[PF_6]$_4$	(1152)[e]	1007	862	717			
[BIPYBIPYEBIXYCY][PF_6]$_4$	1126	980	835	691			
[BHEEN·BIPYBIPYEBIXYCY][PF_6]$_4$	(1462)[e]	1317	1172				
{[2]-[BPP34C10]-[BBIPYEBIXYCY]catenane}	1688	1543	1398	1253	1007	862	(716)[e]
{[2]-[BPP34C10]-[BIPYBIPYEBIXYCY]catenane}	1662	1517	1372	1227	981	836	(691)[e]
{[2]-[1/5NPP36C10]-[BBIPYEBIXYCY]catenane}	(1738)[e]	1593	1448	1303	1007	862	716
{[2]-[1/5NPP36C10]-[BIPYBIPYEBIXYCY]catenane}	(1712)[e]	1567	1422	1277	(981)[e]	836	691
{[2]-[1/5DN38C10]-[BBIPYEBIXYCY]catenane}	1788	1643	1498	1353	1006	861	(716)[e]
{[2]-[1/5DN38C10]-[BIPYBIPYEBIXYCY]catenane}	1762	1617	1472	1327	981	836	691

[a] FABMS were obtained with a Kratos MS80RF mass spectrometer coupled to a DS90 system. The atom gun (Ion Tech Limited) was operated at 7 keV with a tube current of 2 mA. The primary beam of atoms was produced from research grade krypton. Samples were dissolved in a small amount of 3-nitrobenzyl alcohol that had been coated onto a stainless steel probe and spectra were recorded in the positive ion mode at a scan speed of 30 s per decade. [b] Only limited resolution of isotopic species was possible. [c] The molecular weight of the tetrakis(hexafluorophosphate). [d] CE symbolizes the macrocyclic polyether. [e] The numbers in parentheses refer to peaks that were not observed.

Table 4. Stability Constants (K_a) and Derived Free Energies of Complexation ($-\Delta G°$) for the 1:1 Complexes between [PQT][PF_6]$_2$, [BMBIPYEI[PF_6]$_2$, and [BBnBIPYEI[PF_6]$_2$, with BPP34C10 in Acetone at 25 °C and the 1:1 Complexes between the Tetracationic Cyclophanes [BBIPYBIXYCY][PF_6]$_4$ and [BIPYBIPYEBIXYCY][PF_6]$_4$ with BHEEB and 1/5BHEEN in Acetonitrile at 25 °C

1:1 complex	K_a (M^{-1})	$-\Delta G°$ (kcal mol^{-1})
[BPP34C10·PQT][PF_6]$_2$[a]	730[e]	3.9
[BPP34C10·BMBIPYEI[PF_6]$_2$	78 ± 6[e]	2.6 ± 0.1
[BPP34C10·BBnBIPYE][PF_6]$_3$	86 ± 3[f]	2.6 ± 0.1
[BHEEB·BBIPYBIXYCY][PF_6]$_4$[a]	2220 ± 240[e]	4.6 ± 0.1
[BHEEB·BIPYBIPYEBIXYCY][PF_6]$_4$	560 ± 32[d]	3.8 ± 0.1
[1/5BHEEN·BIPYBIPYEBIXYCY][PF_6]$_4$	1459 ± 37[e]	4.3 ± 0.1

[a] Determined by spectrophotometric titration at λ_{max} = 435 nm. [b] Determined by spectrophotometric titration at λ_{max} = 424 nm. [c] Determined by spectrophotometric titration at λ_{max} = 467 nm. [d] Determined by spectrophotometric titration at λ_{max} = 438 nm.

Scheme 7

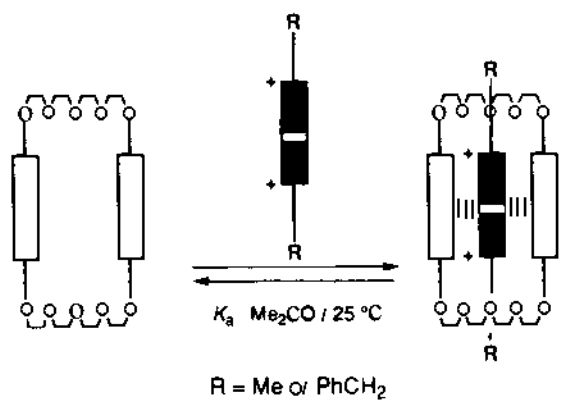

The ^{1}H NMR spectrum of {[2]-[BPP34C10]-[BIPYBIPYEBIXYCY]catenane}[PF_6]$_4$, recorded in CD_3CN at room temperature shows that the protons corresponding to the inside and alongside hydroquinone rings in BPP34C10 resonate as a *broad* signal centered on ca. δ 5.0, reflecting a fast equilibration for process X, probably as a result of the larger size of cyclophane and the somewhat reduced $\pi-\pi$ stacking interaction associated

Scheme 8

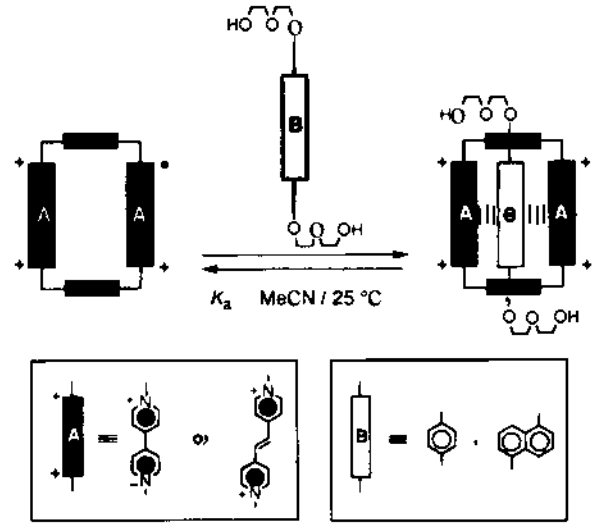

with its π-extended viologen unit. The coalescence of these signals above room temperature allows a $\Delta G_c^{\ddagger}$ value of 13.1 kcal mol^{-1} to be obtained (Table 7) for process X. Figure 10a shows the ^{1}H NMR spectrum of the same [2]catenane recorded in CD_3CN at +40 °C, while Figure 10b shows the spectrum at −20 °C, exhibiting the limiting separation of the chemical shifts for the inside and alongside aromatic protons of BPP34C10 in the [2]catenane. Also, in this [2]catenane, once process Y has been frozen out on the ^{1}H NMR time scale, two translational isomers are possible. The different attractions of the viologen and π-extended viologen units for the π-electron rich hydroquinone rings manifest themselves in a much higher preference for BPP34C10 encircling the viologen unit at low temperatures in CD_3COCD_3, the ^{1}H NMR spectrum (Figure 10c) of this [2]-catenane at +20 °C, with two broad signals at δ 4.40 and 6.22 corresponding respectively to the inside and alongside aromatic protons of the crown ether. The two doublets associated with the β-pyridinium protons and two singlets for the CH_2N^+ protons reflect the presence of two different viologen units in the molecule. At −60 °C, there are two major sets of signals for each type of proton in the cyclophane, indicating that once

Table 5. ^{1}H NMR Chemical Shift Data for the Macrocyclic Polyethers [δ Values ($\Delta\delta$ Values)][a] BPP34C10, 1/5DN38C10, and 1/5NPP36C10, Compounds Containing Bis(pyridinium)ethylene Units and Their 1:1 Complexes in CD_3CN at Ambient Temperature

	dicationic component				macrocyclic polyether (ArH)				
compound or complex	α-CH	β-CH	−CH=CH−[b]	C_6H_4	CH_2N^+	H-4/8	H-3/7	H-2/6	OC_6H_4O
$[BMBIPYE][PF_6]_2$	8.62	8.15	7.82		4.29[c]				
$[BBnBIPYE][PF_6]_2$	8.73	8.15	7.81	7.48[d]	5.70				
$[BBXYBIPYE][PF_6]_2$	8.73	8.15	7.81	7.43/7.53[e]	5.69				
BPP34C10									6.73
$[BPP34C10\cdot BMBIPYE][PF_6]_2$	8.62	8.06	7.64		4.29[c]				6.58
	(0.0)	(−0.09)	(−0.18)		(0.0)				(−0.15)
$[BPP34C10\cdot BBnBIPYE][PF_6]_2$	8.75	7.99	7.49	7.49	5.70				6.61
	(+0.02)	(−0.16)	(−0.32)	(+0.01)[d]	(0.0)				(−0.12)
$[BPP34C10\cdot BBXYBIPYE][PF_6]_2$	8.75	8.06	7.61	7.44/7.55[e]	5.69				6.50
	(+0.02)	(−0.09)	(−0.20)	(+0.01/+0.02)	(0.0)				(−0.23)
1/5DN38C10						7.70	7.21	6.62	
$[1/5DN38C10\cdot BMBIPYE][PF_6]_2$	8.60	8.00	7.52		4.29[c]	7.47	7.12	6.40	
	(−0.02)	(−0.15)	(−0.30)		(0.0)	(−0.23)	(−0.09)	(−0.22)	
$[1/5DN38C10\cdot BBnBIPYE][PF_6]_2$	8.73	7.76	7.05	7.52[d]	5.70	7.42	7.08	6.36	
	(0.0)	(−0.39)	(−0.76)	(+0.04)	(0.0)	(−0.28)	(−0.13)	(−0.26)	
$[1/5DN38C10\cdot BBXYBIPYE][PF_6]_2$	8.73	7.52	6.77	7.53/7.58[e]	5.69	7.53	7.13	6.44	
	(0.0)	(−0.63)	(−1.04)	(+0.10/+0.05)	(−0.01)	(−0.17)	(−0.08)	(−0.18)	
1/5NPP36C10						7.79	7.35	6.66	6.50
$[1/5NPP36C10\cdot BMBIPYE][PF_6]_2$	8.60	8.00	7.53		4.29[c]	7.72	7.31	6.79	6.45
	(−0.02)	(−0.15)	(−0.29)		(0.0)	(−0.07)	(−0.04)	(+0.13)	(−0.05)
$[1/5NPP36C10\cdot BBnBIPYE][PF_6]_2$	8.74	7.88	7.24	7.50[d]	5.70	7.66	7.29	6.71	6.36
	(+0.01)	(−0.27)	(−0.57)	(+0.01)	(0.0)	(−0.13)	(−0.06)	(+0.05)	(−0.14)
$[1/5NPP36C10\cdot BBXYBIPYE][PF_6]_2$	8.73	7.99	7.49	7.46/7.55[e]	5.69	7.70	7.29	6.55	6.40
	(+0.01)	(−0.16)	(−0.32)	(+0.03/+0.02)	(0.0)	(−0.09)	(−0.06)	(−0.11)	(−0.10)

[a] The $\Delta\delta$ values indicated in parentheses under the respective δ values relate to the chemical shift changes experienced by probe protons in both the substrates and the receptors on 1:1 complexation. [b] δ and $\Delta\delta$ values corresponding to the protons of the olefinic double bond. [c] δ and $\Delta\delta$ values for NCH_3^+. [d] δ and $\Delta\delta$ values for C_6H_5. [e] AB system.

Scheme 9

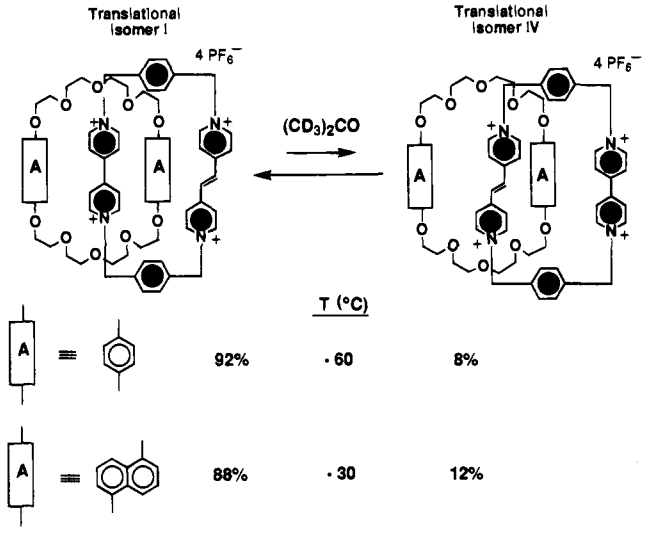

the process Y has been "frozen out", there is one isomer populated predominantly in solution—the one in which the bipyridinium unit occupies the inside position of the crown ether. The presence of a minor isomer was proved by performing a saturation transfer experiment at −50 °C. Irradiation of the low intensity signal at δ 6.60 indicated exchange with the peak at δ 7.16, establishing that these are resonances for the olefinic protons in the inside and alongside positions, respectively. The integration at −60 °C of these two signals for the olefinic protons in the ^{1}H NMR spectrum (Figure 10d) gives a ratio of 8:92 in favor of the isomer in which the bis(pyridinium)ethylene unit occupies the alongside position (translational isomer I in Scheme 9). Measurement of the broadening of the peaks corresponding to the olefinic protons allowed the calculation of $\Delta G^{\ddagger}$ (11.1 kcal mol^{-1}) for the process Y (Table 7). It is also noticeable that in the ^{1}H NMR spectrum at −60 °C, only one peak for the alongside hydroquinone ring protons can be observed at δ 6.17. The peak for the inside hydroquinone ring protons is not detectable because of its broadness, probably as a consequence of a third dynamic process of lower activation energy occurring in the [2]catenane.[19]

In the case of {[2]-[BPP34C10]-[BBIPYEBIXYCY]catenane}-$[PF_6]_4$, both processes (X and Y) are degenerate ones and both are fast on the ^{1}H NMR time scale at room temperature. The broad signal for the hydroquinone ring protons centered on δ 5.63 in the ^{1}H NMR spectrum recorded in CD_3COCD_3 at +47 °C (Figure 11a) separates out into two equal intensity signals resonating at δ 4.81 and 6.32 at −28 °C (Figure 11b). On the other hand, the temperature dependent behavior associated with process Y was accompanied by changes in the ^{1}H NMR spectrum for signals associated with *N*-methylene, α-CH bipyridinium, and olefinic protons in the cyclophane component of the [2]catenane. These changes are reflected in the appearance of two sets of signals for all the different protons corresponding to the tetracationic cyclophane, indicating the difference in the chemical shift induced by the inside and alongside environments in the charged macrocycle. For instance, at −60 °C (Figure 11c), the protons on the olefinic double bond appear as two singlets of equal intensity at δ 6.74 and δ 7.29, respectively, for the inside and alongside π-extended viologen units. The coalescence method was used in all the cases and values for $\Delta G_c^{\ddagger}$ were obtained (Table 7) for both these processes. Again, at low temperatures, the aromatic protons corresponding to the inside hydroquinone ring experience broadening, indicating the onset of a third dynamic process.[19]

The ^{1}H NMR spectra of the {[2]-[1/5DN38C10]-[BBIPYEBIXYCY]catenane}$[PF_6]_4$ at room temperature in both CD_3COCD_3 and CD_3CN are very broad as a consequence of site exchanges for process X which are fast on the NMR time scale.

(19) A third dynamic process (rocking) has been identified in some [2]-catenanes. It involves the protons of the macrocyclic polyether, that exchange between a position pointing toward the phenylene spacer and a position exterior to the cyclophane. See: Ashton, P. R.; Preece, J. A.; Stoddart, J. F.; Tolley, M. S.; White, A. J. P.; Williams, D. J. *Synthesis* **1994**, 1344−1352.

Table 6. ^{1}H NMR Chemical Shift Data [δ Values ($\Delta\delta$ Values)][a] for the Aromatic Threads BHEEB, BHEEN, the Tetracationic Cyclophanes [BBIPYEBIXYCY][PF_6]$_4$, [BIPYBIPYEBIXYCY][PF_6]$_4$, their 1:1 Complexes, and the [2]Catenanes in CD_3CN at Ambient Temperature

		tetracationic component						macrocyclic polyether (ArH)			
compound or complex		α-CH	β-CH	-CH=CH-[b]	C_6H_4-	CH_2N^+		H-4/8	H-3/7	H-2/6	OC_6H_4O
[BBIPYEBIXYCY][PF_6]$_4$		8.75	7.98	7.57	7.59	5.64					
[BIPYBIPYEBIXYCY][PF_6]$_4$	BIPY	8.73	8.18		7.56	5.73					
	BIPYE	8.95	8.39	7.83	7.56	5.84					
BHEEB											6.86
[BHEEB·BIPYBIPYEBIXYCY][PF_6]$_4$	BIPY	8.72	8.19		7.57	5.72					6.82
		(−0.01)	(+0.01)		(+0.01)	(−0.01)					(−0.04)
	BIPYE	8.96	8.40	7.82	7.57	5.84					
		(+0.01)	(+0.01)	(−0.01)	(+0.01)	(0.0)					
1/5BHEEN								7.82	7.40	6.97	
[1/5BHEEN·BIPYBIPYEBIXYCY][PF_6]$_4$	BIPY	8.86	8.30		7.68	5.85		7.88	7.49	7.06	
		(+0.13)	(+0.12)		(+0.12)	(+0.12)		(+0.06)	(+0.09)	(+0.09)	
	BIPYE	9.08	8.50	7.93	7.68	5.96					
		(+0.13)	(+0.11)	(+0.10)	(+0.12)	(+0.12)					
{[2]-[BPP34C10]-[BBIPYEBIXYCY]catenane}		8.72	7.49	6.61	7.68	5.60					5.50
		(−0.03)	(−0.49)	(−0.96)	(+0.09)	(−0.04)					(−1.23)
{[2]-[BPP34C10]-[BIPYBIPYEBIXYCY]catenane}	BIPY	8.71	7.53		7.68	5.70	inside				5.15
		(−0.02)	(−0.65)		(+0.12)	(−0.03)					(−1.58)
	BIPYE	8.88	7.59	6.63	7.79	5.64	alongside				5.70
		(−0.07)	(−0.80)	(−1.20)	(+0.23)	(−0.20)					(−1.03)
{[2]-[1/5DN38C10]-[BBIPYEBIXYCY]catenane}		8.66	7.00	5.68	7.79	5.62	inside	4.12	5.04	6.16	
		(−0.09)	(0.98)	(−1.89)	(+0.20)	(−0.02)		(−3.58)	(−2.17)	(−0.46)	
							alongside	7.29	7.12	6.28	
								(−0.41)	(−0.09)	(−0.34)	
{[2]-[1/5DN38C10]-[BIPYBIPYEBIXYCY]catenane}	BIPY	8.70	6.70		7.86	5.58/5.92	inside	3.25	5.48	6.15	
		(−0.03)	(−1.48)		(+0.30)	(−0.15/+0.19)		(−4.45)	(−1.73)	(−0.47)	
	BIPYE	8.70	7.22	6.01	7.94	5.68	alongside	7.20	7.10	6.37	
		(−0.25)	(−1.17)	(−1.82)	(+0.38)	(−0.16)		(−0.50)	(−0.11)	(−0.25)	
{[2]-[1/5NPP36C10]-[BBIPYEBIXYCY]catenane}		8.75	7.88	5.64	7.85	5.63		6.30	5.67	4.22	6.15
		(0.0)	(−0.10)	(−1.93)	(+0.26)	(0.01)		(−1.49)	(−1.68)	(−2.44)	(−0.35)
{[2]-[1/5NPP36C10]-[BIPYBIPYEBIXYCY]catenane}[c]	BIPY	8.73	7.88		7.06	5.61/5.80	inside	6.26	5.57	3.37	
		(0.0)	(−0.30)		(−0.50)	(−0.12/+0.07)		(−1.53)	(−1.78)	(−3.29)	
	BIPYE	8.73	7.98	6.10	7.27	5.68	alongside				6.09
		(−0.22	(−0.41)	(−1.73)	(−0.29)	(−0.16)					(−0.41)

[a] The $\Delta\delta$ values indicated in parentheses under the respective δ values relate to the chemical shift changes experienced by probe protons in both the substrates and the receptors on 1:1 complexation or in the [2]catenanes. [b] δ and $\Delta\delta$ corresponding to the olefinic protons. [c] Only δ and $\Delta\delta$ for the major translational isomer are indicated.

Table 7. Kinetic and Thermodynamic Parameters Obtained from the Temperature-Dependent 400 MHz ^{1}H NMR Spectra Recorded on the [2]Catenanes Incorporating π-Extended Viologen Units

[2]catenane	probe protons	solvent	$\Delta\nu^a$ (Hz) $(\Delta\nu)^b$	k_c^a (s^{-1}) $(k)^b$	T_c^a (K) $(T)^b$	$\Delta G_c^{\ddagger\,a}$ (kcal mol^{-1}) $(\Delta G^{\ddagger})^b$	process[c]
{[2]-[BPP34C10]-[BIPYBIPYEBIXYCY]catenane}	OC_6H_4O	CD_3CN	832	1848	300	13.1	X
	$-CH=CH-$	$(CD_3)_2CO$	(215)	(675)	(245)	11.1	Y
{[2]-[BPP34C10]-[BBIPYEBIXYCY]catenane}	OC_6H_4O	$(CD_3)_2CO$	612	1360	285	12.5	X
	$-CH$	$(CD_3)_2CO$	48	107	226	11.0	Y
	$-CH=CH-$	$(CD_3)_2CO$	220	489	245	11.2	Y
	CH_2N^+	$(CD_3)_2CO$	44	98	226	11.0	Y
{[2]-[1/5DN38C10]-[BBIPYEBIXYCY]catenane}	H-2/6 $(OC_{10}H_6O)$	CD_3CN	76	169	300	14.5	X
	H-2/6 $(OC_{10}H_6O)$	$(CD_3)_2CO$	32	71	301	15.1	X
	C_6H_4	$(CD_3)_2CO$	27[d]	74[d]	236[d]	11.7[d]	Y
{[2]-[1/5DN38C10]-[BIPYBIPYEBIXYCY]catenane}	H-2/6 $(OC_{10}H_6O)$	$(CD_3)_2SO$	129	287	345	16.4	X
	H-2/6 $(OC_{10}H_6O)$	CD_3CN	76	169	345	16.8	X

[a] Data not in parentheses relates to the *coalescence method* (see ref 18a). [b] Data in parentheses relates to the *exchange method* (see ref 18b). [c] When different translational isomers exist, the data refer to the conversion of the major isomer into the minor one. [d] Data refers to the coalescence of an AB system (see ref 18c).

Scheme 10

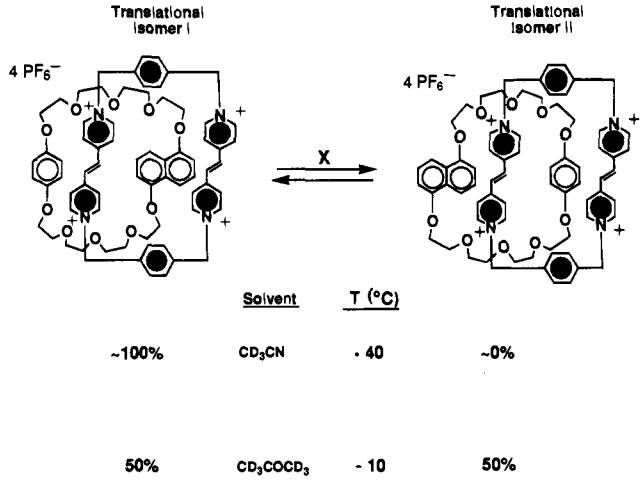

The only signals that can be observed for the naphthalene units in the ^{1}H NMR spectrum at temperatures above room temperature (Figure 12a) are those corresponding to the averaged signal for the H-2/6 protons. However, on cooling down to 0 °C (Figure 12b), two sets of signals emerge, corresponding to the aromatic protons on the naphthalene rings occupying the inside and alongside positions of the tetracationic cyclophane. The coalescence of the resonance for H-2/6 on the naphthalene ring at +28 °C allows the calculation of a $\Delta G_c^{\ddagger}$ value for this process, both in CD_3COCD_3 and CD_3CN (Table 7). The assignment of all the signals corresponding to this [2]catenane at 0 °C was achieved by performing a 2D-COSY experiment. Saturation transfer experiments led to the confirmation of exchange between the two sets of signals associated with all the aromatic protons of the macrocyclic polyether. The energy barrier (Table 7) associated with the second process (Y) was obtained from the coalescence of the signals corresponding to the *p*-phenylene rings above −40 °C (Figure 12c).

The dynamic behavior of {[2]-[1/5DN38C10]-[BIPYBIPYEBIXYCY]catenane}$[PF_6]_4$, has been studied in three different solvents. In CD_3SOCD_3 at room temperature, the process X is already frozen out, leading to the observation of two sets of signals for the aromatic protons of the inside and alongside naphthalene units. A saturation transfer experiment at +37 °C, involving irradiation of the doublet at δ 6.15, proved that this signal is in exchange with the doublet at δ 6.22, associated with the inside and alongside H-2/6 protons, respectively, of the naphthalene units. Coalescence of these signals at +72 °C allowed calculation of the energy for process X (Table 7). The $\Delta G^{\ddagger}$ value for this process X was also obtained in CD_3CN as solvent, following a similar protocol to that used in CD_3SOCD_3. In CD_3COCD_3, all the resonances arising from the [2]catenane were identified at different temperatures, by using (i) 2D-COSY experiments and (ii) saturation transfer experiments for those protons undergoing site exchange. At room temperature (Figure 13a), the resonances for all the protons in the macrocyclic polyether are sharp as a result of a slow process X on the ^{1}H NMR time scale. Again, two sets of signals distinguish the inside and alongside naphthalene units. At this temperature, the only sharp signals for the cyclophane are those corresponding to the methylene protons that appear as two AB systems as a consequence of the C_2 symmetrical naphthalene unit being positioned inside its cavity. A major feature of the [2]catenane, with its cyclophane incorporating one bipyridinium and one *trans*-bis(pyridinium)ethylene unit, is that two translational isomers are possible, with a much higher preference for the isomer wherein the 1/5DN38C10 macrocycle encircles the viologen unit at low temperatures in CD_3COCD_3. Thus, at −30 °C, integration of the signals at δ 6.21 and δ 6.83 for the olefinic protons in the ^{1}H NMR spectrum gives a ratio of 12:88 in favor of the isomer in which the bis(pyridinium)ethylene unit occupies the alongside position (Scheme 9). In Figure 13b, an expansion of the 5−10 ppm region of the ^{1}H NMR spectrum of this [2]-catenane at −45 °C shows the major isomer present in solution, once both processes (X and Y) have been frozen out on the ^{1}H NMR time scale.

Process X is also fast on the ^{1}H NMR time scale at room temperature in CD_3CN in the case of the {[2]-[1/5NPP36C10]-[BBIPYEBIXYCY]catenane}$[PF_6]_4$. The signals observed for the aromatic protons of the neutral macrocycle represent averaged values for the inside and alongside occupations by the hydroquinone and naphthalene rings. Hence, at −40 °C, once the process X has been frozen out, two translational isomers are possible. However, the catenane has a total preference for the one (translational isomer I in Scheme 10) where the naphthalene ring occupies the inside position of the tetracationic cyclophane. This situation is indicated by the presence of only one set of signals for the aromatic protons corresponding to 1/5NPP36C10 in the [2]catenane as well as by the chemical shifts of these protons, whose values are

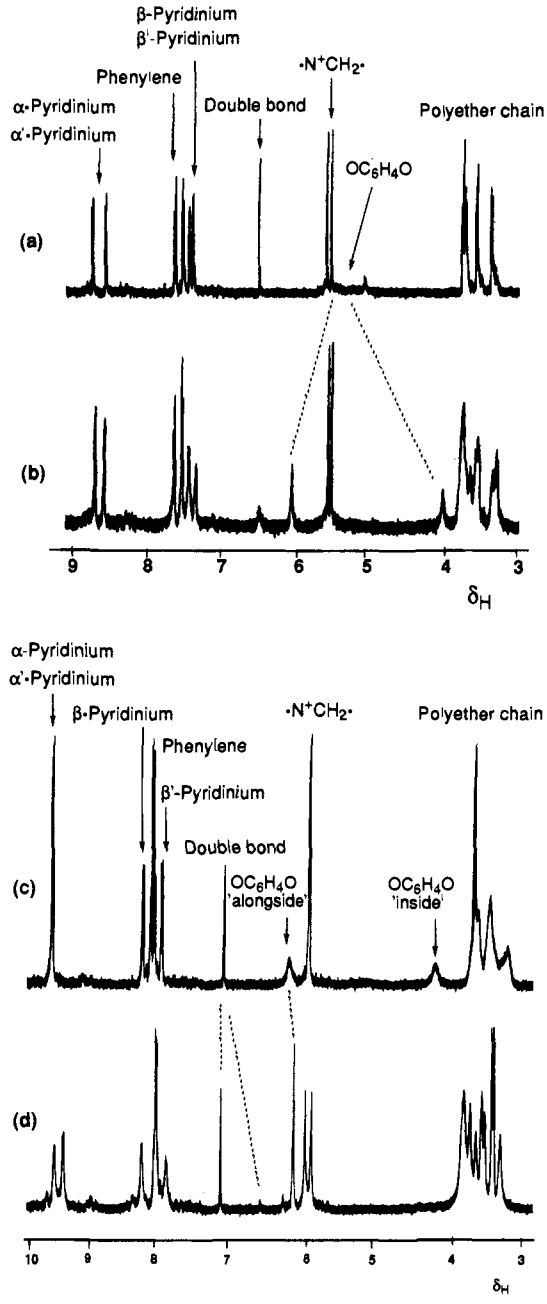

Figure 10. ^{1}H NMR spectra of {[2]-[BPP34C10]-[BIPYBIPYEBIXYCY]catenane}-$[PF_6]_4$, (a) in CD_3CN, at +40 °C, (b) in CD_3CN at −20 °C, (c) in CD_3COCD_3 at +20 °C, and (d) in CD_3COCD_3 at −60 °C.

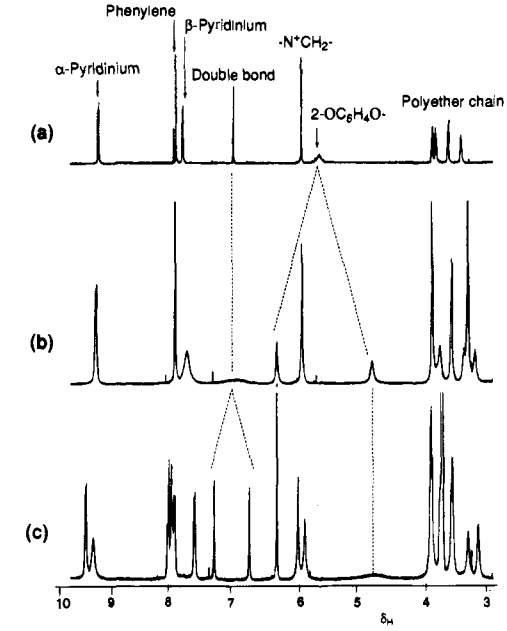

Figure 11. ^{1}H NMR spectra of {[2]-[BPP34C10]-[BBIPYEBIXYCY]-catenane}$[PF_6]_4$ in CD_3COCD_3 (a) at +47 °C, (b) at −28 °C, and (c) at −60 °C.

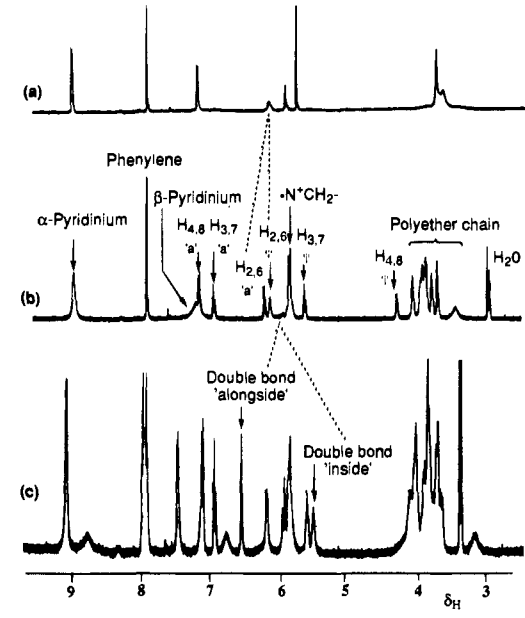

Figure 12. ^{1}H NMR spectra of {[2]-[1/5DN38C10]-[BBIPYEBIXYCY]-catenane}$[PF_6]_4$ in CD_3COCD_3 (a) at +40 °C, (b) at 0 °C, and (c) at −40 °C. For the aromatic protons on the naphthalene ring, "a" stands for alongside and "i" for inside.

comparable to those observed for a hydroquinone ring alongside and a naphthalene unit inside in the symmetric [2]catenanes. In CD_3COCD_3, the ^{1}H NMR spectrum at +45 °C (Figure 14a) exhibits broad signals for the aromatic protons of the neutral macrocycle as a result of the fast equilibration of the two possible (I and II) translational isomers. However, at −10 °C, where their interconversion is slow on the ^{1}H NMR time scale, the averaged resonances for the aromatic protons of the hydroquinone ring and naphthalene residues separate out into two sets of signals (Figure 14b). Integration of the peaks corresponding to the inside/alongside hydroquinone ring and for the inside/alongside naphthalene ring gives a ratio of 50:50 for the occupancies of the translational isomers (I and II in Scheme 10). The solvent dependency of this catenane can be explained in terms of the role that the larger π surface of the naphthalene unit plays as a shield for the positive charges on the cyclophane in apolar solvents[9a] and becomes an important consideration in the construction of controllable [2]catenanes.

The [2]catenane {[2]-[1/5NPP36C10]-[BIPYBIPYEBIXYCY]-catenane}$[PF_6]_4$ consists of four different $\pi-\pi$ interacting systems, and therefore an equilibrium (Scheme 6) between four different translational isomers is possible. However, the differential nature of the recognition processes between its components imbue the system with a high level of structural selectivity. The process X involves the equilibration of the π-electron rich hydroquinone ring and 1,5-dioxynaphthalene unit between inside and alongside environments with respect to the interlocked cyclophane. Both in CD_3COCD_3 and CD_3CN solutions, ^{1}H NMR spectroscopic studies indicate that the circumrotation of 1/5NPP36C10 through the cyclophane is already slow on the ^{1}H NMR time scale at room temperature, i.e., the process X is frozen out and the aromatic π-electron donors (hydroquinone and 1,5-dioxynaphthalene) do not inter-

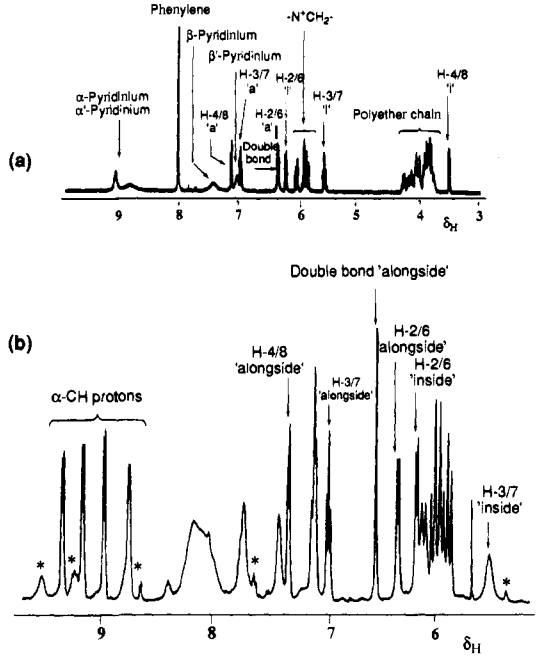

Figure 13. ^{1}H NMR spectra of {[2]-[1/5DN38C10]-[BIPYBIPYEBIXYCY]catenane}$[PF_6]_4$ in CD_3COCD_3 (a) at +25 °C and (b) at −45 °C. The asterisks indicate signals for the minor isomer.

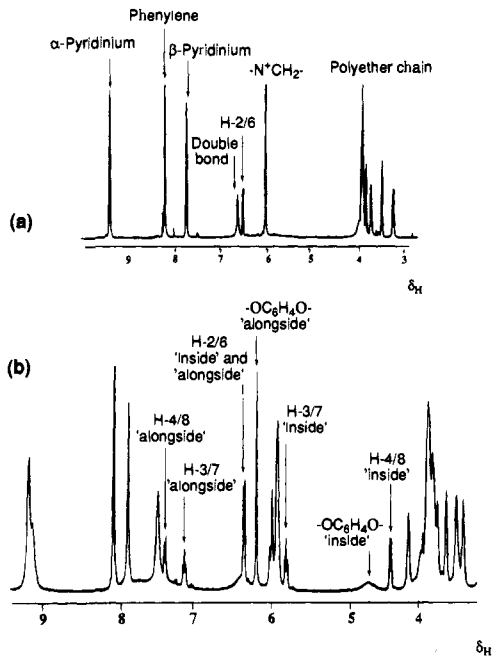

Figure 14. ^{1}H NMR spectra of {[2]-[1/5NPP36C10]-[BBIPYEBIXYCY]-catenane}$[PF_6]_4$ in CD_3COCD_3 (a) at +45 °C and (b) at −10 °C.

change their positions. The equilibrium is predominantly in favor of the translational isomers I and IV, where the 1,5-dioxynaphthalene unit (B in Scheme 6) occupies the inside position of the cyclophane. This conclusion may be drawn from the fact that the ^{1}H NMR spectrum at room temperature in CD_3COCD_3 (Figure 15a) shows *three* well-resolved signals at δ 3.77, 5.71, and 6.37 corresponding to the H-4/8, H-3/7, and H-2/6 protons, respectively, of the 1,5-dioxynaphthalene unit, and *one* well-resolved singlet at δ 6.08 for the hydroquinone ring protons. None of the chemical shifts for these signals undergo any changes at lower temperatures, at least down to −40 °C, i.e., interchange of the two types of aromatic rings is not occurring on the ^{1}H NMR time scale. At +40 °C, the *four* aromatic signals experience a slight broadening, indicating that process

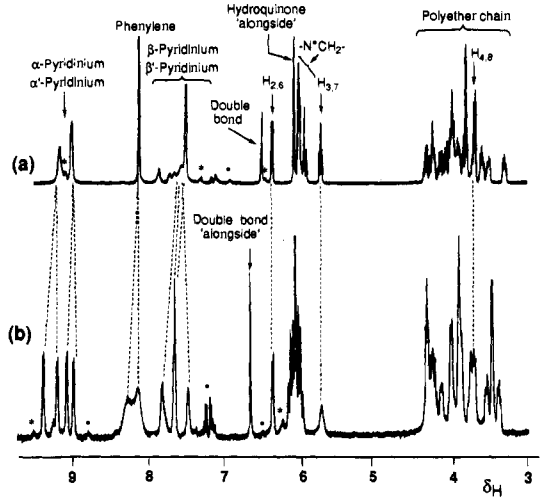

Figure 15. ^{1}H NMR spectra of {[2]-[1/5NPP36C10]-[BIPYBIPYEBIXYCY]catenane}$[PF_6]_4$ in CD_3COCD_3 (a) at +25 °C and (b) at −40 °C. The asterisks indicate signals for the minor isomers.

X is starting to occur on the ^{1}H NMR time scale. At this temperature, saturation transfer experiments led us to the identification of some low intensity broad resonances present in the ^{1}H NMR spectrum, corresponding to the averaged signals resulting from protons in the rapidly equilibrating translational isomers II and III, where the hydroquinone ring (A in Scheme 6) occupies the inside position of the tetracationic cyclophane. Thus, irradiation of these weak signals at δ 7.13 and 7.36, corresponding respectively, to H-3/7 and H-4/8 on the alongside 1,5-dioxynaphthalene unit indicated that they are undergoing exchange with a triplet at δ 5.73 and a doublet at δ 3.68, corresponding to the same protons on the inside 1,5-dioxynaphthalene unit in the rapidly equilibrating translational isomers I and IV. Direct integration of these signals in the ^{1}H NMR spectrum at room temperature—where process X has already been frozen out—gave an equilibrium ratio of 88:12 for the translational isomers I and IV versus II and III. The second dynamic process (process Y in Scheme 6) exhibited by the [2]-catenane involves pirouetting of 1/5NPP36C10 around the tetracationic cyclophane. At room temperature, this process is fast in the ^{1}H NMR time scale. However, below −40 °C, it is frozen out, and the major isomer detected is the translational isomer I, where the π-electron deficient bipyridinium unit (C in Scheme 6) occupies the inside position of the tetracationic cyclophane, as indicated by the relative simplicity of the ^{1}H NMR spectrum, e.g., only *four* major signals are observed for the α-bipyridinium protons—two doublets, corresponding to the bispyridinium unit and two doublets, corresponding to the bis-(pyridinium)ethylene unit (D in Scheme 6). This temperature dependent behavior associated with process Y was accompanied by changes in the ^{1}H NMR spectrum relating to signals associated with all the protons in the cyclophane component of the [2]catenane. Thus, at −40 °C (Figure 15b), the signal corresponding to the olefinic protons of the bis(pyridinium)-ethylene unit in translational isomer I appears at δ 6.60, having experienced only a very slight downfield shift of 0.10 ppm with reference to the room temperature spectrum. This observation confirms that this signal corresponds to translational isomer I, where the π-extended viologen resides alongside the polyether cavity. Once again, a saturation transfer experiment at −20 °C showed the existence of site exchange between a high intensity signal at δ 6.56 (I) and a low intensity signal at δ 6.15 (IV). These signals are associated with site exchange of the olefinic protons of a bis(pyridinium)ethylene unit occupying the alongside and inside positions of the macrocyclic polyether,

Table 8. Halfwave Reduction Potentials (V, *vs* SCE) Obtained in Argon-Purged MeCN Solution at Room Temperature

compound	E_1	E_2	E_3	E_4
BBnBIPY^{2+}	−0.35	−0.78		
t-BBnBIPYE^{2+}	−0.44	−0.64		
$\mathbf{1}^{4+}$	−0.29[a]		−0.71[a]	
$\mathbf{2}^{4+}$	−0.31	−0.43	−0.65	−0.79
$\mathbf{3}^{4+}$	−0.42[a]		−0.62[a]	
$\mathbf{1BB}^{4+}$	−0.31	−0.44	−0.84[a]	
$\mathbf{2BB}^{4+}$	−0.39	−0.49	−0.68	−0.89
$\mathbf{3BB}^{4+}$	−0.43	−0.53	−0.65[a]	
$\mathbf{1BN}^{4+}$	−0.34	−0.48	−0.83	−0.91
$\mathbf{2BN}^{4+}$	−0.40	−0.54	−0.69	−0.88
$\mathbf{3BN}^{4+}$	−0.44	−0.57	−0.73[a]	
$\mathbf{1NN}^{4+}$	−0.35	−0.56	−0.81	−0.89
$\mathbf{2NN}^{4+}$	−0.41	−0.59	−0.73	−0.91
$\mathbf{3NN}^{4+}$	−0.45	−0.59	−0.75[a]	

[a] Two electron process.

i.e., there is evidence for the population of both translational isomers I and IV (Scheme 6). Integration of the signals at −40 °C gave a ratio of 95:5 for the proportions of I to IV. Neither of the other two possible isomers (II or III) was detected at this temperature. The high selectivity exhibited by the [2]catenane {2-[1/5PP36C10]-[BIPYBIPYEBIXYCY]catenane}$[PF_6]_4$ in solution at low temperatures means that it exists as almost *one* amongst the *four* possible translational isomers.

The energy barriers (Table 7) for the dynamic processes observed in [2]catenanes possessing extended π-systems are lower than those described for compounds with smaller cavities, reflecting their "looser" structures.

Electrochemistry. The reported results relate only to *reduction* processes. The oxidation processes are irreversible. The results obtained with the naphthocatenanes $\mathbf{1NN}^{4+}$, $\mathbf{2NN}^{4+}$, and $\mathbf{3NN}^{4+}$, and the benzo/naphthocatenanes $\mathbf{1BN}^{4+}$, $\mathbf{2BN}^{4+}$, and $\mathbf{3BN}^{4+}$ are shown schematically in Figures 16 and 17, respectively, where comparison is made with the known[2,6a] behavior of the corresponding tetracationic cyclophanes. In the following discussion, we will also make reference to previously reported results[6a] concerning the analogous benzo-catenanes (Figure 18). All the electrochemical potentials are gathered in Table 8. For the sake of simplicity, we will first of all compare the behavior of the naphthocatenanes with that of the benzocatenanes. Thereafter, the behavior of the benzo/naphthocatenanes will be discussed.

For compound $\mathbf{1NN}^{4+}$, the degenerate reduction waves of the cyclophane $\mathbf{1}^{4+}$ split and shift to more negative potential (Figure 16), as expected because of the charge-transfer interaction.[2] For the first two waves, the splitting and the shift are larger than for the analogous waves of the benzo-catenane $\mathbf{1BB}^{4+}$ (Figure 18), in agreement with a greater charge-transfer interaction in the case of the naphtho units. An interesting difference can also be observed for the second reduction of the two viologen units. For the benzo-catenane $\mathbf{1BB}^{4+}$, these two reduction processes move to more negative potential, but they remain degenerate, while they split in the case of the naphtho-catenane $\mathbf{1NN}^{4+}$. This observation suggests that, after the second reduction the two viologen units of $\mathbf{1BB}^{4+}$ become equivalent (i.e., they do not occupy "inner" and "outer" positions but either rotate freely or occupy two equivalent positions with respect to the two donor units), whereas they continue to be nonequivalent in the case of $\mathbf{1NN}^{4+}$.

For $\mathbf{3NN}^{4+}$, the first two reduction waves are more split as well as more displaced to negative potential than for $\mathbf{3BB}^{4+}$, indicating again a stronger charge-transfer interaction. The waves corresponding to the second reduction of the vinylogous units, however, do not split but undergo a much stronger shift than in $\mathbf{3BB}^{4+}$. The lack of splitting implies that they do not occupy "inner" and "outer" positions.

Comparison between the behavior of $\mathbf{2BB}^{4+}$ and $\mathbf{2NN}^{4+}$, which contain the desymmetric cyclophane $\mathbf{2}^{4+}$, is very interesting. In both cases, the four waves are separated because the two electron-acceptor units are different. Spectroelectrochemical experiments carried out on $\mathbf{2NN}^{4+}$ have shown that the first reduction process gives rise to spectral changes, which are essentially those expected for the formation of the monoreduced vinylogous unit, whereas, in the case of $\mathbf{2BB}^{4+}$, the first reduction process concerns the viologen unit.[6a] It is clear that the vinylogous unit in $\mathbf{2NN}^{4+}$ lies in the alongside position since its reduction potential is practically the same as that found for the first unit in $\mathbf{3}^{4+}$. This result is in agreement with the lower electron affinity of the vinylogous unit compared with the viologen one, as shown by the smaller displacement of the first two reduction waves for $\mathbf{3BB}^{4+}$ and $\mathbf{3NN}^{4+}$ compared with $\mathbf{1BB}^{4+}$ and $\mathbf{1NN}^{4+}$, respectively (Figures 16 and 18). Furthermore, it is clear that the alongside vinylogous unit does not "feel" the presence of the inside naphtho-unit. The second reduction process of $\mathbf{2NN}^{4+}$ corresponds to reduction of a viologen unit which, being in the inside position, is more difficult to reduce than the (outer) vinylogous unit. It should be recalled that, in the corresponding cyclophane $\mathbf{2}^{4+}$, the viologen unit is reduced at less negative potential than the vinylogous unit. These results show that in $\mathbf{2NN}^{4+}$ the viologen unit interacts very strongly with both the electron-donor units, thereby preventing the inner electron donor interacting with the outer vinylogous unit. The third reduction process is assigned to the second reduction of the vinylogous unit for the following reasons: (a) the second reduction process is always easier for the vinylogous unit (compare the second reduction potential of $\mathbf{1}^{4+}$ and $\mathbf{3}^{4+}$, Table 8 and (b) if the third reduction wave of $\mathbf{2NN}^{4+}$ was arising from the viologen unit, it would occur at a potential very similar to that of the second reduction process of the viologen units in the $\mathbf{1}^{4+}$ cyclophane, while the second reduction of the vinylogous unit would result in a wave which was shifted by a large amount to more negative potential.

Concerning the locations of the vinylogous and viologen units in $\mathbf{2NN}^{4+}$ when the third and fourth reduction processes take place, the following hypothesis can be advanced. After the second reduction process, fast circumrotation of the cyclophane ring around the inside electron donor places the two (monoreduced) electron-acceptor units in equivalent situations. Therefore, the third reduction wave involves the vinylogous unit because its second reduction is easier than the second reduction of the viologen unit. After the third reduction process, the monoreduced viologen unit presumably occupies the inside position, and its second reduction process is therefore displaced to a more negative potential compared to the situation in the case of the free cyclophane.

The behavior of the benzo/naphtho-catenanes $\mathbf{1BN}^{4+}$, $\mathbf{2BN}^{4+}$, and $\mathbf{3BN}^{4+}$ (Figure 17) can be interpreted on the basis of the previously discussed behavior of the benzo- (Figure 18) and naphtho- (Figure 16) catenanes. It is evident that the first reduction of $\mathbf{2BN}^{4+}$ concerns the outer vinylogous unit, as in $\mathbf{2NN}^{4+}$. In the same way, the third and fourth reduction processes of $\mathbf{1BN}^{4+}$ are split as they are in the case of $\mathbf{1NN}^{4+}$.

Figure 19 shows the trend of the potentials of the first and second reduction processes of the symmetrical $\mathbf{1}^{4+}$ and $\mathbf{3}^{4+}$ cyclophanes on changing the nature of the electron-donor crown ether. From this figure—and from the above discussion—it is clear that the reduction patterns are governed by the following properties: (a) 1/5DMN is a better electron donor than 1/4DMB (E_{ox} +1.17[9a] and +1.31 V,[2] vs SCE, respectively); (b) the

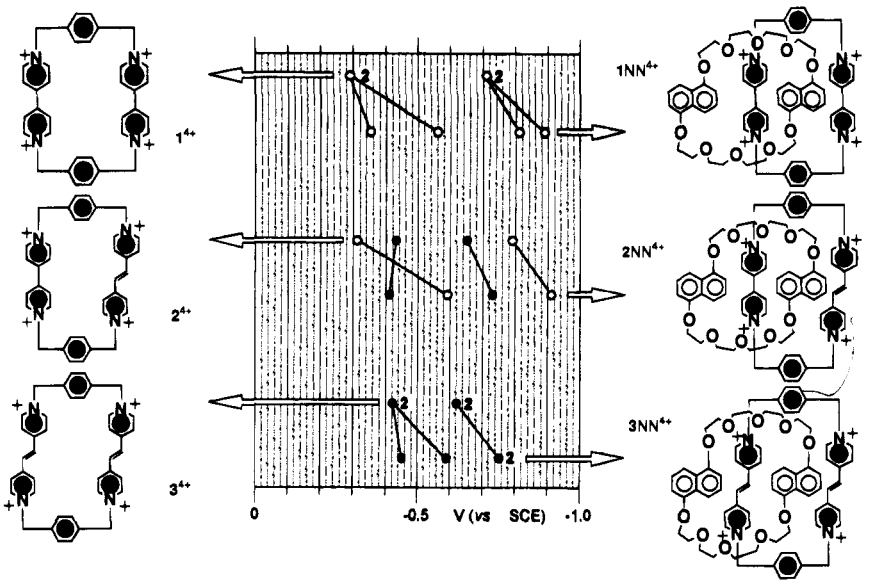

Figure 16. Correlations between the halfwave reduction potentials of each cyclophane with the respective NN catenane. The empty and full circles correspond to reduction of bipyridinium and bis(pyridinium)ethylene units, respectively. Two-electron reduction processes are labelled with the number 2.

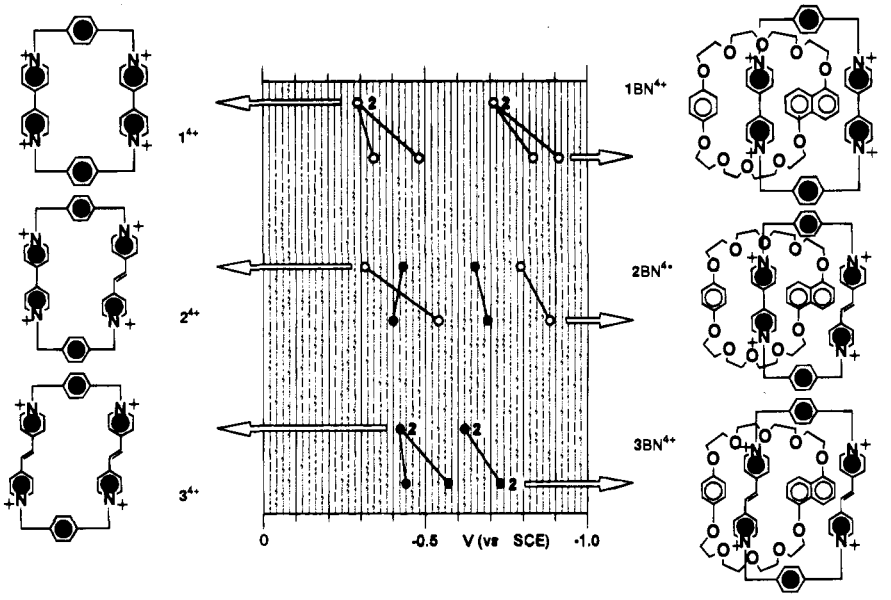

Figure 17. Correlations between the halfwave reduction potentials of each cyclophane with the respective BN catenane. The empty and full circles correspond to reduction of bipyridinium and bis(pyridinium)ethylene units, respectively. Two-electron reduction processes are labelled with the number 2.

viologen unit is a better electron acceptor than the vinylogous unit (first reduction potentials of $\mathbf{1}^{4+}$ and $\mathbf{3}^{4+}$, -0.29 and -0.42 V, respectively, Table 8); and (c) the monoreduced viologen unit is a worse electron acceptor than the monoreduced vinylogous unit (second reduction potential of $\mathbf{1}^{4+}$ and $\mathbf{3}^{4+}$, -0.71 and -0.62 V, respectively, Table 8).

A careful examination of the results obtained for the catenanes shows that a role is also played by structure-related effects when the donor–acceptor interaction is weak (i.e., after the second reduction process). In this regard, two points should be noted: (1) The third and fourth reduction processes of the catenanes of symmetric cyclophanes occur at the same potential (two-electron wave) except for $\mathbf{1NN}^{4+}$ and $\mathbf{1BN}^{4+}$ (Figures 16 and 17). This observation shows that, for $\mathbf{1BB}^{4+}$, $\mathbf{3BB}^{4+}$, $\mathbf{3NN}^{4+}$, and $\mathbf{3BN}^{4+}$, the alongside/inside distinction for the two electron-acceptor units is no longer valid after the second reduction process. This situation could be a result of a fast circumrotation of the cyclophane ring around the inside electron-donor unit, which makes the two (monoreduced) units of the cyclophane equivalent. Such a fast circumrotation apparently cannot take place in either $\mathbf{1NN}^{4}$ or $\mathbf{1BN}^{4+}$, both of which contain the smallest cyclophane ring and one or two bulky electron-donor units, i.e., naphtho units. (2) The shift of the third, two-electron wave with respect to that of the corresponding cyclophane is larger for $\mathbf{1BB}^{4+}$ than for $\mathbf{3BB}^{4+}$, in spite of the better electron-acceptor properties of the monoreduced vinylogous unit. This observation suggests that the actual interaction is larger in $\mathbf{1BB}^{4+}$ because the electron-donor unit fits better the smaller cavity of the viologen cyclophane.

Absorption and Emission Spectra. Most of the data concerning absorption and emission spectra are collected in Table 9.

Components. The absorption and emission spectra of the aromatic crown ethers BB and NN in MeCN solution at room temperature are shown in Figure 20. As previously observed,[2] the absorption spectrum of BB has the shape expected for two

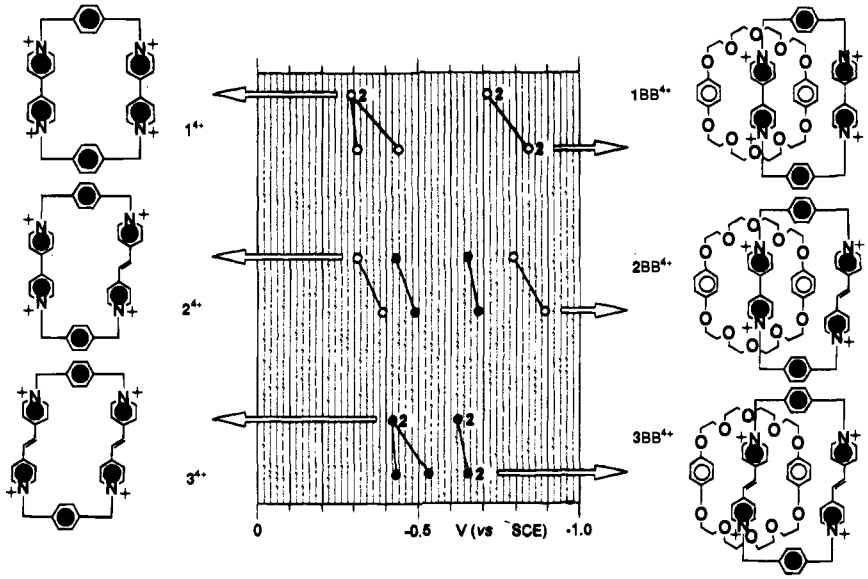

Figure 18. Correlations between the halfwave reduction potentials of each cyclophane with the respective BB catenane. The empty and full circles correspond to reduction of bipyridinium and bis(pyridinium)ethylene units, respectively. Two-electron reduction processes are labeled with the number 2.

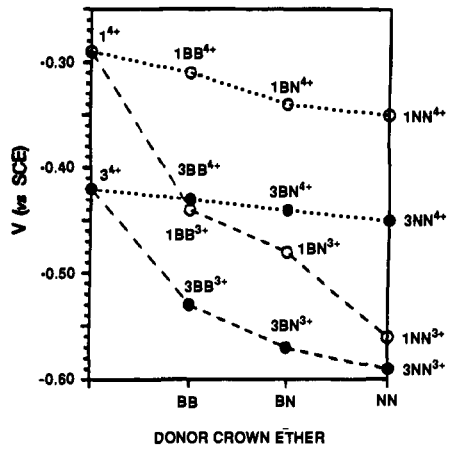

Figure 19. Trend of the potentials of the first (dotted lines) and second (dashed lines) reduction processes of the symmetrical $\mathbf{1}^{4+}$ (○) and $\mathbf{3}^{4+}$ (●) cyclophanes on changing the nature of the interlocked electron-donor crown ether.

1/4DMB units, but it is less intense; its fluorescence spectrum is identical to that of 1/4DMB, except for a lower (~30%) intensity. For compound NN, the absorption spectrum is very similar both in shape and intensity to that of two 1/5DMN units; its fluorescence spectrum is slightly red-shifted with respect to that of 1/5DMN, about 30% less intense in its maximum, and slightly more intense in the tail above 370 nm. The absorption spectrum of BN is that expected for its two chromophoric units. The luminescence spectrum of BN shows only the band of the 1/5DMN unit, regardless of the excitation wavelength. The excitation spectrum shows that energy transfer from the 1/4DMB to the 1/5DMN unit is practically 100% efficient. The luminescence quantum yield is equal to that of the 1/5DMN component.

The absorption spectra of $BBnBIPY^{2+}$ and *t*-1,2-bis(1-benzyl-4-pyridinium)ethylene (*t*-$BBnBIPYE^{2+}$) (Figure 21) are practically identical to those of the PQT^{2+} and *t*-1,2-bis(1-methyl-4-pyridinium)ethylene (*t*-$BMBIPYE^{2+}$) parent compounds which contain methyl instead of benzyl substituents in the 1-pyridinium positions. *t*-$BBnBIPYE^{2+}$ (Figure 21) and *t*-$BMBIPYE^{2+}$ [20] exhibit the characteristic fluorescence band of *t*-bis(pyridinium)-ethylene unit.[21] However, the fluorescence quantum yield of *t*-$BBnBIPYE^{2+}$ is very low (~6% of that of *t*-$BMBIPYE^{2+}$, for which $\Phi = 0.01$[20a,c] has been reported). This observation can be attributed (Figure 22) to the presence in *t*-$BBnBIPYE^{2+}$ of a charge-transfer excited state (hereafter indicated by CT-(*intra*) for a reason that will be explained later) at an energy comparable to or lower than that of the fluorescent S_1 ($^1\pi\pi^*$) level ($E^{00} \sim 3.6$ eV, from the first feature of the fluorescence spectrum at 77 K). The presence of a charge-transfer excited state at relatively low energy is, in fact, expected since the bis-(pyridinium)ethylene moiety is a strong electron acceptor ($E_{1/2}$ *t*-$BMBIPYE^{2+/+} = -0.53$ V *vs* SCE),[20b] and the benzyl moiety is a weak electron donor ($E_{1/2}$ $C_6H_5Me^{0/+} = 1.98$ V *vs* SCE).[22]

Table 9. Absorption and Emission Properties in Air-Equilibrated MeCN Solution at Room Temperature

	absorption		emission	
compound	λ_{max} (nm)	ϵ_{max} (M^{-1} cm^{-1})	λ_{max} (nm)	Φ_{em}
BB	290	5200	320	0.11
BN	295	11500	330	0.38
NN	295	17600	330	0.26
$BBnBIPY^{2+}$	260	20000		
$BBnBIPYE^{2+}$	324	42000	372	6×10^{-4}
$\mathbf{1}^{4+}$	261	40000		
$\mathbf{2}^{4+}$	263	26000	374	2×10^{-3}
	324	42000		
$\mathbf{3}^{4+}$	316	48000	376	4×10^{-4}
$\mathbf{1}BB^{4+}$	263	36500		
	478	700		
$\mathbf{2}BB^{4+}$	267	27000		
	335	17500		
	460[a]	2200		
$\mathbf{3}BB^{4+}$	319	49000		
	440	1100		
$\mathbf{1}BN^{4+}$	267	31700		
	505	740		
$\mathbf{2}BN^{4+}$	278	28200		
	492	900		
$\mathbf{3}BN^{4+}$	316	55700		
	470	920		
$\mathbf{1}NN^{4+}$	268	30600		
	529	1100		
$\mathbf{2}NN^{4+}$	277	31000		
	325	24000		
	515	1000		
$\mathbf{3}NN^{4+}$	307	49000		
	490	1100		

[a] Asymmetrical band with a shoulder at 420 nm (ϵ = 2000 M^{-1} cm^{-1}).

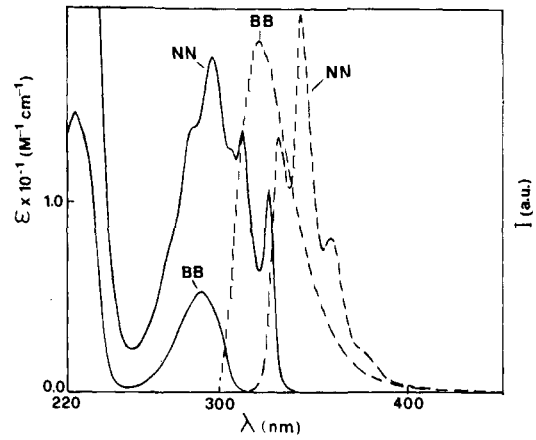

Figure 20. Absorption (—) and emission (– –) spectra of the BB and NN crown ethers in air-equilibrated MeCN solution at room temperature.

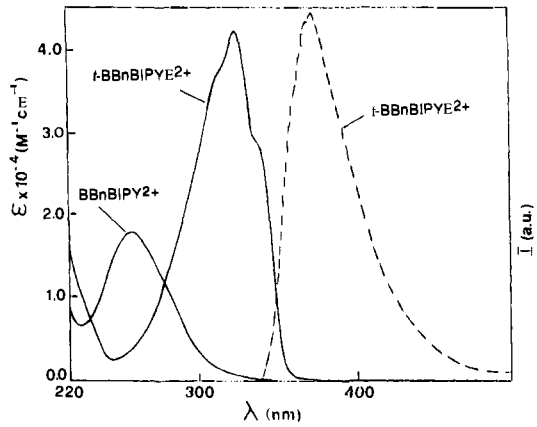

Figure 21. Absorption spectra (—) of *t*-BBnBIPYE^{2+} and BBnBIPY^{2+} and emission spectrum (– –) of *t*-BBnBIPYE^{2+} in air-equilibrated MeCN solution at room temperature.

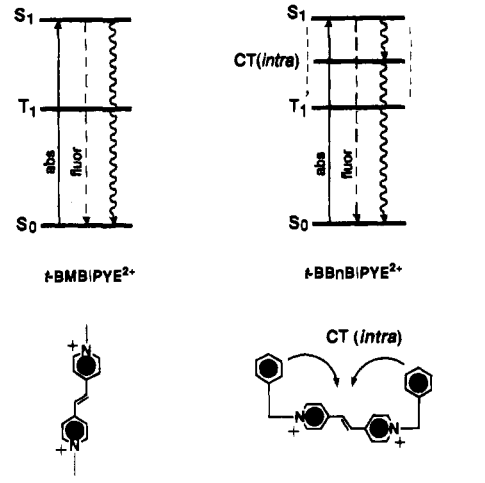

Figure 22. Schematic energy-level diagrams for *t*-BMBIPYE^{2+} and *t*-BBnBIPYE^{2+}.

This CT(*intra*) excited state cannot be seen in absorption, presumably because the charge-transfer transition exhibits a very weak molar extinction coefficient compared to that exhibited by the $^1(\pi \rightarrow \pi^*)$ transition ($\epsilon_{max} = 4.2 \times 10^4$ M^{-1} cm^{-1}). We will see later on that the presence of a CT(*intra*) excited state below S_1 is also needed to explain the photochemical results.

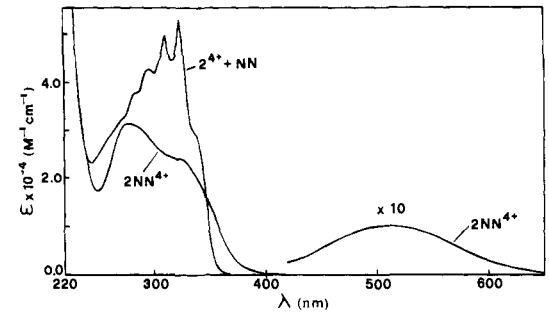

Figure 23. Comparison of the absorption spectrum of the **2**NN^{4+} catenane with the sum of the spectra of the separated components (MeCN solution).

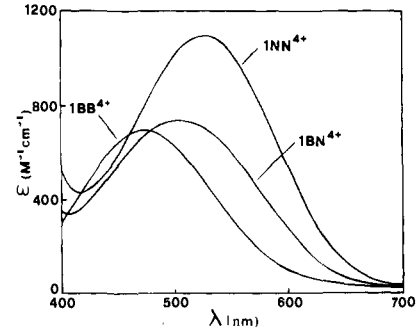

Figure 24. CT(*inter*) absorption band of **1**BB^{4+}, **1**BN^{4+}, and **1**NN^{4+} (MeCN solution).

The absorption spectrum of the tetracationic cyclophane **1**$^{4+}$ is exactly twice that of the BBnBIPY^{2+} component. It should be noted that solutions of **1**$^{4+}$ can show a weak irreproducible luminescence around 550 nm, depending on the experimental conditions. The presence of spurious luminescence bands in solutions containing PQT^{2+} has previously been observed and has caused several misinterpretations.[23] Compound **2**$^{4+}$ shows an absorption spectrum which is similar but not identical to the sum of the spectra of its two chromophoric units, BBnBIPY^{2+} and *t*-BBnBIPYE^{2+}. A fluorescence band, identical to that exhibited by *t*-BBnBIPYE^{2+} except for a somewhat stronger intensity, is observed. The same fluorescence band is exhibited by **3**$^{4+}$, with an intensity similar to that of *t*-BBnBIPYE^{2+}. The absorption spectrum of **3**$^{4+}$, however, is slightly different in shape and much weaker than twice that of *t*-BBnBIPYE^{2+}.

Catenanes. The absorption spectra of the catenanes are different from the summation of the spectra of the respective components (Table 9). As shown for **2NN**$^{4+}$ (Figure 23), the intensity of the UV bands of its **2**$^{4+}$ and NN components is considerably reduced in intensity, and noticeable changes in the structure of the bands are also observed. Furthermore, **2**NN^{4+} exhibits a tail in the 350–400 nm region and a new, broad, relatively weak band in the visible region. Such spectral changes indicate that the two macrocyclic components interact strongly in the catenated structure. In particular, the new band in the visible region can be assigned[2] to charge-transfer transitions from the electron-donor units of the macrocyclic polyether to the electron-acceptor units of the tetracationic cyclophane. This assignment is fully consistent with the blue shift of the visible band when 1/4DMB replaces 1/5DMN as the donor and when the vinylogous unit replaces the viologen one as the acceptor (Figures 24 and 25), as expected on the basis of the redox potentials. It should be noticed that the CT

(20) (a) Ebbesen, T. W.; Previtali, C. M.; Karatsu, T.; Arai, T.; Tokumaru, K. *Chem. Phys. Lett.* **1985**, *119*, 489–493. (b) Ebbesen, T. W.; Akaba, R.; Tokumaru, K.; Washio, M.; Tagava, S.; Tabata, Y. *J. Am. Chem. Soc.* **1988**, *110*, 2147–2151. (c) Ebbesen, T. W.; Tokumaru, K.; Sumitani, M.; Yoshihara, K. *J. Phys. Chem.* **1989**, *93*, 5453–5457.

(21) Favaro, G.; Beggiato, G. *Gazz. Chim. Ital.* **1970**, *100*, 326–333.

(22) Mann, C. K.; Barnes, K. K. In *Electrochemical Reactions in Non-Aqueous Systems*; Dekker: New York, 1970.

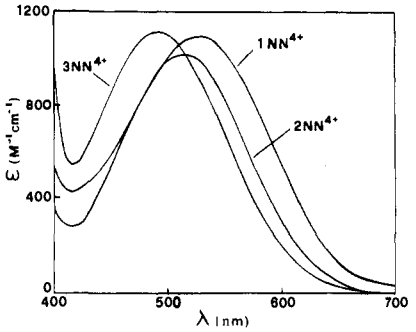

Figure 25. CT(*inter*) absorption band of $\mathbf{1NN}^{4+}$, $\mathbf{2NN}^{4+}$, and $\mathbf{3NN}^{4+}$ (MeCN solution).

bands of the catenanes in the visible region, hereafter indicated by CT(*inter*), to avoid confusion with the CT(*intra*) discussed above (Figure 22), receive contributions from a number of electronic transitions. In fact, in the symmetrical $\mathbf{1BB}^{4+}$, $\mathbf{1NN}^{4+}$, $\mathbf{3BB}^{4+}$, and $\mathbf{3NN}^{4+}$ catenanes, as one can appreciate by considering their structures, three CT(*inter*) transitions can be expected (i.e., from external donor to internal acceptor, from internal donor to external acceptor, and from internal donor to internal acceptor). On the same basis, six different CT(*inter*) transitions can be expected for the desymmetrical $\mathbf{2BB}^{4+}$, $\mathbf{2NN}^{4}$, $\mathbf{1BN}^{4+}$ and $\mathbf{3BN}^{4+}$ catenanes, since they can exist as two different translational isomers (i.e., with each component of the desymmetric macrocycle in the inside or alongside positions). For $\mathbf{2BN}^{4+}$, which in principle can exist as four different translational isomers, such transitions may be as many as 12. The contributions of transitions of different energies explain why the CT(*inter*) bands are generally very broad (Figures 24 and 25), and in one case (i.e., for $\mathbf{2BB}^{4+}$, Table 9) such a band presents a pronounced shoulder.

None of the catenanes shows the fluorescent bands characteristic of their chromophoric units. Clearly, the low energy CT(*inter*) levels offer to the S_1 fluorescent levels of the components a fast radiationless decay route, as illustrated in Figure 26 for $\mathbf{3BB}^{4+}$.

In principle, luminescence could be expected to occur from the low-lying CT(*inter*) levels (Figure 26). A very weak CT luminescence band has in fact been reported to occur for a [2]-rotaxane made of $\mathbf{1}^{4+}$ and a hydroquinone-containing dumbbell component.[7k] However, we have observed that such a band is very similar to that of $\mathbf{1}^{4+}$ alone, and that both bands are casual and irreproducible. Furthermore, when the band is present, its excitation spectrum does not match the absorption spectrum. For these reasons, we thought that no *bona fide* luminescence occurred for that particular [2]rotaxane.[2] Similar weak, casual, and irreproducible emission bands can be observed for the catenanes studied in this paper. Again, the excitation spectrum does not match the absorption spectrum. This observation leads us to reiterate that no *bona fide* CT luminescence is present in these compounds.

Photochemical Behavior. This discussion relates firstly to the components and then to the [2]catenanes.

Components. The macrocyclic species BB, BN, and NN are slightly photosensitive. Their reactions, which are probably a result of interactions between the two aromatic units of the crown, have not been investigated further.

Light excitation of PQT^{2+}, $BBnBIPY^{2+}$, and $\mathbf{1}^{4+}$ in MeCN solution does not cause any appreciable change in the absorption spectra. *t*-$BBnBIPYE^{2+}$ undergoes a reaction in MeCN solution when irradiated with 313 nm light. As shown in Figure 27, the photoreaction causes a decrease in the intensity of the absorption band with $\lambda_{max} = 324$ nm, while two isosbestic points

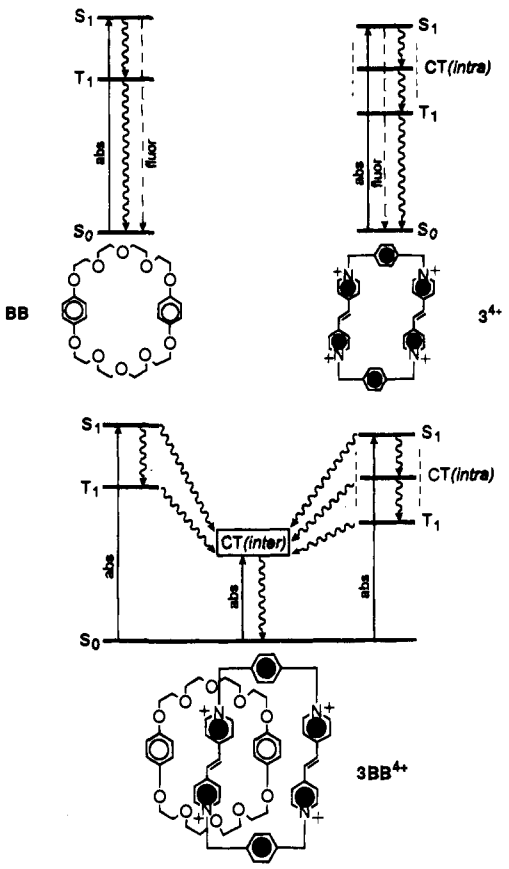

Figure 26. Schematic energy-level diagrams for $\mathbf{3BB}^{4+}$ and its components.

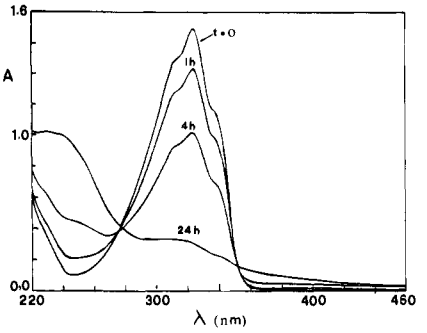

Figure 27. Changes in the absorption spectrum of *t*-$BBnBIPYE^{2+}$ upon direct irradiation with 313 nm light in air-equilibrated MeCN solution.

(at 275 and 355 nm) are observed. After prolonged irradiation, the isosbestic points become "fuzzy", and the 324 nm band disappears. This reaction takes place both in aerated and deaerated solutions, but it is slower in the latter case. The quantum yield for reactant disappearance, measured from the changes in the absorption spectra at 340 nm, where the absorbance of the photoproduct can be neglected, is shown in Table 10. From the beginning, we could exclude the possibility that the observed photoreaction is the *trans* → *cis* photoisomerization. The latter reaction, in fact, has been reported to occur[20a,c] for *t*-$BMBIPYE^{2+}$ (which exhibits the same absorption spectrum as *t*-$BBnBIPYE^{2+}$) with maintenance of an isosbestic point at 286 nm. The excited state, which is responsible for the observed direct photoreaction of *t*-$BBnBIPYE^{2+}$, will be discussed below. In order to identify the nature of the photoproduct, the photoreaction was carried out on a large scale. The analysis of the reaction mixture by ^{1}H NMR spectroscopy and FABMS indicated that it was composed of the starting material, *t*-$BBnBIPYE^{2+}$, and a cyclobutene derivative (Scheme 11). The formation of similar cyclobutene derivatives has been

Table 10. Direct Photochemistry of Air-Equilibrated MeCN Solutions of Components and Catenanes Containing the *t*-BBnBIPYE^{2+} Unit

compound	λ_{irr} (nm)	Φ_{dir}[a]
t-BBnBIPYE^{2+}	313	8×10^{-4}
$\mathbf{2}^{4+}$	313	1×10^{-3}
$\mathbf{3}^{4+}$	313	7×10^{-4}
$\mathbf{2BB}^{4+}$	313	$<5 \times 10^{-5}$
	>420	$<1 \times 10^{-5}$
$\mathbf{3BB}^{4+}$	313	$<8 \times 10^{-5}$
	>420	$<2 \times 10^{-5}$
$\mathbf{2BN}^{4+}$	313	$<2 \times 10^{-4}$
	>420	$<1 \times 10^{-5}$
$\mathbf{3BN}^{4+}$	313	$<4 \times 10^{-4}$
	>420	$<1 \times 10^{-5}$
$\mathbf{2NN}^{4+}$	313	$<2 \times 10^{-4}$
	>420	$<5 \times 10^{-5}$
$\mathbf{3NN}^{4+}$	313	$<2 \times 10^{-4}$
	>420	$<2 \times 10^{-5}$

[a] For reactant disappearance.

Scheme 11

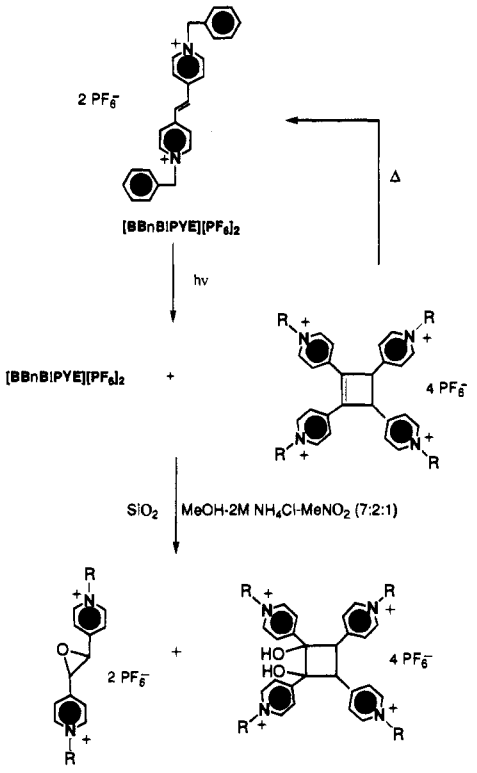

reported previously,[24] as the photoproducts of photoreactions carried out on similar substrates. The compounds oxidize very easily. During an attempt to isolate the photoproduct from the reaction mixture by column chromatography on silica gel, the corresponding epoxide and dihydroxycyclobutane derivative were obtained (Scheme 11), as indicated by FABMS. Furthermore, the photoadduct was difficult to characterize, on account of its instability, whereby it is transformed slowly to *t*-BBnBIPYE^{2+}.

In order to explore the possibility of obtaining a photoinduced *trans* → *cis* isomerization of *t*-BBnBIPYE^{2+}, we have performed photosensitization experiments using biacetyl as a triplet sensitizer. In such experiments, a degassed MeCN solution containing 6.0×10^{-2} M biacetyl and 4.0×10^{-5} M *t*-BBnBIPYE^{2+} was excited with 436 nm light, which is absorbed only by biacetyl. The biacetyl phosphorescence was quenched with a rate constant of 1.5×10^{9} M^{-1} s^{-1} and the spectral variations observed are shown in Figure 28. As one can see, an isosbestic point at 286 nm is present, as expected for the

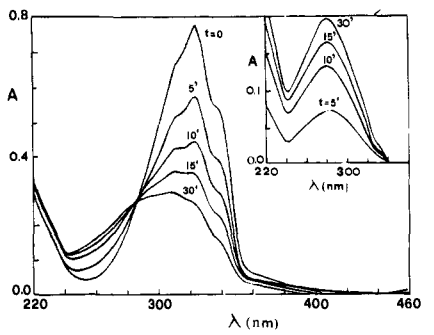

Figure 28. Spectral changes obtained for the sensitized (biacetyl) reaction of *t*-BBnBIPYE^{2+} in degassed MeCN solution (λ_{irr} = 436 nm); the absorption due to the photosensitizer has been subtracted. The inset shows the spectral changes obtained when the absorption due to the residual concentration of *t*-BBnBIPYE^{2+} is also subtracted.

Table 11. Quantum and Chemical Yields of the Sensitized Photoisomerization in Degassed MeCN Solution

	photosensitizer			
	biacetyl		benzanthrone	
compound	$\Phi_{t\rightarrow c}$[a]	% cis[b]	$\Phi_{t\rightarrow c}$[a]	% cis[b]
t-BBnBIPYE^{2+}	0.4	65	0.2	18
$\mathbf{2}^{4+}$	0.8	46	0.4	12
$\mathbf{3}^{4+}$	0.3	47	*c*	*c*

[a] Extrapolated at $t = 0$. [b] At the steady state. [c] Not investigated.

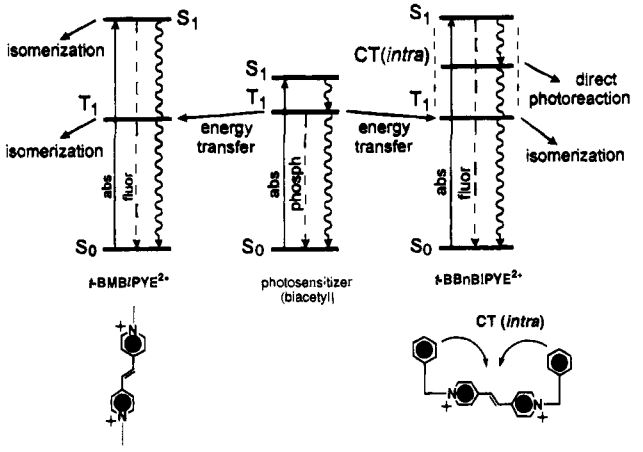

Figure 29. Schematic energy-level diagrams illustrating the photophysical and photochemical processes taking place in the *t*-BMBIPYE^{2+} and *t*-BBnBIPYE^{2+} vinylogous compounds.

trans → *cis* photoisomerization. As shown by the inset of Figure 28, the spectrum of the photoproduct is, in fact, that of *c*-BBnBIPYE^{2+}.[20c] On prolonged irradiation the solution reaches a photostationary state which corresponds to a *trans* → *cis* conversion of 65%. When benzanthrone is used as a triplet photosensitizer, the *trans* → *cis* photoisomerization is again obtained, with a photostationary state less favorable to the *cis* isomer (18%) and a lower quantum yield (Table 11).

The photochemical behavior of $\mathbf{2}^{4+}$ and $\mathbf{3}^{4+}$ is like that of their *t*-BBnBIPYE^{2+} component. Upon direct excitation with 313 nm light, the disappearance of the 324 nm band is observed, whereas the use of triplet photosensitizers causes the *trans* → *cis* isomerization of the *t*-BBnBIPYE^{2+} units. The quantum yields of the direct photoreaction and of the photosensitized isomerization are gathered together in Tables 10 and 11.

The results obtained for *t*-BBnBIPYE^{2+}, $\mathbf{2}^{4+}$, and $\mathbf{3}^{4+}$ can be interpreted on the basis of the energy-level diagrams shown in Figure 29. For *t*-BMBIPYE^{2+}, photoisomerization is known to occur by both the direct (S_1)[20c] and sensitized (T_1)[20a,25] routes.

Table 12. Crystal Data and Data Collection Parameters of {[2]-[1/5NPP36C10]-[BIPYBIPYEBIXYCY]catenane}$[PF_6]_4$ (A), {[2]-[1/5DN38C10]-[BIPYBIPYEBIXYCY]catenane}$[PF_6]_4$ (B), and {[2]-[1/5DN38C10]-[BBIPYEBIXYCY]catenane}$[PF_6]_4$ (C)

data	A	B	C
formula	$C_{78}H_{88}N_8O_{10}P_4F_{24}$	$C_{82}H_{90}N_8O_{10}P_4F_{24}$	$C_{76}H_{80}N_4O_{10}P_4F_{24}$
solvent	4MeCN	4MeCN·H_2O	1.5MeCN·H_2O
formula weight	1877.4	1945.5	1789.3
lattice type	monoclinic	monoclinic	monoclinic
space group	*C2/c*	$P2_1/n$	*C2/c*
T, K	293	293	293
cell dimensions			
a, Å	35.075(10)	14.995(4)	29.301(6)
b, Å	14.171(3)	14.199(2)	15.354(7)
c, Å	20.020(6)	43.316(10)	41.866(9)
α, deg			
β, deg	119.43(2)	90.28(2)	105.04(1)
γ, deg			
V, Å^3	8669(4)	9222(4)	18189
Z	4	4	8
D_c, g cm^{-3}	1.44	1.40	1.37
F(000)	3872	4016	7704
μ, mm^{-1}	1.8	1.7	0.18[a]
θ range, deg	1.5−58	1.5−55	1.75−22.5[a]
no. of unique reflns			
measd	6043	9457	11756
obsd	4063	4840	4067
no. of variables	566	896	785
R, %	0.116	0.093	0.1470
R_w, %	0.129	0.096	0.4608
weighting factor			
p	0.00050	0.00050	0.3018/0[b]

[a] Mo-Kα radiation. [b] SHELXL93.

Furthermore, excitation to S_1 causes a relatively strong fluorescence.[20a,c] For *t*-BBnBIPYE^{2+}, however, direct (S_1) excitation gives a very weak fluorescence (see above) and does not lead to photoisomerization but to another type of photoreaction. These results indicate that, in *t*-BBnBIPYE^{2+}, excitation to S_1 is followed by a fast deactivation to the CT(*intra*) excited state, which is the state likely to be responsible for the direct photoreaction (Figure 29). When a triplet photosensitizer is used, the upper excited states are bypassed, and only the T_1 excited state of *t*-BMBIPYE^{2+} and *t*-BBnBIPYE^{2+} is populated (Figure 29). Under such conditions, the usual *trans* → *cis* photoisomerization reaction of bis(pyridinium)ethylene units is in fact obtained. This behavior is common to *t*-BBnBIPYE^{2+} and its $\mathbf{2}^{4+}$ and $\mathbf{3}^{4+}$ cyclophane derivatives.

Catenanes. Direct light excitation of the nine catenanes does not cause any appreciable photoreaction. No photoreaction can be observed, even when the biacetyl and benzanthrone triplet sensitizers are used for the catenanes containing the *t*-BBnBIPYE^{2+} unit. This behavior can be easily accounted for on the basis of the diagram shown in Figure 26. In the catenanes, besides the levels for the two macrocyclic components, other very low-lying levels, namely the CT(*inter*) levels, are present. As shown by the position of the CT(*inter*) absorption bands, such levels lie certainly below the S_1 and CT(*intra*) levels, and therefore they are expected to quench the processes which can originate from such excited states. This scenario explains the lack of any fluorescence and direct photoreaction when the catenanes containing the *t*-BBnBIPYE^{2+} unit are excited in their UV bands. Judging from the extension to the red of the tail of the CT(*inter*) absorption bands, the lowest CT(*inter*) level can be as low as 15 000−16 000 cm^{-1}, i.e., lower than T_1 level of the photosensitizer (biacetyl: 19 250 cm^{-1}; benzanthrone: 16 450 cm^{-1}),[26] and even lower than the T_1 level of the bis(pyridinium)ethylene unit.[27] Therefore, the photosensitization path becomes ineffective for the catenanes since the potentially reactive T_1 level of the isomerizable moiety is either not populated or, if populated, it can be quenched by the presence of the new CT state.

Scheme 12

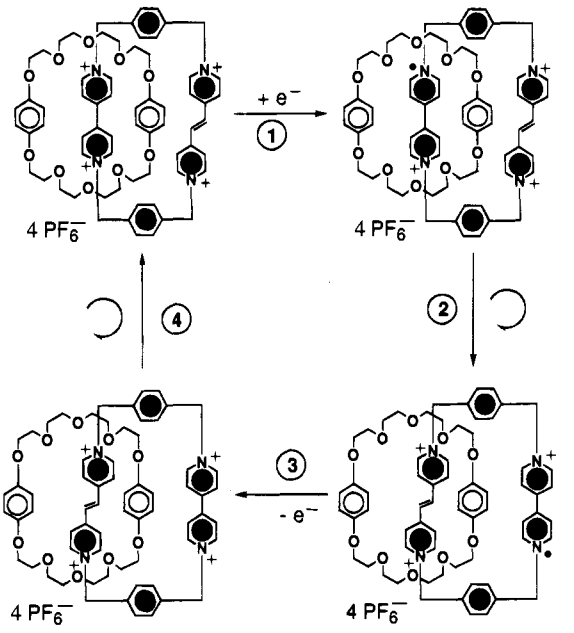

In conclusion, the results obtained show that the photochemical, photophysical, and electrochemical behavior of the cyclophane and crown ether components is very similar to that of the respective components, whereas different properties appear when a cyclophane and a crown ether are interlocked in a catenated structure. This difference is clearly a consequence of the presence of a charge-transfer interaction which (i) introduces new, low-lying excited states (Figure 26) and (ii) perturbs the electron donor/acceptor properties of the various components. The consequence of the former process is a drastic, qualitative change in the photochemical and photophysical properties since the reactive and/or luminescent levels of the components are quenched by the lower-lying CT levels. This is the reason why the luminescence of the crown ethers and the luminescence and the direct and sensitized photoreactions of the cyclophanes containing vinylogous units are not observed in the catenanes. On the electrochemical side, the charge-transfer interaction affects the redox potentials of the components and thereby causes the removal of degeneracy and other changes in the pattern of the successive electrochemical properties (Figures 16−18).

It should be noted that the charge-transfer interaction plays the role of a brake as far as the rotation of the two rings is concerned, since it stabilizes some preferred geometrical arrangements. Successive reduction of the electron-acceptor components (or oxidation of the electron-donor ones) amounts to the release of the charge-transfer brake, thereby leaving the two rings much freer to rotate. These redox properties confer upon such systems, the potential to control the translational isomerism according to the scheme outlined in Scheme 12. The [2]catenane $\mathbf{2BB}^{4+}$ can exist as two different translational isomers—either the viologen unit or the π-extended viologen unit is inside the macrocyclic polyether. The predominant isomer in solution is the one represented in the **top left-hand corner**, in which the viologen occupies the inside position of the macrocyclic polyether, because this dication is a better acceptor than the π-extended viologen dication which occupies the alongside position. However, we can switch this situation

electrochemically, according to the following sequence: (1) Reduction of the [2]catenane: the first reduction occurs in the bipyridinium unit (inside)—because of its lower reduction potential compared with the π-extended viologen ('alongside')—becoming a monoradical cation, as represented in the **top right-hand corner** in Scheme 12. (2) After being reduced, the unit inside loses its ability to bind the π-electron rich units of the macrocyclic polyether. And so, thereafter a situation prevails wherein the π-extended viologen (alongside) which is still a dication prefers to bind the macrocyclic polyether. In consequence, the tricationic macrocycle circumrotates within the neutral macrocycle in order to locate the π-extended viologen dication inside. The predominant translational isomer is now the one represented in the **bottom right-hand corner**. (3) This process is reversible by oxidation, producing again a tetracationic compound, drawn in the **bottom left-hand corner**. In this state, the original preference obtains again, and so the viologen recovers its ability to bind the aromatic units of the macrocyclic polyether. (4) And so, circumrotation takes place, returning the equilibrium to be in favor of the original translational isomer, shown in the **top left-hand corner.** This principle has already been exploited on similar compounds to construct light-driven[7j] and electrochemically driven[7c] mechanical molecular machines.

Conclusion. Several conclusions can be drawn from the results reported in this paper. They are as follows:

●It is possible to use the concept of self-assembly to construct a wide range of [2]catenanes between (1) donor macrocyclic polyethers, incorporating both hydroquinone and 1,5-dioxynaphthalene units and (2) acceptor tetracationic cyclophanes, incorporating both viologen units and the extended analog, bis(pyridinium)ethylene, and still retain quite remarkable efficiencies (38−64% yields) for template-directed syntheses.

●Both variable temperature NMR spectroscopy and electrochemical measurements on the [2]catenanes reveal that their molecular structures are highly ordered in solution and that the particular translational isomers which predominate at equilibrium are the expected ones on the basis of the relative π-donating and π-accepting characteristics of the donor and acceptor units, respectively.

●The solution state behavior exhibited by the [2]catenanes equates well with the solid state structures of three representative catenanes at a molecular level.

●The fact that translational isomerism is not only solvent dependent but can be controlled electrochemically means that the [2]catenanes can be induced to behave as simple switching devices at a molecular level.

●Although the *trans* carbon−carbon double bond in the bis(pyridinium)ethylene units can be isomerized photochemically within a free tetracationic cyclophane, this configurational change does not take place within the corresponding [2]catenanes.

The findings reported herein are now being employed in the design of catenanes that can be controlled and switched according to a prescribed set of stimuli on the molecules. Our aim is to express one function of a molecule in terms of another function and to amplify this transfer of information at a supramolecular level.

(23) Novakocic, V.; Hoffman, M. Z. *J. Am. Chem. Soc.* **1987**, *109*, 2341−2346.

(24) (a) Horner, M.; Hünig, S. *J. Am. Chem. Soc.* **1977**, *99*, 6120−6122. (b) Horner, M.; Hünig, S. *J. Am. Chem. Soc.* **1977**, *99*, 6122−6124. (c) Horner, M.; Hünig, S. *Liebigs Ann. Chem.* **1982**, 1409−1422.

(25) Whitten, D. G.; McCall, M. T. *J. Am. Chem. Soc.* **1969**, *91*, 5097−5103.

Experimental Section

General Methods. 2,3-Butanedione (biacetyl), 1,4-dimethoxybenzene, 1,5-dimethoxynaphthalene, and tetraethylammonium tetrafluoroborate were obtained from Fluka, and benzanthrone (7H-benz[*de*]-anthracene-9-one) was Baker "reagent grade". The following chemicals were purchased from Aldrich and used as received, unless it is indicated that they have been recrystallized—benzyl bromide, 4,4′-bipyridine (BP), 1,4-bis(bromomethyl)benzene (BBB), 1,4-bis(2-hydroxyethoxy)benzene (BHEB), (*E*)-1,2-bis(4-pyridyl)ethylene (BPE) (recrystallized from MeCN), 2-(2-chloroethoxy)ethanol, 1,4-dihydroxybenzene (1/4DHB), 1,5-dihydroxynaphthalene (1/5DHN), methyl iodide, tetraethylene glycol, and *p*-toluenesulfonyl (tosyl) chloride (recrystallized from hexane-$CHCl_3$). The Aldrich products, 1,1′-dimethyl-4,4′-bipyridinium dichloride (PQT^{2+}) and 1,1′-dibenzyl-4,4′-bipyridinium dichloride ($BBnBIPY^{2+}$), were converted into their hexafluorophosphate salts. Solvents were distilled and dried [DMF (from CaH_2), MeCN (from P_2O_5), Me_2CO (from K_2CO_3), and CH_2Cl_2 (from CaH_2)] according to literature procedures.[29] For the photophysical and photochemical experiments, the solvent used was MeCN Merck Uvasol and Aldrich extra-dry for the electrochemical experiments. The following compounds were prepared according to published procedures—1,4-bis[2-(2-hydroxyethoxy)ethoxy]benzene (BHEEB),[2] 1,4-bis[2-(2-hydroxyethyoxy)ethoxy]benzene bis(4-methylbenzenesulfonate) (BTEEB),[2] 1,5-bis[2-(2-hydroxyethoxy)ethoxy]naphthalene (1/5BHEEN),[30] 1,5-bis[2-(2-hydroxyethoxy)ethoxy]naphthalene bis(4-methyl-benzenesulfonate) (1/5BTEEN),[9a] tetraethylene glycol bis(4-methylbenzenesulfonate),[31] 1,4,7,10,13,20,23,26,29,32-decaoxa[13.13]paracyclophane (BPP34C10),[2,11] 1,4,7,10,13,22,25,28,31,34-decaoxa[13.13](1,5)naphthalenophane (1/5DN38C10),[10,12] 1,5-bis[2-[2-[2-(2-hydroxyethoxy)ethoxy]ethoxy]ethoxy]-naphthalene bis(4-methylbenzenesulfonate) (1/5BTEEEEN),[10] and 1,1′-[1,4-phenylenebis(methylene)]-bis(4,4′-bipyridinium) bis(hexafluorophosphate) ([BBIPYXY][PF_6]$_2$).[2,32] Thin-layer chromatography (TLC) was performed on aluminium sheets, coated with silica gel 60 F_{254} (Merck 5554). After being developed, the plates were air dried, analyzed under an UV lamp, and exposed to a SiO_2-I_2 tank. Column chromatography was carried out on silica gel 60 (Merck 9385, 230−400 mesh). Melting points were determined on a electric melting-point apparatus with a digital display (Electhrothermal 9200) and are uncorrected. UV-visible spectra were measured on a Perkin-Elmer 559. Low-resolution mass spectra were obtained on a Kratos Profile Mass Spectrometer using either electron impact mass spectrometry (EIMS) or chemical ionization mass spectrometry (CIMS) using ammonia. Fast atom bombardment mass spectrometry (FABMS), using a krypton primary atom beam in conjunction with a 3-nitrobenzyl alcohol matrix, was performed on a Kratos MS80RF mass spectrometer coupled to a DS90 system. ^{1}H NMR spectra were recorded on either a Bruker AC 300 (300 MHz) or a Bruker AMX400 (400 MHz) spectrometer. ^{13}C NMR spectra were recorded on either the Bruker AC300 (75.5 MHz) or the Bruker AMX400 (100 MHz) spectrometer. Microanalyses were performed by the University of Birmingham Microanalytical Service. All single crystals, which were subjected to X-ray crystal structure analysis, were grown using the vapor diffusion method.[33]

1,4,7,10,13,20,23,26,29,32-Decaoxa[13]paracyclo[13](1,5)-naphthalenophane (1/5NPP36C10). Method B. A solution of 1/4DHB (0.15 g, 1.4 mmol) in dry MeCN (200 mL) was added under nitrogen over 30 min to a degassed suspension of Cs_2CO_3 (2.26 g, 7.0 mmol) and CsOTs (0.93 g, 3.1 mmol) in dry MeCN (400 mL), while the temperature was raised to reflux. After 15 min, a solution of 1/5BTEEEEN[10] (1.14 g, 1.4 mmol) in dry MeCN (200 mL) was added, and the reaction mixture was then heated under reflux for 5 days. After

(26) (a) Murov, S. L.; Carmichael, I.; Hug, G. L. *Handbook of Photochemistry*; Dekker: New York, 1993. (b) Görner, H. *J. Phys. Chem.* **1982**, *86*, 2028−2035.

(27) (a) $E_T \approx 17\,500$ cm^{-1} for *t*-1,2-bis(4,4′-pyridyl)ethylene (ref 24). (b) $E_T = 17\,500$ cm^{-1} for the conjugate acid of *t*-1,2-bis(4,4′-pyridyl)-ethylene (ref 28).

(28) Orlandi, G.; Poggi, G.; Marconi, G. *J. Chem. Soc., Faraday II* **1980**, *76*, 598−605.

(29) Perrin, D. D.; Armarego, W. L. *Purification of Laboratory Chemicals*, 3rd ed.; Pergamon Press: New York, 1988.

(30) Brown, C. L.; Philp, D.; Spencer, N.; Stoddart, J. F. *Israel J. Chem.* **1992**, *32*, 61−67.

being cooled down to room temperature, the suspension was filtered, the solid was washed with MeCN (2 × 50 mL), and the solvent was removed in vacuo. The brown residue was partitioned between CH_2Cl_2 (50 mL) and H_2O (30 mL). The aqueous phase was extracted again with CH_2Cl_2 (2 × 50 mL), and the organic extracts were washed with brine (2 × 50 mL), dried (Na_2SO_4), and concentrated in vacuo. Column chromatography [SiO_2, $Et_2O-CHCl_3-MeOH$ (68:30:2)] afforded 1/5NPP36C10 as a white solid (0.26 g, 32%): mp 94 °C [lit.[9a] mp 78–9 °C]; FABMS 586 $(M)^+$; ^1H NMR ($CDCl_3$) δ 3.66–3.83 (24H, m), 3.98–4.04 (4H, m), 4.18–4.27 (4H, m), 6.56 (4H, s), 6.74 (2H, d, J = 7.5 Hz), 7.38 (2H, dd, J = 7.5 Hz and J = 8.5 Hz), 7.87 (2H, d, J = 8.5 Hz); ^{13}C NMR ($CDCl_3$) δ 68.0, 68.1, 69.7, 69.8, 70.8, 70.9, 71.0, 105.7, 114.6, 115.4, 125.2, 126.8, 152.9, 154.4. Anal. ($C_{32}H_{42}O_{10}$) C, H.

(*E*)-1,2-Bis(*N*-methyl-4-pyridinium)ethylene Bis(hexafluorophosphate) ([BMBIPYE][PF_6]$_2$). A solution of methyl iodide (1.71 g, 27.4 mmol) in dry MeCN (10 mL) was added to a solution of (*E*)-1,2-bis-(4-pyridyl)ethylene (1.0 g, 5.5 mmol) in dry MeCN (100 mL), and the reaction mixture was refluxed under nitrogen for 2 h. After cooling down to room temperature, the suspension was evaporated in vacuo, and the residue was dried. The solid was then dissolved in H_2O (200 mL), and a saturated aqueous solution of NH_4PF_6 was added until no further precipitation was observed. The precipitate was filtered off and washed with H_2O (15 mL). Finally, it was recrystallized from Me_2CO to afford [BMBIPYE][PF_6]$_2$ as a yellow solid (2.50 g, 91%): mp 294 °C; FABMS 357 $(M - PF_6)^+$, 212 $(M - 2PF_6)^+$; ^1H NMR (CD_3CN) δ 4.29 (6H, s), 7.82 (2H, s), 8.15 (4H, d, J = 7.0 Hz), 8.62 (4H, d, J = 7.0 Hz); ^{13}C NMR (CD_3CN) δ 49.0, 126.6, 134.8, 146.7, 151.9. Anal. ($C_{14}H_{16}N_2F_{12}P_2$) C, H, N.

[BPP34C10·BMBIPYE][PF_6]$_2$, [1/5DN38C10·BMBIPYE][PF_6]$_2$, and [1/5NPP36C10·BMBIPYE][PF_6]$_2$. The complexes were obtained by mixing equimolar solutions of the free components. The ^1H NMR spectra were recorded immediately after their preparation. Slow evaporation of the solvent afforded orange-to-red solids that were analyzed by FABMS.

(*E*)-1,2-Bis(*N*-benzyl-4-pyridinium)ethylene Bis(hexafluorophosphate) ([BBnBIPYE][PF_6]$_2$). A solution of benzyl bromide (3.75 g, 22.0 mmol) in dry MeCN (10 mL) was added under nitrogen to a solution of (*E*)-1,2-bis(4-pyridyl)ethylene (1.0 g, 5.5 mmol) in dry MeCN (85 mL), and the reaction mixture was heated under reflux for 2 h. After cooling down to room temperature, the yellow precipitate was filtered off, washed with MeCN (15 mL), and dried before being dissolved in warm H_2O (250 mL). A saturated aqueous solution of NH_4PF_6 was then added until no further precipitation was observed. After filtration, the precipitate was washed with H_2O (20 mL) and dried to give [BBnBIPYE][PF_6]$_2$ as a white solid (2.60 g, 72%): mp 266 °C; FABMS 509 $(M - PF_6)^+$, 364 $(M - 2PF_6)^+$; ^1H NMR 9CD_3CN) δ 5.70 (4H, s), 7.43–7.53 (10H, m), 7.81 (2H, s), 8.15 (4H, d, J = 7.0 Hz), 8.73 (4H, d, J = 7.0 Hz); ^{13}C NMR (CD_3CN) δ 65.1, 127.2, 130.2, 130.6, 130.9, 133.9, 135.1, 145.7, 152.5. Anal. ($C_{26}H_{24}N_2F_{12}P_2$) C, H, N.

[BPP34C10·BBnBIPYE][PF_6]$_2$, [1/5DN38C10·BBnBIPYE][PF_6]$_2$, and [1/5NPP36C10·BBnBIPYE][PF_6]$_2$. The complexes were obtained by mixing equimolar solutions of the free components. The ^1H NMR spectra were recorded immediately after their preparation. Slow evaporation of the solvent afforded orange-to-red solids that were analyzed by FABMS.

(*E*,*E*)-1,1′-[1,4-Phenylenebis(methylene)]bis[4-[2-(4-pyridyl)ethenyl]pyridinium] Bis(hexafluorophosphate) ([BBIPYEXY][PF_6]$_2$). A solution of 1,4-bis(bromomethyl)benzene (1.98 g, 7.5 mmol) in dry MeCN (180 mL) was added dropwise over 6 h to a solution of (*E*)-1,2-bis(4-pyridyl)ethylene (3.0 g, 16.5 mmol) in dry MeCN (60 mL) heated under reflux. The reaction mixture was refluxed for a further 12 h under nitrogen. After the suspension had been cooled down to room temperature, the precipitate was filtered off and washed with MeCN (2 × 15 mL). The residue was subjected to column chromatography [SiO_2: MeOH/2M-NH_4Cl/$MeNO_2$ (5:2:3)]. The fractions containing the product were concentrated to give a residue which was dissolved in hot H_2O (750 mL). Then, a saturated aqueous NH_4PF_6 solution was added until no further precipitation was observed. The precipitate was filtered off, washed with H_2O (3 × 10 mL) and dried to give [BBIPYEXY][PF_6]$_2$ as a white solid (4.8 g, 84%) which must be protected from light: mp 209 °C; FABMS 613 $(M - PF_6)^+$, 468 $(M - 2PF_6)^+$; ^1H NMR (CD_3CN) δ 5.68 (4H, s), 7.52 (4H, s), 7.56 (2H, d, J = 16.3 Hz), 7.57 (4H, d, J = 5.0 Hz), 7.75 (2H, d, J = 16.3 Hz), 8.10 (4H, d, J = 6.5 Hz), 8.64 (4H, d, J = 6.5 Hz), 8.68 (4H, d, J = 5.0 Hz); ^{13}C NMR (CD_3SOCD_3) δ 62.2, 121.9, 125.1, 127.7, 129.6, 135.4, 138.2, 142.2, 144.8, 150.4, 152.4. Anal. ($C_{32}H_{28}N_4F_{12}P_2$) C, H, N.

(1*E*,23*E*)-6,17,28,39-Tetraazonia[2.1.1.2.1.1]paracyclophan-1,23-diene Tetrakis(hexafluorophosphate) ([BBIPYEBIXYCY][PF_6]$_4$). 1,4-Bis(bromomethyl)benzene (35 mg, 0.13 mmol) and NaI (5 mg) were added to a solution of [BBIPYEXY][PF_6]$_2$ (100 mg, 0.13 mmol) and BHEEN (133 mg, 0.39 mmol) in dry DMF (5 mL). A red precipitate was formed in the reaction mixture. After stirring at room temperature for 15 days, Et_2O (20 mL) was added, and the precipitate was filtered off and dried in vacuo. Decomplexation was effected by continuous extraction of an aqueous solution (250 mL) with $CHCl_3$ for 3 days. The aqueous solution was concentrated in vacuo to 5 mL and a saturated aqueous solution of NH_4PF_6 was added until no further precipitation occurred. The suspension was filtered off, and the residue was washed with H_2O (2 × 2 mL) and dried. Recrystallization from MeCN/H_2O gave [BBIPYEBIXYCY][PF_6]$_4$ as a white crystalline solid (53 mg, 35%): mp 263 °C; FABMS 1007 $(M - PF_6)^+$, 862 $(M - 2PF_6)^+$, 717 $(M - 3PF_6)^+$; ^1H NMR (CD_3CN) δ 5.64 (8H, s), 7.57 (4H, s), 7.59 (8H, s), 7.98 (8H, d, J = 7.0 Hz), 8.75 (8H, d, J = 7.0 Hz); ^{13}C NMR (CD_3CN) δ 65.0, 128.5, 131.3, 135.1, 135.8, 147.0, 152.9. Anal. ($C_{40}H_{36}N_4F_{24}P_4$) C, H, N. Use of either BHEB or BHEEB, instead of BHEEN, as potential templates for the formation of [BBIPYEBIXYCY][PF_6]$_4$, did not afford any of this tetracationic cyclophane.

***N*,*N*′-Bis(4-bromomethylbenzyl)-4,4′-bipyridinium Bis(hexafluorophosphate) ([BBXYBIPY][PF_6]$_2$).** A solution of 4,4′-bipyridine (1.0 g, 6.4 mmol) in dry MeCN (20 mL) was added dropwise during 1 h to a solution of 1,4-bis(bromomethyl)benzene (16.92 g, 64.1 mmol) in dry MeCN (70 mL) heated under reflux. The reaction mixture was refluxed under nitrogen for 6 h. After cooling down to room temperature, the yellow precipitate was filtered off and washed with MeCN (20 mL) and Et_2O (500 mL). The residue was then dissolved in H_2O (1500 mL), and a saturated aqueous solution of NH_4PF_6 was added until no further precipitation was observed. The suspension was filtered off, and the solid was washed with H_2O (100 mL) and dried to afford [BBXYBIPY][PF_6]$_2$ as a white solid (3.63 g, 70%): mp > 330 °C [lit.[17] mp > 250 °C]; FABMS 669 $(M - PF_6)^+$, 524 $(M - 2PF_6)^+$; ^1H NMR (CD_3CN) δ 4.62 (4H, s), 5.82 (4H, s), 7.48 (4H, d, J = 8.0 Hz), 7.56 (4H, d, J = 8.0 Hz), 8.36 (4H, d, J = 7.5 Hz), 8.98 (4H, d, J = 7.5 Hz); ^{13}C NMR (CD_3SOCD_3) δ 33.6, 63.1, 127.3, 129.3, 130.2, 132.7, 139.5, 145.8, 149.4.

(*E*)-1,2-Bis[*N*-(4-bromomethylbenzyl)-4-pyridinium]ethylene Bis(hexafluorophosphate) ([BBXYBIPYE][PF_6]$_2$). A solution of (*E*)-1,2-bis(4-pyridyl)ethylene (1.0 g, 5.5 mmol) in dry MeCN (100 mL) was added dropwise over 3 h to a solution of 1,4-bis(bromomethyl)-benzene (14.5 g, 55.0 mmol) in dry MeCN (100 mL) heated under reflux. The reaction mixture was refluxed under nitrogen for a further 12 h. After cooling down to room temperature, the solvent was removed in vacuo, and the yellow residue was suspended in Et_2O (500 mL). The solid was then filtered off and washed with Et_2O (2 × 30 mL), before being dissolved in H_2O (2 L). A saturated aqueous solution of NH_4PF_6 was added until no further precipitation was observed. The precipitate was filtered, washed with H_2O (20 mL), and dried to give [BBXYBIPYE][PF_6]$_2$ as a white solid (1.55 g, 34%): mp 205 °C;

(31) Ouchi, M.; Inoue, Y.; Liu, Y.; Nagamune, S.; Nakamura, S.; Wada, K.; Hakushi, K. *Bull. Chem. Soc. Jpn.* **1990**, *63*, 1260–1262.
(32) Geuder, W.; Hunig, S.; Suchy, A. *Tetrahedron* **1986**, *42*, 1655–1677.
(33) Jones, P. G. *Chem. Br.* **1981**, *17*, 222–225.
(34) Berlman, I. B. *Handbook of Fluorescence Spectra of Aromatic Compounds*; Academic Press: London, 1965.
(35) (a) Hatchard, C. G.; Parker, C. A. *Proc. R. Soc. London A* **1956**, *235*, 518–536. (b) Fisher, E. *EPA Newsletters* **1984**, July 33.
(36) Benesi, H. A.; Hildebrand, J. H. *J. Am. Chem. Soc.* **1949**, *71*, 2703–2707.
(37) Sheldrick, G. M. SHELXTL, *An Integrated System for Solving, Refining and Displaying Crystal Structures from Diffraction Data*; Revision 5.2. University of Göttingen, Germany, 1985.
(38) Sheldrick, G. M. *J. Appl. Cryst.* Manuscript in preparation.

FABMS 695 $(M - PF_6)^+$, 550 $(M - 2PF_6)^+$; ^1H NMR (CD_3CN) δ 4.61 (4H, s), 5.70 (4H, s), 7.44 (4H, d, J = 8.0 Hz), 7.54 (4H, d, J = 8.0 Hz), 7.82 (2H, s), 8.16 (4H, d, J = 7.0 Hz), 8.74 (4H, d, J = 7.0 Hz); ^{13}C NMR (CD_3CN) δ 33.4, 64.5, 127.0, 130.4, 130.9, 133.8, 134.9, 141.0, 145.6, 152.4. Anal. ($C_{28}H_{26}N_2Br_2F_{12}P_2$) C, H, N.

[BPP34C10·BBXYBIPYE][PF_6]$_2$, [1/5DN38C10·−BBXYBIPYE]-[PF_6]$_2$, and [1/5NPP36C10·BBXYBIPYE][PF_6]$_2$. The complexes were obtained by mixing equimolar solutions of the free components. The ^1H NMR spectra were recorded immediately after their preparation. Slow evaporation of the solvent afforded orange-to-red solids that were analyzed by FABMS.

(*E*)-6,17,26,37-Tetraazonia[2.1.1.0.1.1]paracyclo-1-phene Tetrakis(hexafluorophosphate) ([BIPYBIPYEBIXYCY][PF_6]$_4$). Method C. (*E*)-1,2-Bis(4-pyridyl)ethylene (22.5 mg, 0.12 mmol) and NaI (5 mg) were added to a solution of [BBXYBIPY][PF_6]$_2$ (100 mg, 0.12 mmol) and BHEEN (125 mg, 0.36 mmol) in dry DMF (5 mL). A red precipitate was formed in the reaction mixture. After stirring at room temperature for 15 days, Et_2O (20 mL) was added, and the precipitate was filtered off and dried in vacuo. Decomplexation was effected by continuous extraction of an aqueous solution (250 mL) with $CHCl_3$ for 5 days. The aqueous solution was concentrated in vacuo to 5 mL, and a saturated aqueous solution of NH_4PF_6 was added until no further precipitation was observed. The suspension was filtered off, and the solid was recrystallized from $MeNO_2$/EtOAc and then from Me_2CO/H_2O to give [BIPYBIPYEBIXYCY][PF_6]$_4$ as a yellow crystalline solid (73 mg, 53%): mp 285 °C dec; FABMS 1126 $(M)^+$, 980 $(M - PF_6)^+$, 835 $(M - 2PF_6)^+$, 691 $(M - 3PF_6)^+$; ^1H NMR (CD_3CN) δ 5.73 (4H, s), 5.84 (4H, s), 7.56 (8H, s), 7.83 (2H, s), 8.18 (4H, d, J = 7.0 Hz), 8.39 (4H, d, J = 6.6 Hz), 8.73 (4H, d, J = 7.0 Hz), 8.95 (4H, d, J = 6.6 Hz); ^{13}C NMR (CD_3CN) δ 64.4, 65.0, 127.2, 128.6, 131.2, 131.3, 135.1, 135.6, 135.6, 145.9, 146.7, 151.5, 152.7. Anal. ($C_{38}H_{34}N_4F_{24}P_4$) C, H, N. Use of BHEEB instead of BHEEN as the template gave [BIPYBIPYEBIXYCY][PF_6]$_4$ in only 12% yield.

Method D. Following a procedure similar to that described in method C, [BIPYBIPYEBIXYCY][PF_6]$_4$ was obtained in 42% yield by reaction of 4,4′-bipyridine (18.7 mg, 0.12 mmol) with [BBXYPYE]-[PF_6]$_2$ (100 mg, 0.12 mmol) in DMF (6 mL) using a catalytic amount of NaI (5 mg) and BHEEN (125 mg, 0.12 mmol) as the template.

{[2]-[1,4,7,10,17,20,23,26,29,32-Decaoxa[13.13]paracyclophane]-[(1*E*,23*E*)-6,17,28,39-tetraazonia[2.1.1.2.1.1]paracyclophan-1,23-diene]catenane} Tetrakis(hexafluorophosphate) ({[2]-[BPP34C10]-[BBIPYEBIXYCY]catenane}[PF_6]$_4$). Method E Using MeCN as Solvent. A solution of [BBIPYEXY][PF_6]$_2$ (113 mg, 0.15 mmol) in dry MeCN (10 mL) was added to a stirred solution of BPP34C10 (200 mg, 0.37 mmol) in dry MeCN (10 mL). A deep yellow color was formed immediately, and a solution of 1,4-bis(bromomethyl)benzene (43 mg, 0.16 mmol) in dry MeCN (10 mL) was added. After 2 h, the reaction mixture became a deep orange color, which preceded the precipitation of an orange solid. After the reaction mixture had been stirred at room temperature for 7 days, the solvent was removed in vacuo. The residue was purified by column chromatography [SiO_2, MeOH−2M NH_4Cl−$MeNO_2$ (7:2:1)]. The [2]catenane containing fractions were combined and evaporated in vacuo at 25 °C, and the residue was purified by column chromatography [SiO_2, MeOH−2M NH_4Cl−$MeNO_2$ (5:2:3)]. The fractions containing the product were concentrated and dried, and the residue was dissolved in H_2O (15 mL) before a saturated aqueous NH_4PF_6 solution was added until no further precipitation was observed. The precipitate was filtered off and dried to afford {[2]-[BPP34C10]-[BBIPYEBIXYCY]catenane}[PF_6]$_4$ as an orange solid (48 mg, 19%): mp > 300 °C; FABMS 1688 $(M)^+$, 1543 $(M - PF_6)^+$, 1398 $(M - 2PF_6)^+$, 1253 $(M - 3PF_6)^+$; ^1H NMR (CD_3CN) δ 3.14−3.22 (8H, m), 3.49−3.55 (8H, m), 3.72−3.77 (8H, m), 3.78−3.83 (8H, m), 5.50 (8H, br s), 5.60 (8H, s), 6.61 (4H, s), 7.49 (8H, d, J = 6.5 Hz), 7.68 (8H, s), 8.72 (8H, d, J = 6.5 Hz); ^{13}C NMR (CD_3CN) δ 65.1, 68.0, 70.7, 71.2, 71.4, 115.2, 126.9, 131.2, 132.6, 137.5, 145.0, 151.4, 152.8. Anal. ($C_{68}H_{76}N_4O_{10}F_{24}P_4$·$2H_2O$) C, H, N.

Method E Using DMF as Solvent. A solution of [BBIPYEBIXY]-[PF_6]$_2$ (100 mg, 0.13 mmol) in dry DMF (2 mL) was added to a stirred solution of BPP34C10 (177 mg, 0.33 mmol) in dry DMF (1 mL). A deep yellow colored solution was formed immediately, and a solution of 1,4-bis(bromomethyl)benzene (38 mg, 0.15 mmol) in dry DMF (2 mL) was added. After 2 h, the reaction mixture became a deep orange color, which preceded the precipitation of an orange solid. After the reaction mixture had been stirred at room temperature for 15 days, it was poured into Et_2O (50 mL). The orange solid was filtered off, washed with Et_2O (2 × 5 mL), and dried, before being dissolved in a mixture of H_2O/Me_2CO (4:1) (50 mL). Then, a saturated aqueous NH_4PF_6 solution was added until no further precipitation was observed. The orange precipitate was filtered off, washed with H_2O (2 × 5 mL), and dried. Recrystallization from MeCN/Et_2O afforded {[2]-[BPP34C10]-[BBIPYEBIXYCY]catenane}[PF_6]$_4$ (62 mg, 38%).

{[2]-[1,4,7,10,17,20,23,26,29,32-Decaoxa[13.13]paracyclophane]-[(*E*)-6,17,26,37-tetraazonia[2.1.1.0.1.1]paracyclo-1-phene]catenane} Tetrakis(hexafluorophosphate) ({[2]-[BPP34C10]-[BIPYBIPYEBIXYCY]catenane}[PF_6]$_4$). Method F Using MeCN as Solvent. [BBXYBIPY][PF_6]$_2$ (200 mg, 0.25 mmol) and (*E*)-1,2-bis-(4-pyridyl)ethylene (50 mg, 0.30 mmol) were added to a solution of BPP34C10 (330 mg, 0.60 mmol) in dry MeCN (20 mL). The reaction mixture, which turned red immediately, was stirred at room temperature during 5 days. The solvent was then evaporated off to afford a red solid which was subjected to column chromatography [SiO_2, MeOH−2M NH_4Cl−$MeNO_2$ (7:2:1)]. The fractions containing the product were concentrated, and the residue was dissolved in H_2O (2 mL) before a saturated aqueous NH_4PF_6 solution was added until no further precipitation occurred. The suspension was filtered off, and the solid recrystallized from MeCN/H_2O to give {[2]-[BPP34C10]-[BIPYBIPYEBIXYCY]-catenane}[PF_6]$_4$ as a red solid (93 mg, 23%): mp > 300 °C; FABMS 1662 $(M)^+$, 1517 $(M - PF_6)^+$, 1372 $(M - 2PF_6)^+$, 1227 $(M - 3PF_6)^+$; ^1H NMR (CD_3CN) δ 3.41−3.47 (8H, m), 3.62−3.68 (8H, m), 3.78−3.88 (16H, m), 5.15 (4H, br s), 5.64 (4H, s), 5.70 (4H, br s), 5.73 (4H, s), 6.63 (2H, s), 7.53 (4H, d, J = 6.5 Hz), 7.59 (4H, d, J = 7.2 Hz), 7.68 (4H, d, J = 8.5 Hz), 7.79 (4H, d, J = 8.5 Hz), 8.71 (4H, d, J = 6.5 Hz), 8.88 (4H, d, J = 7.2 Hz); ^{13}C NMR (CD_3CN) δ 65.1, 65.2, 67.0, 70.6, 70.8, 71.3, 126.0, 126.8, 128.4, 130.5, 131.1, 131.7, 133.0, 136.4, 137.9, 144.6, 145.7, 146.5, 151.8. Anal. ($C_{66}H_{74}N_4O_{10}F_{24}P_4$) C, H, N.

Method F Using DMF as Solvent. A suspension of [BBXYBIPY]-[PF_6]$_2$ (100 mg, 0.12 mmol) in dry DMF (3 mL) was added to a stirred solution of BPP34C10 (165 mg, 0.31 mmol) in dry DMF (1 mL). A deep red colored solution was formed immediately, and a solution of (*E*)-1,2-bis(4-pyridyl)ethylene (25 mg, 0.13 mmol) in dry DMF (1 mL) was added. After it had been stirred at room temperature for 15 days, the reaction mixture was poured in Et_2O (50 mL). The red solid was filtered off, washed with Et_2O (2 × 5 mL), and dried before being dissolved in a mixture of H_2O/Me_2CO (5:1) (50 mL). Then, a saturated aqueous NH_4PF_6 solution was added, and the solution was left to stand overnight. The solid precipitate was filtered, washed with H_2O (2 × 10 mL), and dried. Recrystallization from MeCN/iPr_2O gave {[2]-[BPP34C10]-[BIPYBIPYEBIXYCY]catenane}[PF_6]$_4$ (87 mg, 43%).

Method G Using DMF as Solvent. A suspension of [BBXYBI-PYE][PF_6]$_2$ (100 mg, 0.12 mmol) in dry DMF (3.5 mL) was added to a stirred solution of BPP34C10 (160 mg, 0.30 mmol) in dry DMF (1 mL). A deep orange colored solution was formed immediately, and a solution of 4,4′-bipyridine (20.4 mg, 0.13 mmol) in dry DMF (0.5 mL) was added. The reaction mixture was stirred at room temperature for 15 days. Workup according to method F (DMF) afforded {[2]-[BPP34C10]-[BIPYBIPYEBIXYCY]catenane}[PF_6]$_4$ (75 mg, 38%).

{[2]-[1,4,7,10,13,22,25,28,31,34-Decaoxa[13.13](1.5)-naphthalenophane]-[(1*E*,23*E*)-6,17,28,39-tetraazonia[2.1.1.2.1.1]-paracyclophan-1,23-diene]catenane} Tetrakis(hexafluorophosphate) ({[2]-[1/5DN38C10]-[BBIPYEBIXYCY]catenane}[PF_6]$_4$). Method E Using DMF as Solvent. A solution of [BBIPYEXY][PF_6]$_2$ (100 mg, 0.13 mmol) in dry DMF (2 mL) was added to a solution of 1/5DN38C10 (210 mg, 0.33 mmol) in dry DMF (5 mL). A deep yellow color developed immediately, and a solution of 1,4-bis(bromomethyl)-benzene (38 mg, 0.15 mmol) in dry DMF (3 mL) was added. After 4 h, the reaction mixture became a deep red color, which preceded the precipitation of a red solid. After the reaction mixture had been stirred at room temperature for 15 days, the suspension was poured into Et_2O (50 mL). The precipitate was filtered off, washed with Et_2O (2 × 5 mL), and dried. The red solid was then suspended in a solution of hexane−Me_2CO (99:1) and stirred for 15 min. The suspension was then filtered, the residue was washed with hexane−Me_2CO (99:1) (3

mL) and CH_2Cl_2 (2 × 5 mL) and dried before being dissolved in H_2O–Me_2CO (2:1) (15 mL). A saturated aqueous NH_4PF_6 solution was then added, and the solution was concentrated in vacuo to remove the Me_2CO, which induced the precipitation of a solid that was filtered off, washed H_2O (2 × 3 mL), and dried. The residue was suspended in CH_2Cl_2 (15 mL), stirred for 30 min, filtered off, and washed with CH_2Cl_2 (10 mL). Recrystallization from Me_2CO–Et_2O gave {[2]-[1/5DN38C10]-[BBIPYEBIXYCY]catenane}$[PF_6]_4$ as a pure compound (120 mg, 51%): mp > 350 °C; FABMS 1788 $(M)^+$, 1643 $(M - PF_6)^+$, 1498 $(M - 2PF_6)^+$, 1353 $(M - 3PF_6)^+$; ^{1}H NMR (CD_3COCD_3) δ 3.37–4.08 (32H, m), 4.28 (2H, br s), 5.63 (2H, br s), 5.83 (8H, s), 5.98 (4H, br s), 6.16 (2H, br s), 6.23 (2H, br s), 6.98 (2H, br s), 7.22 (2H, br s), 7.22 (8H, d, J = 7.5 Hz), 7.95 (8H, s), 9.00 (8H, d, J = 7.5 Hz); ^{13}C NMR (CD_3CN at 273 K) δ 61.7, 64.5, 68.4, 70.5, 71.0, 71.4, 71.7, 71.9, 72.0, 72.9, 105.2, 106.2, 112.3, 114.6, 125.5, 126.2, 126.3, 126.4, 130.0, 130.8, 144.2, 150.65, 153.3, 154.4. Anal. ($C_{76}H_{80}N_4O_{10}F_{24}P_4 \cdot H_2O$) C, H, N. Single crystals, suitable for X-ray crystallography, were grown by vapor diffusion of i-Pr_2O into a solution of the catenane in MeCN.

{[2]-[1,4,7,10,13,22,25,28,31,34-Decaoxa[13.13](1.5)-naphthalenophane]-[(*E*)-6,17,26,37-tetraazonia[2.1.1.0.1.1]paracyclo-1-phene]catenane} Tetrakis(hexafluorophosphate) ({[2]-[1/5DN-38C10]-[BIPYBIPYEBIXYCY]catenane}$[PF_6]_4$). Method F Using DMF as Solvent. A solution of [BBXYBIPY]$[PF_6]_2$ (100 mg, 0.12 mmol) in dry DMF (3 mL) was added to a stirred suspension of 1/5DN38C10 (195 mg, 0.31 mmol) in dry DMF (3 mL). A deep red colored solution was formed immediately, and a solution of (*E*)-1,2-bis(4-pyridyl)ethylene (25 mg, 0.13 mmol) in dry DMF (2 mL) was added. After 2 h, the reaction mixture became a deep purple color, and a purple solid precipitated. After the reaction mixture had been stirred at room temperature for 15 days, the suspension was poured into Et_2O (30 mL). The precipitate was filtered off, washed with Et_2O (2 × 5 mL), and dried before being suspended in H_2O (20 mL). The purple solution was filtered to remove some noncolored material, and a saturated aqueous NH_4PF_6 solution was added until no further precipitation occurred. The precipitate was filtered off, washed with H_2O (10 mL) CH_2Cl_2 (15 mL), and dried. Recrystallization from MeCN/Et_2O gave {[2]-[1/5DN38C10]-[BIPYBIPYEBIXYCY]catenane}-$[PF_6]_4$ as a purple solid (139 mg, 64%): mp > 350 °C; FABMS 1762 $(M)^+$, 1617 $(M - PF_6)^+$, 1472 $(M - 2PF_6)^+$, 1327 $(M - 3PF_6)^+$; ^{1}HNMR (CD_3CN) δ 3.25 (2H, d, J = 8.5 Hz), 3.65–4.20 (32H, m), 5.48 (2H, dd, J = 7.5 Hz and 8.5 Hz), 5.58 (2H, d, J = 13.5 Hz), 5.68 (4H, s), 5.92 (2H, d, J = 13.5 Hz), 6.01 (2H, br s), 6.15 (2H, d, J = 7.5 Hz), 6.37 (2H, d, J = 7.0 Hz), 6.70 (4H, br s), 7.10 (2H, dd, J = 7.0 Hz and 9.0 Hz), 7.20 (2H, d, J = 9.0 Hz), 7.22 (4H, br s), 7.86 (4H, d, J = 8.0 Hz), 7.94 (4H, d, J = 8.0 Hz), 8.70 (8H, br s); ^{13}C NMR (CD_3COCD_3) δ 65.2, 65.3, 68.3, 68.6, 70.7, 71.2, 71.4, 72.1, 72.1, 104.9, 106.5, 110.8, 114.7, 125.2, 126.4, 126.9, 130.9, 132.1, 132.8, 136.4, 139.0, 144.5, 151.5, 152.9, 154.3. Anal. ($C_{74}H_{78}N_4O_{10}F_{24}P_4$) C, H, N. Single crystals, suitable for X-ray crystallography, were grown by vapor diffusion of i-Pr_2O into a solution of the catenane in MeCN.

Method G Using DMF as Solvent. A solution of [BBXYBIPYE]-$[PF_6]_2$ (100 mg, 0.12 mmol) in dry DMF (1 mL) was added to a stirred suspension of 1/5DN38C10 (189 mg, 0.30 mmol) in dry DMF (3 mL). A deep red colored solution was formed instantaneously, and a solution of 4,4′-bipyridine (20.4 mg, 0.13 mmol) in dry DMF (1 mL) was added. After 3 h, the reaction mixture became a deep purple color, and some purple precipitate appeared. After the reaction mixture had been stirred at room temperature for 15 days, a workup according to method F afforded {[2]-[1/5DN38C10]-[BIPYBIPYEBIXYCY]catenane}$[PF_6]_4$ (124 mg, 59%).

{[2]-[1,4,7,10,13,20,23,26,29,32-Decaoxa[13]paracyclo[13](1,5)-naphthalenophane]-[(1*E*,23*E*)-6,17,28,39-tetraazonia[2.1.1.2.1.1]-paracyclophan-1,23-diene]catenane} Tetrakis(hexafluorophosphate) ({[2]-[1/5NPP36C10]-[BBIPYEBIXYCY]catenane}$[PF_6]_4$). Method E Using DMF as Solvent. A solution of [BBIPYEXY]$[PF_6]_2$ (65 mg, 0.16 mmol) in dry DMF (2 mL) was added to a solution of 1/5NPP36C10 (100 mg, 0.41 mmol) in dry DMF (2 mL). A deep yellow color developed immediately, and a solution of 1,4-bis-(bromomethyl)benzene (19 mg, 0.18 mmol) in dry DMF (1 mL) was added. After 4 h, the reaction mixture became a deep red color, and some red precipitate appeared. After the reaction mixture had been stirred at room temperature for 15 days, the suspension was poured into Et_2O (25 mL), the precipitate was filtered off, washed with Et_2O (2 × 3 mL), and dried. The red residue was then suspended in a solution of Et_2O–Me_2CO (10:1) and stirred for 15 min. The suspension was then filtered, and the residue washed with Et_2O–Me_2CO (10:1) (2 × 3 mL) and CH_2Cl_2 (2 × 2 mL) and dried, before being dissolved in a solution of H_2O–Me_2CO (2:1) (15 mL). A saturated aqueous NH_4PF_6 solution was then added, the Me_2CO was removed in vacuo, and the precipitate formed was filtered, washed with H_2O (3 mL), and dried. Recrystallization from MeCN–CH_2Cl_2 afforded {[2]-[1/5NPP36C10]-[BBIPYEBIXYCY]catenane}$[PF_6]_4$ as a red solid (73 mg, 49%): mp > 300 °C; FABMS 1593 $(M - PF_6)^+$, 1448 $(M - 2PF_6)^+$, 1303 $(M - 3PF_6)^+$; ^{1}H NMR (CD_3CN) δ 3.10–4.22 (34H, m), 5.63 (8H, s), 5.64 (4H, br s), 5.65 (2H, br s), 6.15 (4H, br s), 6.30 (2H, d), 7.25 (8H, d J = 8.0 Hz), 7.85 (8H, s), 8.75 (8H, d, J = 8.0 Hz); ^{13}C NMR (CD_3CN) δ 64.9, 68.0, 68.7, 70.3, 70.7, 71.3, 71.3, 71.55, 71.8, 126.6, 126.6, 130.9, 130.9, 131.9, 137.8, 144.5, 151.1, 153.9. Anal. ($C_{72}H_{78}N_4O_{10}F_{24}P_4 \cdot H_2O$) C, H, N.

{[2]-[1,4,7,10,13,20,23,26,29,32-Decaoxa[13]paracyclo[13](1,5)-naphthalenophane]-[(*E*)-6,17,26,37-tetraazonia[2.1.1.0.1.1]paracyclo-1-phene]catenane} Tetrakis(hexafluorophosphate) ({[2]-[1/5NPP36-C10]-[BIPYBIPYEBIXYCY]catenane}$[PF_6]_4$). Method F Using DMF as Solvent. A solution of [BBXYBIPY]$[PF_6]_2$ (53.4 mg, 0.06 mmol) in dry DMF (5 mL) was added to a solution of 1/5NPP36C10 (77 mg, 0.13 mmol) in dry DMF (4 mL). A deep red color was formed immediately, and a solution of (*E*)-1,2-bis(4-pyridyl)ethylene (13 mg, 0.07 mmol) in dry DMF (1 mL) was added. After the reaction mixture had been stirred at room temperature for 15 days, the suspension was poured into Et_2O (50 mL), and the red solid was filtered off, washed with Et_2O (10 mL), CH_2Cl_2 (10 mL), and dried, before being dissolved in H_2O (15 mL) and Me_2CO (5 mL). Then a saturated aqueous solution of NH_4PF_6 was added, and the solution was left to stand overnight, which induced the formation of purple crystals. The suspension was filtered, the crystals were washed with H_2O (2 × 3 mL) and dried to give {[2]-[1/5NPP36C10][BIPYBIPYEBIXYCY]catenane}$[PF_6]_4$ as a purple solid (65 mg, 58%): mp > 350 °C; FABMS 1567 $(M - PF_6)^+$, 1422 $(M - 2PF_6)^+$, 1277 $(M - 3PF_6)^+$; ^{1}H NMR (CD_3CN) δ 3.20–4.40 (32H, m), 3.37 (2H, d, J = 8.0 Hz), 5.57 (2H, dd, J = 7.5 Hz and 8.0 Hz), 5.61 (2H, d, J = 13.5 Hz), 5.68 (4H, s), 5.80 (2H, d, J = 13.5 Hz), 6.09 (4H, s), 6.10 (2H, s), 6.26 (2H, d, J = 7.5 Hz), 7.06 (4H, br s), 7.27 (4H, br s), 7.88 (4H, d, J = 8.5 Hz), 7.98 (4H, d, J = 8.5 Hz), 8.73 (8H, br s); ^{13}C NMR (CD_3COCD_3) δ 65.2, 65.3, 68.4, 68.7, 70.4, 70.4, 71.6, 71.6, 71.65, 72.1, 105.0, 111.0, 115.9, 125.45, 125.8, 127.9, 130.7, 131.0, 131.8, 132.2, 133.0, 136.6, 139.2, 144.7, 145.3, 151.7, 153.0, 153.1. Anal. ($C_{70}H_{76}N_4O_{10}F_{24}P_4$) C, H, N. Single crystals, suitable for X-ray crystallography, were grown by vapor diffusion of i-Pr_2O into a solution of the catenane in MeCN.

Macrophotochemical Experiment. A solution of [BBnBIPYE]-$[PF_6]_2$ (50 mg, 0.08 mmol) in MeCN Merck Uvasol (300 mL) was irradiated with a Hg medium pressure immersion lamp using a Pyrex filter (clear for λ > 300 nm). After 30 h, the solvent was removed in vacuo. Analysis of the crude reaction mixture by FABMS and ^{1}H NMR spectroscopy showed that it was composed of a mixture (6:4) of the starting material [BBnBIPYE]$[PF_6]_2$ and 1,2,3,4-tetrakis(1-benzyl-4-pyridinium)cyclobutene: FABMS 1161 $(M - PF_6)^+$, 925 $(M - 2PF_6 - Bn)^+$, 866 $(M - 3PF_6)^+$, 720 $(M - 4PF_6)^+$.

The residue was then subjected to column chromatography [SiO_2: MeOH/2M-NH_4Cl/$MeNO_2$ (7:2:1)]. The fractions containing the product were concentrated to give a residue which was dissolved in H_2O (10 mL). Then, saturated aqueous NH_4PF_6 solution was added until no further precipitation was observed. The precipitate was filtered off, washed with H_2O (2 × 2 mL), and dried to give a residue that was analyzed by FABMS and ^{1}H NMR spectroscopy. The analysis showed the product to be a mixture of the epoxide of [BBnBIPYE]$[PF_6]_2$ and 1,2,3,4-tetrakis(1-benzyl-4-pyridinium)cyclobutane-1,2-diol in a ratio of 8:2. The instability of these compounds precluded their isolation. The epoxide of [BBnBIPYE]$[PF_6]_2$ had FABMS 525 $(M - PF_6)^+$, 380 $(M - 2PF_6)^+$, 289 $(M - 2PF_6 - Bn)^+$, whereas 1,2,3,4-tetrakis(1-benzyl-4-pyridinium)cyclobutane-1,2-diol had FABMS 1195 $(M - PF_6)^+$, 941 $(M - 2PF_6 - Bn - OH)^+$.

Absorption and Emission Spectra. Absorption spectra were

recorded with a Perkin Elmer λ6 spectrophotometer. Uncorrected emission and corrected excitation spectra were obtained with a Perkin Elmer LS50 spectrofluorimeter. Emission spectra in MeCN rigid matrix were recorded at 77 K using quartz tubes immersed in a quartz Dewar filled with liquid nitrogen. Luminescence quantum yields were determined using naphthalene in degassed cyclohexane as a standard ($\Phi = 0.23$).[34] The experimental error was ±15%.

Photochemistry. Photochemical experiments were carried out in spectrofluorimetric cells on 5×10^{-5} M solutions at room temperature with a medium pressure Q400 Hanau mercury lamp, whose light was filtered with interference filters ($\lambda = 313$ nm for direct photochemistry, $\lambda = 365$ nm and 436 nm for benzanthrone and biacetyl photosensitized reactions, respectively). For the photosensitized experiments, the solutions were degassed by the "freeze−thaw−pump" method. The incident light intensity was measured using the ferric oxalate actinometer.[35] In the direct irradiation experiments, the photon intensity was of the order of 10^{-7} Nhν/min; in the photosensitized experiments, the intensity was reduced by means of a grey filter ($T = 1\%$). The experimental error on the photochemical quantum yields was ±20%.

Electrochemistry. Electrochemical measurements were carried out at room temperature in argon-purged solutions with a Princeton Applied Research 273 multipurpose instrument interfaced to a personal computer. A glassy carbon electrode (0.08 cm^2, Amel) was used as the working electrode. The counter electrode was a Pt wire, and the reference electrode was an SCE (saturated calomel electrode) separated with a fine glass frit. The concentration of the examined compounds was 5.0×10^{-4} M, and 0.05 M tetraethylammonium tetrafluoroborate was added as supporting electrolyte. Cyclic voltammograms were obtained at sweep rates of 20, 50, 200, and 500 mV s^{-1}. All the reduction processes were fully reversible. The criteria for reversibility were (i) the separation between cathodic and anodic peaks, (ii) the close to unity ratio of the intensities of the cathodic and anodic currents, and (iii) the constancy of the peak potential on changing sweep rate. The experimental error on the potential values was estimated to be ±20 mV. Spectroelectrochemical experiments were made in a spectrophotometric cell using a Pt grid as working electrode; the counter electrode was a Pt wire, separated with a fine glass frit and the reference electrode was an Amel Ag/AgCl. Absorption spectra of the reduced species were recorded with a Kontron Uvikon 860 spectrophotometer.

NMR Spectroscopy. Saturation-transfer experiments were performed on the [2]catenanes in a similar manner to NOE experiments with standard Bruker software. During irradiation, saturation is transferred by chemical exchange, and the site to which it occurs is identified as an additional irradiation point. The resulting difference spectrum contains NOEs generated both by the actual irradiated resonance and by that which has been saturated by exchange. The temperature for the experiment was chosen by careful judgment of the onset of line broadening as a result of chemical exchange in the signal of interest. Standard Bruker software was used to perform 2D-COSY-45 correlation experiments.

Stability Constant Determinations by Spectrophotometric Titration Procedures. The method employed for the evaluation of the stability constants of the complexes described in this paper was based on the use of a spectrophotometric titration procedure, by employing the charge-transfer band as a quantitative spectroscopic probe, and observing changes in optical densities of solutions where the relative concentration of one component is increased wtih respect to the other component. The stability constants were determined in dry Me_2CO or MeCN at 25 °C. The experiments were performed according to previously reported protocols.[2] The data were subjected to a Benesi-Hildebrand treatment.[36] The inclusion nature of the 1:1 complexes was confirmed by FABMS and ^1H NMR spectroscopy.

X-ray Crystallography. X-ray diffraction measurements were performed on a Siemens P4/RA diffractometer with graphite-monochromated Cu-Kα radiation with ω scans. Crystal data and data collection parameters are given in Table 12. Lattice parameters were determined by least-squares fits from 18 to 22 centered reflections. Intensities were corrected for the decay of two control reflections, measured either every 50 or 100 reflections, and for Lorentz and polarization factors and empirically for absorption. The structures were solved by direct methods and refined by full-matrix least-squares. Reflections with $|F_o| > 4\sigma(|F_o|)$ were considered to be observed and were included in the refinements (based on F_o for structures A and B and on F_o^2 for structure C). A weighting function of the form $w^{-1} = \sigma^2(F) + pF^2$ was applied in the case of structures A and B and of the form $w = q/[\sigma^2(F_o^2) + (aP)^2 + bP + d + e\sin\theta]$ for structure C. All hydrogen atoms, where calculable, were included in the refinement in calculated positions (C−H distance 0.96 Å) and allowed to ride on their parent carbon atoms ($U(H) - 1.2U_{eq}(C)$). Parameters refined were the overall scale factor, isotropic extinction parameter g (correction of F_c where $F^* = F_c[1.0 + 0.002gF^2/\sin(2\theta)]^{0.25}$), and positional parameters for the non-hydrogen atoms. In structure A, all major occupancy non-hydrogen atoms were refined anisotropically. In structures B and C, due to a shortage of observed data, only selected atoms were allowed to refine anisotropically. In structure B, the atoms of the rigid tetracationic cyclophane were refined isotropically; the major occupancy atoms of the polyether macrocycle were refined anisotropically, the minor occupancy atoms, isotropically. Similarly, the major and minor occupancy atoms of the PF_6^- counterions and the included solvent molecules (MeCN and H_2O) were refined anisotropically and isotropically, respectively. In structure C, again because of observed data limitations, the tetracationic cyclophane was refined isotropically as were the naphthalene rings of the crown ether. The major occupancy PF_6^- counterions and the oxygen and carbon atoms of the polyether linkages were refined anisotropically. The 1,5-naphtho and *p*-phenylene rings were refined as rigid bodies. The major and minor occupancy MeCN solvent molecules were refined anisotropically and isotropically, respectively. Refinements converged with shift:error ratios less than unity for all variables, except occasionally for disordered atoms. Final difference Fourier maps showed no significant features. Calculations for structures A and B were carried out using the SHELXTL program system,[37] those for structure C, using SHELXTL-93.[38]

Acknowledgments. This work was supported by the Engineering and Physical Sciences Research Council in the United Kingdom, and by Ministero dell'Università e della Ricerca Scientifica e Tecnologica and Progetto Strategico CNR Tecnologie Chimiche Innovative in Italy. We thank the Ministerio de Educación y Ciencia in Spain for a Fleming Postdoctoral Fellowship (to L.P.-G.) and CIBA-GEIGY Divisione Additivi for a fellowship (to A.C.). We are grateful to Mr. Damien J.F.-Marquis for a preliminary study. We thank Mr. Malcolm S. Tolley for his assistance in the recording of the NMR spectra. We also thank Dr. Mark A. Blower for the donation of a sample of 1/5NPP36C10. We would like to thank Dr. Norma A. Stoddart for assistance during the preparation of the manuscript.

Supporting Information Available: Tables listing atomic coordinates, temperature factors, bond lengths and angles, and torsion angles (20 pages). This material is contained in many libraries on microfiche, immediately follows this article in the microfilm version of the journal, can be ordered from the ACS, and can be downloaded from the Internet; see any current masthead page for ordering information and Internet access instructions.

JA943898Z